Structural and Mechanistic Studies

on β-Methylaspartate Ammonia-Lyase

a thesis presented by

Susan Helen Richardson

to the

UNIVERSITY OF ST ANDREWS

in application for

THE DEGREE OF DOCTOR OF PHILOSOPHY

St Andrews July 2000

'Anyone of common mental and physical health can practise scientific research..... Anyone can try by patient experiment what happens if this or that substance be mixed in this or that proportion with some other under this or that condition. Anyone can vary the experiment in any number of ways. He that hits in this fashion on something novel and of use will have fame.....The fame will be the product of luck and industry. It will not be the product of special talent.'

Hillaire Belloc (1870-1953)[1]

DECLARATIONS

In submitting this thesis to the University of St Andrews I understand that I am giving permission for it to be made available for use in accordance with the regulations of the University library for the time being in force, subject to any copyright vested in the work not being affected thereby. I also understand that the title and abstract will be published, and that a copy of the work may be made and supplied to any *bona fide* library or worker.

Date ..24th July 2000.. Signature of candidate

I, Susan Helen Richardson, hereby certify that this thesis, which is approximately 40,000 words in length, has been written by me, that it is the record of work carried out by me and that it has not been submitted in any previous application for a higher degree.

Date 24th July 2000.... Signature of candidate

I was admitted as a research student in October, 1995 and as a candidate for the degree of Ph.D. in October 1996: the higher study for which is a record which was carried out in the University of St Andrews between 1995 and 2000.

Date 24th July 2000.... Signature of candidate

I hereby certify that the candidate has fulfilled the conditions of the Resolution and Regulations appropriate for the degree of Ph.D. in the University of St Andrews and that the candidate is qualified to submit this thesis in application for that degree.

Date 24 July 2000 Signature of supervisor

ACKNOWLEDGEMENTS

I would like to thank Professor Gani for his supervision of this work and the Universities of St Andrews and Birmingham for financial support.

I would also like to thank Dr Trevor Rutherford for all his help with the NMR studies, and Dr Mahmoud Akhtar for his valuable scientific input.

I am extremely grateful to Dr John Pollard for his guidance and unwavering moral support which was invaluable and especially appreciated when writing this thesis.

Thank you to Nigel, Saqib, Nadia and Pui Shan, for making life in the lab so enjoyable and for cheering me up when things became a bit too much! To my closest friends Pui Shan, Karen and Caroline, thank you for showing me true friendship and for keeping me sane, despite everything.

Last but by no means least, a huge thank you to Mum, without whose love and support I would not have come so far.

ABSTRACT

Methylaspartase catalyses the reversible *anti*-elimination of ammonia from L-*threo*-(2*S*,3*S*-3-methylaspartic acid (**2**) to afford mesaconic acid (**3**), the second step in the metabolic pathway for (2*S*)-glutamic acid in *Clostridium tetanomorphum*.

This thesis describes the purification to near homogeneity and studies toward the active site structure of an N-terminal His-tagged construct of methylaspartase. In particular the role of the proposed dehydroalanine (dhala) catalytic residue has been addressed.

Kinetic characterization of the purified protein involved an anlysis of the isotope effects over the pH range 6.5-9.0. This showed that the presence of the His-tag and a 5 amino acid C-terminal extension had the effect of removing the primary isotope effect on V at each pH when compared to the wild type enzyme.

An attempt was made to label the active site by incorporation of a ^{13}C-label into the catalytic dhala residue by supplementing the growth media with ^{13}C enriched serine, the proposed pre-cursor of dhala. Analysis of the labeled protein by 2-D NMR spectroscopy showed that the ^{13}C-enriched serine had been metabolized and the label incorporated into a range of alternative residues.

In an attempt to isolate and characterize an active site peptide, the known ability of hydrazine analogues to irreversibly inactivate the enzyme was utilized in the design of a solid phase inhibitor (**99**). The enzyme was irreversibly inhibited and the solid phase bound enzyme was then treated with a protease to strip away the bulk protein and both the liberated peptides and solid support (**100**) were analysed by a range of techniques. Unfortunately, no evidence was gathered to show the presence of a peptide bound covalently to the solid supported inhibitor.

The mechanism of inactivation by hydrazines/hydrazides and analogues was subsequently studied in detail. Phenylhydrazine was found to be the most potent irreversible inactivator of methylaspartase (K_i 5.18 mM) with a pH inactivation rate profile that displayed a unit slope of two, indicative of the involvement of two ionisable groups in the inactivation mechanism. Addition of 2-mercaptoethanol to the inactivation incubation had the effect of reducing the rate of inactivation, with evidence suggesting that this acted as a competitive inhibitor for inactivation. Further, addition of 2-mercaptoethanol to partially inactivated methylaspartase had the effect of dramatically rescuing enzyme activity. This remarkable ability was also observed (to a lesser degree) with both DTT and tributylphosphine. Finally, analysis of the intermediates and products of inactivation by a range of NMR spectroscopic techniques provided strong evidence that the N-N bond in phenylhydrazine was facile and was rapidly degraded under aqueous conditions. Furthermore, evidence was provided for the formation of an Enz-C-N-H bond system at the active site, consistent with the nucleophilic attack of phenylhydrazine at dhala.

A unified mechanism of inactivation by the family of hydrazine analogues has been proposed which may explain these observations.

CONTENTS

LIST OF SCHEMES

Scheme :

LIST OF FIGURES

LIST OF TABLES

LIST OF ABBREVIATIONS

CoA	Coenzyme A
COT	Cyclooctatetraenyl
CV	Column volume
DACM	*N*-(7-dimethylamino-4-methylcoumarynyl)maleimide
DBU	(1,8-diazabicyclo [5.4.0] undec-7-ene)
DEP	Diethylpyrocarbonate
DMB	Davis minimal broth
DMSO	Dimethylsulfoxide
DTT	Dithiothreitol
ES/MS	Electrospray/ mass spectrometry
FPLC	Fast protein liquid chromatography
HAL	Histidine ammonia-lyase
HMQC	Heteronuclear multiple-quantum correlation
HPLC	High performance liquid chromatography
HSQC	Heteronuclear single-quantum correlation
IPTG	Isopropylβ-D-thiogalactoside
IR	Infrared
L-ASA	(2*S*)-Aspartate β-semialdehyde
LB	Luria-Bertani
MAL	Methylaspartate ammonia-lyase
MIO	4-Methylidene-imidazole-5-one

MLE I	Muconate lactonising enzyme I
NAD	Nicotinamide adenine dinucleotide
NEM	N-ethylmaleimide
NMR	Nuclear magnetic resonance
NTA	Nitrilotriacetic acid
OD	Optical density
PAL	Phenylalanine ammonia-lyase
p-CMB	para-Chloromercuribenzoate
PEG	Polyethylene glycol
PKU	Phenylketonuria
PLP	Pyridoxal 5'-phosphate
PMSF	Phenylmethylsulfonyl fluoride
SDS-PAGE	Sodium dodecyl sulfate polyacrylamide gel electrophoresis
TFA	Trifluoroacetic acid
THF	Tetrahydrofuran
TMS	Tetramethylsilane
Tris	Tris [Hydroxymethyl] aminomethane

AMINO ACID CODES

Alanine	Ala	A
Arginine	Arg	R
Asparagine	Asn	N
Aspartic acid	Asp	D
Cysteine	Cys	C
Glutamic acid	Glu	E
Glutamine	Gln	Q
Glycine	Gly	G
Histidine	His	H
Isoleucine	Ile	I
Leucine	Leu	L
Lysine	Lys	K
Methionine	Met	M
Phenylalanine	Phe	F
Proline	Pro	P
Serine	Ser	S
Threonine	Thr	T
Tryptophan	Trp	W
Tyrosine	Tyr	Y
Valine	Val	V

Chapter 1 : Introduction

Despite the enormous variety in living organisms, from a single-celled to complex multi-cellular organisms, there exists a remarkable similarity in the biochemical processes which sustain them.[2] The cells are organised so that the biochemical reactions which are essential to sustain the cell life-cycle can be accomplished with exquisite precision and efficiency. The rates of these transformation reactions are controlled by enzymes, Nature's catalysts.[2] Enzymes are macromolecules which catalyse anabolic (synthesis) and catabolic (degradation) reactions and are commonly used in series to complete metabolic processes.[3] The regulation of metabolic pathways is important in ensuring that adequate energy and synthetic precursors are available for the biosynthesis of more complex molecules.[2]

1.1 Amino acid biosynthesis and metabolism

Mammals are only able to synthesise about half of the amino acids that are required for protein synthesis. The remaining essential amino acids are obtained from dietary sources, the biosynthetic pathways for which are found only in plants and certain bacteria.[2] The enzymes which synthesise essential amino acids in mammals, have apparently been eradicated during evolution, due to their high natural abundance in the diet of primitive animals. Thus, as a result of evolutionary pressure and competition between micro-organisms and mammals for a limited supply of natural resources, individual bacterial species have developed specialised metabolic pathways in order to

process vital organic molecules. The array of enzymes responsible for mediating these essential synthetic and degradative pathways in bacteria, has gradually broadened by the sequential evolution of new enzyme-catalysed reactions which are responsible for the generation of fundamental molecular building blocks.[2]

1.1.1 Amino acid degradation by aerobic bacteria

When animals and plants die, a number of compounds such as polysaccharides, nucleic acids and proteins become available to micro-organisms. These are digested by enzymes such as nucleases and proteases, into low molecular weight peptides, amino acids and nucleic acids, which are then subsequently broken down *via* a range of metabolic pathways, into simple building blocks known as primary metabolites. These primary metabolites are then fed into alternative pathways in order to generate secondary metabolites such as steroids and pheromones.

Many aerobic bacteria have enormous flexibility as to the range of substrates they can utilise. *Pseudomonas putida* for example, was found to be able to use over 200 individual organic compounds as a source of carbon.

Many of the amino acids are structurally similar to central intermediates involved in cellular metabolism. The first step usually involves deamination of the amino acid. A pre-requisite for this reaction is the presence of a substituent at the β-carbon, which facilitates removal of ammonia. Scheme 1.1 shows the degradative pathway for histidine.[4] Subsequent steps in the pathway involve a range of enzyme catalysed reactions such as hydrolytic C-N bond cleavage and hydrolysis.

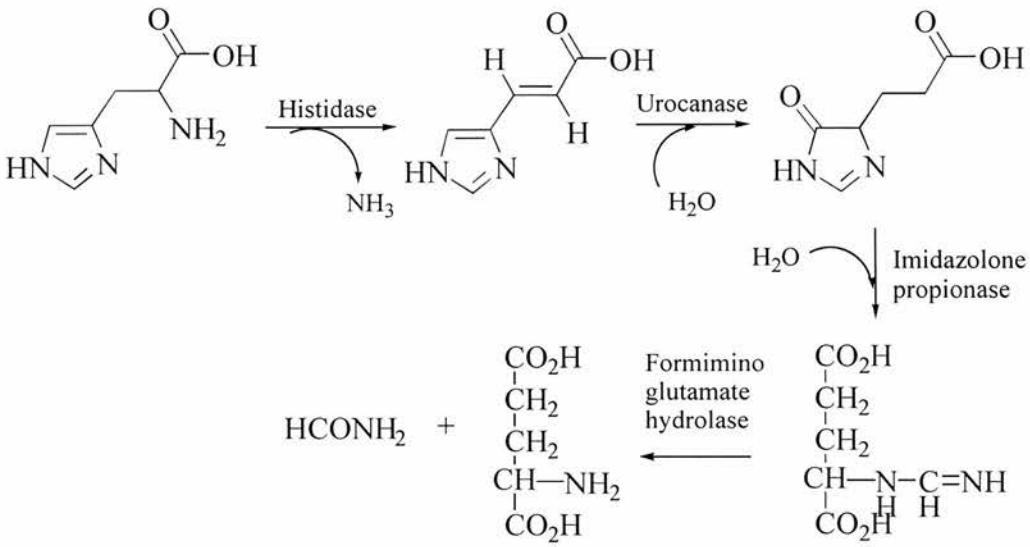

Scheme 1.1: *Degradative pathway for histidine*

1.1.2 Amino acid degradation by anaerobic bacteria

Over the past thirty years, much interest has centered on the determination of the reaction pathways specific to certain anaerobic bacteria (and the enzymes therein) degradation of amino acids.[5] Of particular interest was the discovery that *Clostridium tetanomorphum* is able to metabolise glutamate. The pathway for glutamate fermentation in *C. tetanomorphum* was first delineated in 1958 (Scheme 1.2).[5, 6, 7] (2*S*)-Glutamic acid (**1**) initially undergoes a carbon chain rearrangement catalysed by the co-enzyme B_{12} dependent enzyme glutamate mutase to afford (2*S*,3*S*)-3-methylaspartic acid (**2**). Deamination catalysed by methylaspartase then affords mesaconic acid (**3**). A stereospecific hydration, catalysed by mesaconase then affords (2*S*)-citramalic acid (**4**) which is cleaved by citramalate lyase, to afford pyruvic acid (**5**) and acetic acid. Subsequent oxidative decarboxylation of pyruvic acid produces acetyl CoA (**6**).[7] The

primary metabolites, acetyl CoA and pyruvic acid can then go on to participate in a number of further essential metabolic processes such as the tricarboxylic acid cycle.[7]

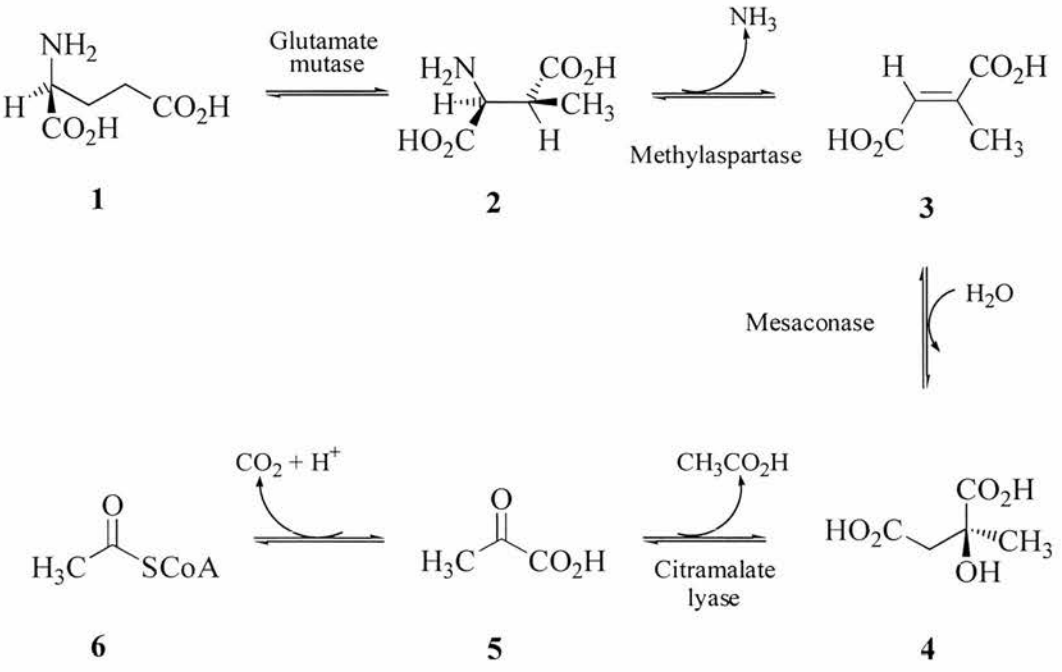

1 **2** **3** **6** **5** **4**

Scheme 1.2: *Glutamate fermentation by* Clostridium tetanomorphum

Peptococcus aerogenes however, is also able to utilise glutamate as the sole carbon source, by a significantly different degradation pathway (Scheme 1.3).[5, 7] In this case the linear carbon chain of glutamate does not undergo rearrangement but instead the amine functionality is replaced by an α-keto group. This reaction is catalysed by glutamate dehydrogenase.[7] Reduction of the α-keto group by 2-hydroxyglutarate dehydrogenase affords 2-hydroxyglutarate. The subsequent enzyme catalysed steps leading to the formation of butyrate (**7**) and acetate still remain in doubt, however, it has been shown that crotonyl-CoA is a product of the degradation pathway.[7]

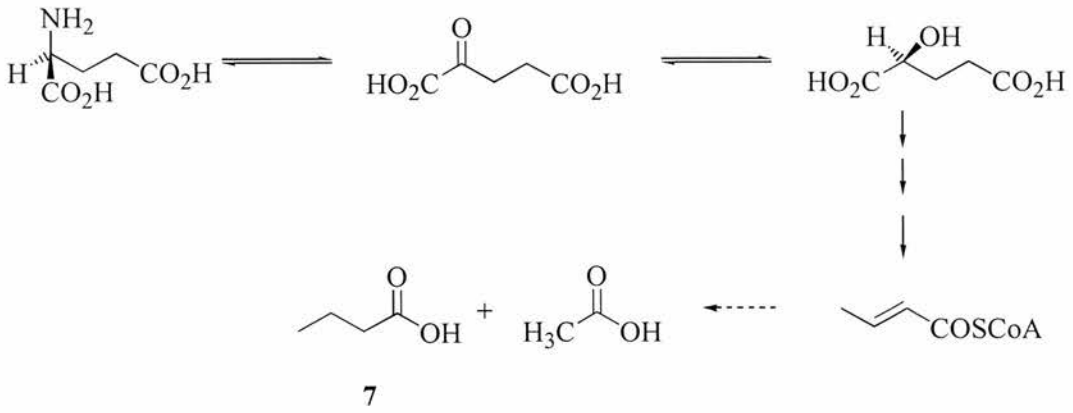

7

Scheme 1.3: *Glutamate metabolism* via *the 2-oxoglutarate pathway*

The two pathways, which are used to degrade glutamate, demonstrate that the metabolism of a specific substrate to identical products in different bacteria, can often proceed with a range of alternative enzyme catalysed reactions.[5] In the case of glutamate fermentation, the two different pathways detailed in this section include several enzymes, which are unique to those bacteria. This most likely reflects a long evolutionary separation of the bacteria and the response of the host organism to differing environmental factors.[5]

1.2 Enzyme-catalysed elimination reactions

As has been highlighted in the previous section, the reversible elimination or lysis of a substrate to generate a double bond is an essential metabolic and biosynthetic reaction. Examples include the elimination of ammonia in amino acid degradation or the introduction of a hydroxy functionality in the degradation of unsaturated hydrocarbons.[2]

These reactions are catalysed by a class of enzymes known as the lyases. The most common elimination reactions involve small molecules such as water (hydratases)[8] carbon dioxide (decarboxylases)[9] and ammonia (ammonia-lyases).[10]

1.2.1 The ammonia-lyase enzymes

The enzyme catalysed reversible elimination of ammonia in biochemical pathways is carried out by a class of enzymes known as the ammonia-lyases.[11] These enzymes are all located on metabolic pathways for amino acids such as (2*S*)-phenylalanine, (2*S*)-histidine, (2*S*)-aspartic acid and (2*S*)-glutamic acid. Some of these are shown in Table 1.1.

Table 1.1: *Reactions catalysed by the ammonia-lyase enzymes*

Enzyme	*Co-factor*	*Reaction*
Glucosaminate ammonia-lyase (EC 4.3.1.9)[12]	PLP	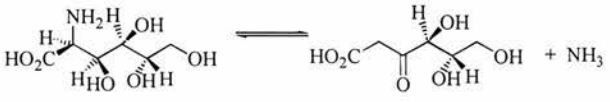
Ethanolamine ammonia-lyase (EC 4.3.1.1)[13]	Co-enzyme B_{12}	
Ornithine *cyclo*-deaminase (EC 4.3.1.12)[14]	NAD^+	
Formimino-tetrahydrofolate *cyclo*-deaminase (EC 4.3.1.4)[15]	-	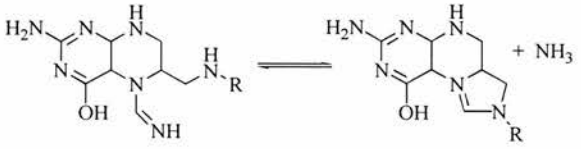
3-alanyl-CoA ammonia-lyase (EC 4.3.1.6)[16]	-	
Aspartate ammonia-lyase (EC 4.3.1.1)[17, 18, 19, 20]	-	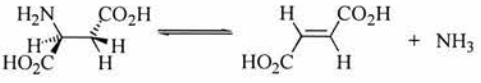
Phenylalanine ammonia-lyase (EC 4.3.1.5)[21, 22, 23]	-	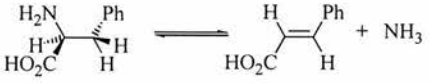
Histidine ammonia-lyase (EC 4.3.1.3)[24, 25, 26]	-	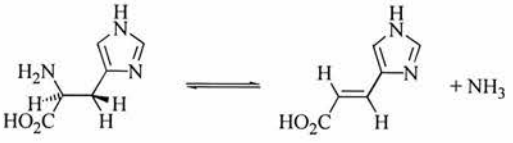
Methylaspartate ammonia-lyase (EC 4.3.1.2)[27, 28, 29]	K^+, Mg^{2+}	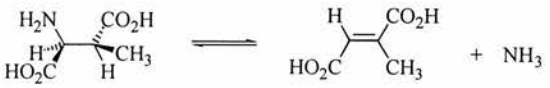

Elimination reactions are known to proceed *via* one of three mechanisms designated as E1, $E1_{cb}$ and E2. These mechanisms differ only in the timing of C-H and C-N bond cleavage.[30] Scheme 1.4 shows the three possible mechanisms for elimination of, in the case of this example, ammonia as is observed with the enzymes methylaspartase (MAL)[27] phenylalanine-ammonia lyase (PAL)[21] and histidase (HAL).[24]

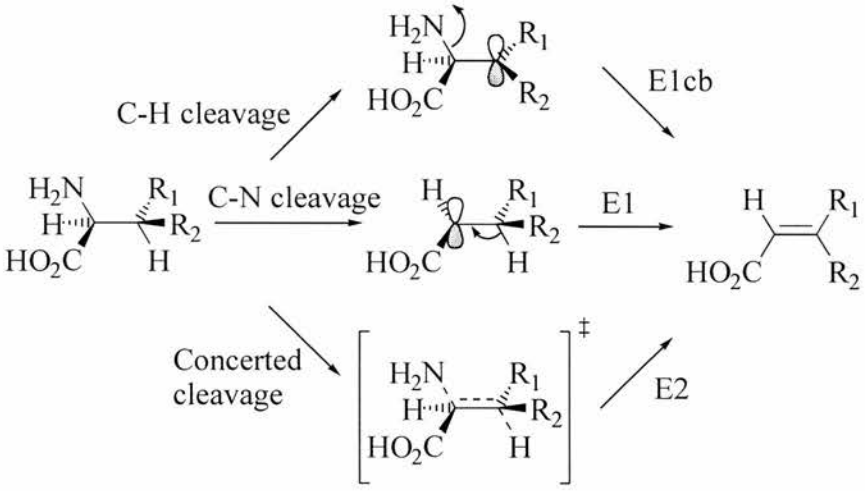

Scheme 1.4: *Mechanisms for elimination of ammonia*

E1 mechanism - An E1 mechanism is a unimolecular elimination, which occurs when the C-N bond is cleaved first, in the rate-determining step, to afford a carbocation intermediate. Subsequent rapid C-H bond cleavage results in the unsaturated product (Scheme 1.4, middle). Although common in organic reactions, this mechanism is rare in enzymatic systems.[31] A probable explanation for this is that in many of the substrates for

elimination, a neighbouring electron-withdrawing group such as a carbonyl group is present. This then acts to destabilise the positive charge, making the intermediate a very high energy species. In chemical systems the direction of the double bond will form mainly at the more highly substituted carbon atom (Scheme 1.5).[32]

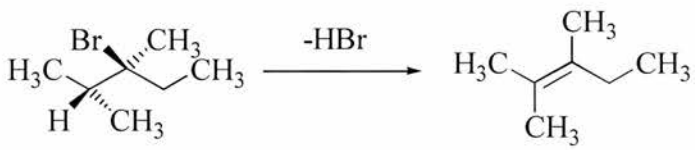

Scheme 1.5: *Elimination of HBr from 3-bromo-2,3-dimethylpentane*

$E1_{cb}$ mechanism - In an $E1_{cb}$ (unimolecular elimination using a conjugate base) mechanism the C-H bond is broken first, in the rate determining step, to form a carbanion.[30] This step is followed by rapid cleavage of the C-N bond to afford the unsaturated product (Scheme 1.4, Top). In a non-enzymatic $E1_{cb}$ elimination reaction a strong base is required to abstract the proton, generating the carbanionic intermediate (Scheme 1.6).[33]

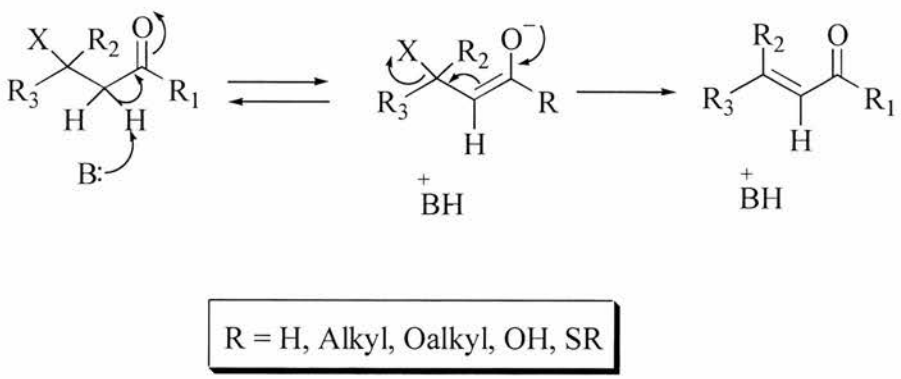

Scheme 1.6: *Base-catalysed non-enzymatic elimination reaction ($E1_{cb}$)*

The carbanionic intermediate which is formed can then partition down two reaction pathways. The intermediate can either undergo C-N cleavage to give the product, or it can pick up a proton from the bulk solvent to give back the starting material. Thus, hydrogen exchange is evidence for an $E1_{cb}$ mechanism.[33] It should be noted however that in an enzyme catalysed reaction, a lack of exchange with the bulk solvent is not necessarily sufficient evidence, in isolation, to rule out an $E1_{cb}$ mechanism, since the active site may not be accessible to solvent and therefore exchange can not occur. Despite this, a number of enzyme reactions have been proposed to operate *via* an $E1_{cb}$ mechanism, on the basis of observed hydrogen exchange.[33] These include triose phosphate isomerase and enolase.[33] Exchange of the α-proton of the substrate with bulk solvent was observed, suggesting the formation of an intermediate carbanion.

In some enzyme-catalysed reactions where the natural substrate contains a carboxylate group adjacent to the site of proton abstraction, an $E1_{cb}$ mechanism would involve the formation of an unfavorable dianion after removal of the α-proton. However, in an enzyme active site *e.g.* mandelate racemase, the anionic carboxylate group of the substrate binds directly with a metal ion.[33] The intermediate can also be stabilised through favourable interactions with the enzyme, through ion-pair interactions with active site residues.[33]

Reactions, which are initiated by proton abstraction, generally undergo *anti*-elimination, thus implying that the α-proton and the β-substituent are in an *anti*-periplanar relationship. This is necessary in order to achieve maximal overlap of the negative charge and the *anti*-bonding orbital of the scissile bond. The *anti* stereochemical course has been attributed to a two base mechanism as the conjugate acid of the base

must be acidic enough to protonate the leaving group, thus a second more acidic group is required.[34]

E2 mechanism – An E2 mechanism (bimolecular) is a one step process involving a rate-determining concerted cleavage of the C-H bond and the C-N bond bond which proceeds through a single transition state (Scheme 1.4, Bottom).[30] The reaction, which is initiated by attack of a base to remove the proton, proceeds *via* a planar transition state. In synthetic reactions the deprotonation step usually requires a strong base.

For the E2 elimination a *trans* β-proton is generally necessary, if this is available at only one adjacent carbon centre the location of the double bond is pre-determined. When β-hydrogens are available on 2 or 3 carbons, the structural isomer formed will depend on the substrate structure and the nature of the leaving group.

The stereochemistry of synthetic elimination reactions is defined by the mechanism through which the reaction proceeds. In the case of enzyme-catalysed β-elimination reactions however, a profound fidelity to the conservation of stereochemistry is observed and the products of reactions involving elimination from a carboxylate anion are almost always *trans*.[34, 35]

For a concerted elimination to proceed, strong orbital overlap is required between the bonding σ-orbital of the scissile C-H bond and the σ* *anti*-bonding orbital of the C-X bond. Except in the case of a few enzymes (discussed below) this can only be achieved with a *trans* peri-planar relationship.

The ability of some enzymes to stabilise high-energy intermediates means that occasionally *syn* products are observed. Examples of enzymes which catalyse *syn*-elimination reactions include muconate lactonising enzyme, which catalyses the

reversible cycloisomerisation of *cis,cis*-muconate to muconolactone[36, 37] and dehydroquinase which catalyses the reversible dehydration of 3-dehydroquinic acid (**8**) to 3-dehydroshikimic acid (**9**) (Scheme 1.7).[38]

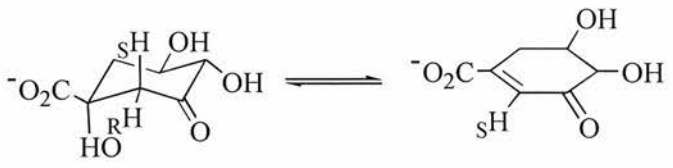

8 **9**

Scheme 1.7: *Reaction catalysed by dehydroquinase*

It has been suggested that concerted *syn* elimination reactions will have a certain degree of carbanion character due to faster C-H bond cleavage compared to C-leaving group bond cleavage. Crotonase, has been proposed to operate *via* a concerted mechanism (Scheme 1.8).[39]

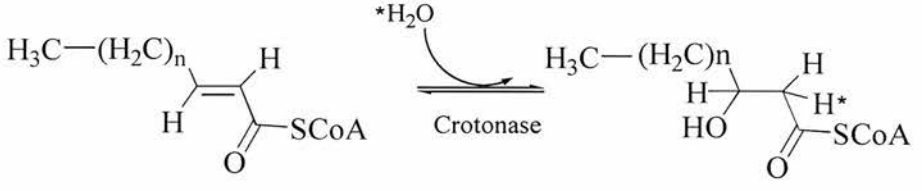

Scheme 1.8: *Reaction catalysed by Crotonase*

1.3 3-Methylaspartate ammonia-lyase

3-Methylaspartate ammonia-lyase (EC 4.3.1.2) is the second enzyme in the glutamate metabolic pathway and catalyses the reversible *anti*-elimination of ammonia from L-*threo*-(2*S*,3*S*)-3-methylaspartic acid (**2**) to give mesaconic acid (**3**) (Scheme 1.9).

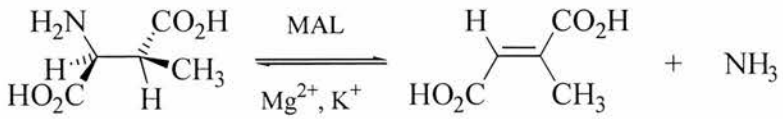

2 **3**

Scheme 1.9: *Reaction catalysed by methylaspartase*

The native enzyme was first isolated from cell free extracts of the obligate anaerobe *C. tetanomorphum* by Barker *et al.* and was shown to have a native molecular weight of 90 kDa, as determined from sedimentation equilibrium measurements.[42]

Addition of 6 M guanidine hydrochloride cleaved the enzyme into two subunits of 45 kDa and an eight-fold molar excess of *p*-chloromercuribenzoate (*p*-CMB) effected cleavage of the enzyme into four identical subunits of ~25 kDa.[43] However, only two moles of *p*-CMB were required for complete inactivation of the enzyme. These observations led to the conclusion that the native enzyme contained two types of sub-unit, only one of which possessed catalytic activity,[41] the morphology being $(AB)_2$. The enzyme has a pH optimum for V_{max} of 9.7.

Methylaspartase migrated in polyacrylamide gel electrophoresis as a single protein band with a molecular weight of 100 kDa. [44, 42] However, in a later study, it was shown by SDS-PAGE and Edman sequencing that the enzyme was constructed from a single sub-unit species with a mass of 49 kDa,[45] consistent then with a homodimeric morphology. A 2.2 kb section of *Clostridial* DNA containing the complete gene for methylaspartase was excised from the *Clostridial* chromosome using the *Hind*III restriction enzyme.[46] This was subsequently ligated into the plasmid vectors pMTL21 and

pMTL32 and transformed into an *E. coli* host, pSG4. The DNA sequence of the mal gene was determined and from this a 413 amino acid sequence was inferred (Fig 1.1).[46]

```
MKIVDVLCTP  GLTGFYFDDQ  RAIKKGAGHD  30
GFTYTGSTVT  EGFTQVRQKG  ESISVLLVLE  60
DGQVAHGDCA  AVQYSGAGGR  DPLFLAKDFI  90
PVIEKEIAPK  LIGREITNFK  PMAEEFDKMT  120
VNGNRLHTAI  RYGITQAILD  AVAKTRKVTM  150
AEVIRDEYNP  GAEINAVPVF  AQSGDDRYDN  180
VDKMIIKEAD  VLPHALINNV  EEKLGLKGEK  210
LLEYVKWLRD  RIIKLRVRED  YAPIFHIDVY  240
GTIGAAFDVD  IKAMADQIQT  LAEAAKPFHL  270
RIEGPMDVED  RYKQMEAMRD  LRAELDGRGV  300
DAELVADEWC  NTVEDVKFFT  DNKAGHMVQI  330
KTPDLGGVNN  IADAIMYCKA  NGMGAYCGGT  360
CNETNRSAEV  TTNIGMACGA  RQVLAKPGMG  390
VDEGMMIVKN  EMNRVLALVG  RRK         413
```

Figure 1.1: *Inferred amino acid sequence of methylaspartase*

In addition to being an ammonia-lyase enzyme, methylaspartase is also a member of the enolase superfamily of enzymes, which are related due to their ability to catalyse the removal of the proton α- to a carboxylic acid.[47] The members of this family are sub-divided into three groups based on the identity of the active site base. Methylaspartase belongs to the Muconate lactonising enzyme I group (MLE I).[47] Enzymes in this group

contain two lysine residues in a KX (K/R) motif which are thought to act as active-site bases.[47] It was shown, by incubating the enzyme with the substrate in tritiated water that the proton at C-3 was able to undergo exchange with the bulk solvent. This was analysed as ^{3}H incorporation into the substrate pool.

The pH rate profile for exchange of the C-3 proton of the substrate showed an inflection at pH 7.8.[27] On this basis it was proposed that a nucleophile with a pk_a of 7.8 was responsible for β-proton abstraction. It was suggested that a cysteine residue was a possible candidate.[48] Further evidence to support this was obtained in a kinetic study with the cysteine dependent chemical modifying agent (*N*-ethylmaleimide) (NEM).[42] The enzyme was rapidly and irreversibly inhibited with NEM but protection from inhibition was afforded upon pre-incubation of the enzyme with the substrate. This indicated that the amino acid that had been modified was at or near the active site of the enzyme and was most probably a cysteine residue.[48]

1.3.1 Metal ion cofactor requirements

Methylaspartase has a requirement for both a monovalent and divalent metal ion for catalytic activity.[49] Magnesium ion was found to be the most effective divalent cation although nickel, cobalt, iron, zinc, manganese and cadmium were also shown to provide activation, but to a lesser degree.[49, 50] Further investigations showed that divalent metal ions with an ionic radius smaller than that for Ca^{2+} (<1.0 Å) were activators of methylaspartase and ions with a radius larger than that for Ca^{2+} (>1.0 Å) acted as inhibitors.[51, 52]

The requirement for a monovalent cation was found to be relatively non-specific, with a wide range of monovalent ions capable of activating the enzyme.[28] Potassium was found to be the most effective activator at 2 mM (K_M=3 mM).[28] In addition, it was found that other monovalent ions such as ammonia, lithium, sodium and cesium also activated the enzyme. It was also shown that in the absence of an activator such as potassium, the enzyme still displayed catalytic activity. This observation was rationalised by proposing that ammonium ion, as a protonated product of the forward deamination reaction, could promote autocatalysis.[51]

1.3.2 Substrate specificity

In addition to the natural substrate (2*S*,3*S*)-3-methylaspartic acid, it was demonstrated that methylaspartase is able to catalyse the deamination of a wide range of 3-alkyl aspartic acids (Scheme 1.10).[53, 54]

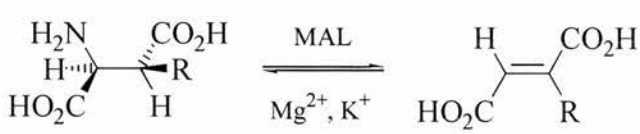

2; R = CH_3

10; R = H

11; R = Et

3; R = CH_3

12; R = H

13; R = Et

Scheme 1.10: *Deamination of 3-substituted aspartic acids by methylaspartase*

The kinetic parameters for the deamintion of a range of 3-alkyl aspartic acids are shown in Table 1.2.[55] Whilst K_m values only vary by about 10-fold over the three

analogues it is evident that V_{max} changes by up to 150-fold. From this study it was concluded that the size of the C-3 substituent is critical in lowering the activation energy of the reaction (and hence increasing V_{max}), most probably through favourable interactions with the active site.[55]

Table 1.2: *Kinetic parameters for deamination of 3-substituted aspartic acids*

Substrate	K_m *(mM)*	V_{max} *(x* 10^{-6} *mol* dm^{-3} min^{-1}*)*
(2*S*,3*S*)-3-metylaspartic acid **2**	10.5 ± 0.82	4.8
(2*S*)-aspartic acid **10**	2.37 ± 0.2	654.0
(2*S*,3*S*)-3-ethylaspartic acid **11**	17.08 ± 1.4	292.0

It was suggested that the low rate of deamination of (2*S*)-aspartic acid (**10**), was due to poor orbital alignment of the σ -bonding orbital of the C-H bond with the σ*-antibonding orbital of the C-N bond in the transition state (Scheme 1.10).[55] The ability of the enzyme to accept a range of alkyl groups at the C-3 position of the substrate prompted an investigation into the potential application of the reverse-physiological enzyme reaction[29] in the biosynthesis of novel and synthetically challenging amino acids. A range of substituted fumaric acids were prepared and incubated with ammonia in the presence of the enzyme and the necessary metal ions.[56] In each case, the reaction gave exclusively the product of *anti* addition (Scheme 1.11).[56]

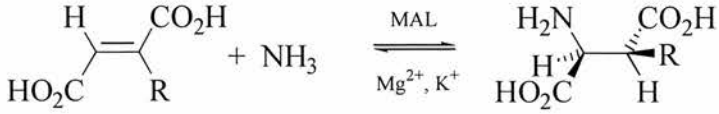

3	R = -CH_3,	**2**	R = -CH_3,
12	R = -H,	**10**	R = -H,
13	R = -Et,	**11**	R = -Et,
14	R = -nPr,	**19**	R = -nPr,
15	R = -iPr,	**20**	R = -iPr,
16	R = -Cl,	**21**	R = -Cl,
17	R = -Br	**22**	R = -Br
18	R = -F	**23**	R = -F

Scheme 1.11: *Amination of 3-substituted fumaric acids by methylaspartase*

The kinetic parameters for the amination of selected substituted fumaric acids are shown in Table 1.3. The value of V_{max} for substrates containing an ethyl (or smaller) substituent at the C-3 position such as for chlorofumaric acid (**16**) and mesaconic acid (**3**) are similar. This indicated that changes in electronic or steric properties of the substrate at the C-3 position do not significantly influence the rate of amination. However, the values of K_m for fumaric acid (**12**) (~23 mM) and mesaconic acid (**3**) (~1.23 mM) differ by one order of magnitude.[56] It was proposed that this resulted from a conformational change in the enzyme due to the alteration in the size of the C-3 substituent, which affects substrate binding interactions.[55]

Table 1.3: *Kinetic parameters for amination of some substituted fumaric acids*

Substrate	K_m *(mM)*	V_{max} *(x* 10^{-6} *mol* dm^{-3} min^{-1}*)*
Fumaric acid **12**	23 ± 2.2	1702
Mesaconic acid **3**	1.24 ± 0.085	894
Ethylfumaric acid **13**	1.05 ± 0.2	583
Chlorofumaric acid **16**	3.52 ± 0.71	382
Bromofumaric acid **17**	2.64 ± 0.53	425
n-Propylfumaric acid **14**	2.1 ± 1.3	4.2

Fluorofumaric acid was apparently found to produce very little aminated product. This behaviour was shown to be due to the fact that ammonia is able to add at either C-2 or the fluorophilic C-3 position (Scheme 1.11, (**18**). However, both the chlorofumaric acid (**16**) and bromofumaric acid (**17**) analogues were moderate substrates for methylaspartase, and were converted into the corresponding halogeno-aspartic acids.[57] In addition bromoaspartic acid (**22**), the product of the amination of bromofumaric acid (**17**), was found to inhibit the enzyme over the time course of the incubation required to produce bromoaspartic acid (**22**). Upon addition of a second aliquot of methylaspartase to the incubation no further inactivation was observed. The chemical species present in the incubation mixture was isolated and shown to be an aziridine dicarboxylic acid (**24**) (Scheme 1.12). A mechanism for its formation was then proposed (Scheme 1.12). It was noted however that the aziridine was incapable of inactivating the enzyme.[57]

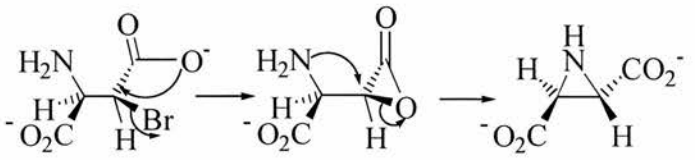

(24) **(26)**

Scheme 1.12: *Aziridine ring formation*

Further investigation showed that inactivation of methylaspartase by bromoaspartic acid (**22**) was greatly reduced in the presence of the natural substrate (2*S*,3*S*)-3-methylaspartic acid (**2**), thus indicating that the inhibitor is directed at or near the active site of the enzyme. The mode of inactivation was believed to be due to alkylation of an active site base through substitution of the bromide as shown in Scheme 1.13.[57]

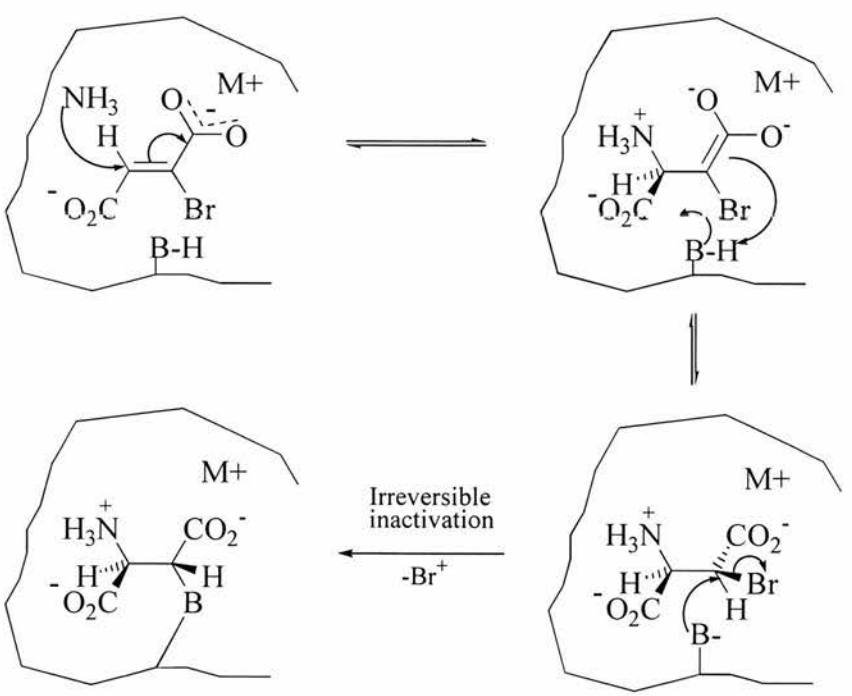

Scheme 1.13: *Alkylation of an active-site base/nucleophile*

1.3.3 *L*-erythro activity

During initial investigations into the substrate specificity of methylaspartase, it was found that the opposite *L*-erythro diastereoisomer of the natural substrate (2*S*,3*S*)-3-methylaspartic acid), (2*S*,3*R*)-3-methylaspartic acid (**25**), was capable of acting as a slow substrate, V_{max} was ~1% of that for the natural substrate (Scheme 1.14).[58, 59] Two possibilities were proposed to explain this observation. Either the elimination of ammonia catalysed by methylaspartase is non-stereospecific, or the enzyme extract used in this experiment contained a racemase activity. This could be due to the presence of a separate, distinct racemase enzyme, or an additional role for methylaspartase (Scheme 1.14).[59]

In an attempt to address this question, the enzyme was incubated with (2*S*,3*R*)-3-methylaspartic acid (**25**) and the mixture was analysed at various time intervals by ^{1}H-NMR spectroscopy.[60] The deamination reaction proceeded rapidly to give mesaconic acid (**3**) and then on a slower time scale the mesaconic acid was re-aminated to afford (2*S*,3*S*)-3-methylaspartic acid (**2**) (Scheme 1.14). This study suggested that the enzyme did not simply racemise the substrate, but was catalysing the *syn* elimination of ammonia from (2*S*,3*R*)-3-methylaspartic acid.[60]

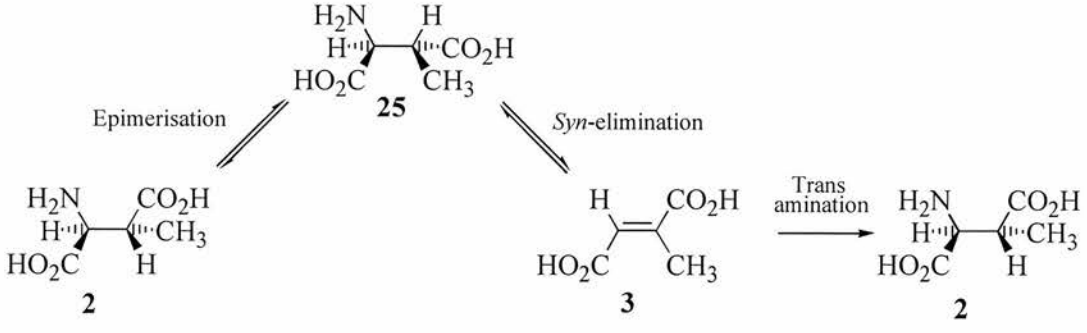

Scheme 1.14: Epimerisation/ syn-elimination mechanism for methylaspartase

1.3.4 Analogues of ammonia

The active site structure of methylaspartase was probed further by carrying out a series of incubations utilising the *retro* physiological reaction in the direction of amination with mesaconic acid and a range of N-nucleophiles.[61] The substrates that were used and the extent of the conversions to the corresponding unsaturated products are shown in Table 1.4.[61]

Table 1.4: *N-nucleophile analogues of ammonia in the retro-physiological MAL reaction*

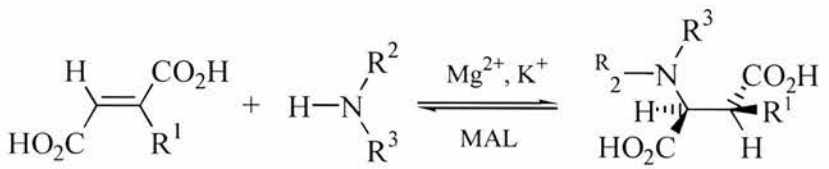

Compound no.	*R^1*	*R^2*	*R^3*	*% Conversion*
26	H	NH_2	H	89
27	CH_3	NH_2	H	91
28	Et	NH_2	H	90
29	^{n}Pr	NH_2	H	90
30	^{i}Pr	NH_2	H	90
31	H	CH_3	H	55
32	CH_3	CH_3	H	54
33	Et	CH_3	H	60
34	^{n}Pr	CH_3	H	0
35	^{i}Pr	CH_3	H	0
36	H	Et	H	5
37	H	CH_3	CH_3	70
38	CH_3	CH_3	CH_3	0
39	H	OH	H	90
40	CH_3	OH	H	90
41	Et	OH	H	60
42	H	OCH_3	H	80
43	CH_3	OCH_3	H	70
44	Et	OCH_3	H	0

Both hydrazine and hydroxylamine proved to be efficient substrate analogues with conversions in excess of 60% (**26**)-(**30**) and (**39**)-(**41**) (Table 1.4). The enzyme was able to tolerate alkyl substituents on either the fumarate analogue (**27**)-(**30**) or the N-nucleophile (**31**) and (**36**), however, if both were present then an alkyl substituent larger than an ethyl group (**34**) and (**35**) could not be processed with methylamine.[61]

In addition, it was shown that methylaspartase was unable able to catalyse the addition of methyoxylamine to methyl fumaric acid (**43**). From these results it was concluded that the N-nucleophile and the C-3 alkyl substituent of fumaric acid appear to occupy similar regions of the enzyme active site, presumably a small hydrophobic pocket.[61] Figure 1.2 shows the anticipated transition states for the addition of dimethylamine to fumaric acid (**45**) and mesaconic acid (**46**).[61]

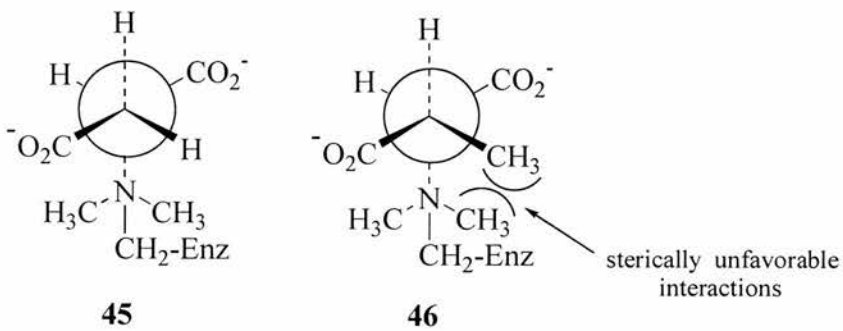

Figure 1.2: *Transition states for addition of dimethylamine to fumaric acid and mesaconic acid*

1.3.5 Mechanistic studies with methylaspartase

In order to distinguish between the three possible elimination mechanisms, a series of early kinetic isotope effect experiments were performed with (2*S*,3*S*)-3-methylaspartic acid (**2**) and (2*S*,3*S*)-[^{2}H]-3-methylaspartic acid.[27, 62, 63, 64] The rate of mesaconic acid formation was measured for both substrates. However, no primary isotope effect was observed for the deamination reaction over the pH range 5.5 – 10.5.[40]

In addition methylaspartase was incubated with mesaconic acid (**3**) and ammonia in deuterium oxide, and in a separate experiment with (2*S*,3*S*)-[^{2}H]-3-methylaspartic acid (**2**) in water.[40] In both experiments, analysis by ^{1}H-NMR spectroscopy showed that hydrogen exchange had occured at the C-3 position of (2*S*,3*S*)-3-methylaspartic acid with hydrogen derived from the bulk solvent.[40] Determination of the rate of exchange (v_{ex}) and the rate of deamination (v_{deam}) showed that exchange was occurring at a faster rate than deamination, at pH 9. These results, in addition to the observation that the enzyme was able to catalyse the elimination of ammonia from (2*S*,3*R*)-3-methylaspartic acid, led to the proposal that methylaspartase operates *via* a step-wise mechanism.[40] This would involve the abstraction of the C-3 proton to form an intermediate carbanion.[27, 40] On the basis of this mechanism it was proposed that the role of the magnesium ion was that of a Lewis acid, enhancing the acidity of the C-3 proton.[48] In a second step elimination of ammonia would take place to form mesaconate.[48]

The effect on the rate of exchange at varied pH was studied and it was shown that the exchange reaction reaches a maximum at pH 7.8.[27]

1.3.5.1 Identification of an active-site base

Methylaspartase was shown to be readily inhibited by NEM (MAL 17) and (*p*-CMB).[42] The enzyme was completely protected against inactivation by the inclusion of the substrate in the incubation.[48] This led to the proposal that this involved shielding of an enzyme residue, which lies near the C-3 carbon of the substrate. On the basis of the pH rate profile for the exchange reaction (optimum at pH 7.8) it was proposed that a thiol group was the nucleophile responsible for abstraction of the C-3 proton.[27]

Labelling experiments were also conducted using *N*-[1-^{14}C]-ethylmaleimide. Methylaspartase was treated with the radiolabelled inhibitor and subsequently digested using the protease enzyme, trypsin to afford a total of 55 peptides, eight of which had been radiolabelled. It was therefore proposed that 8 cysteine residues had been covalently modified by S-alkylation by NEM (**30**) (Scheme 1.15).[43] In a repeat experiment the enzyme active-site was saturated with excess substrate before addition of the unlabelled NEM. Unreacted NEM and substrate were removed before treatment of the enzyme with [^{14}C]-NEM.[43]

After tryptic digestion one radiolabelled peptide was isolated. The total amino acid composition of the peptide was determined from acid hydrolysis. The results showed the presence of ~40 amino acid residued in the peptide, one of which was an unusual amino acid and was attributed to a half cysteine residue (**48**) (Scheme 1.15). It was presumed that this resulted from the product of hydrolysis of a Cys-NEM adduct (**47**).[43] This further supported the proposal of a cysteine residue being at the active-site.

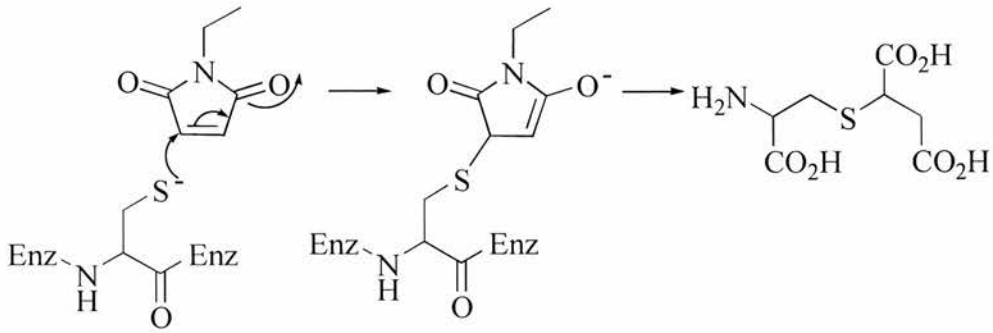

47 **48**

Scheme 1.15: *Modification of cysteine residue with N-ethylmaleimide*

In a recent study, the properties of the active site of methylaspartase were further investigated by labelling experiments using NEM.[65] NEM showed simple saturation kinetics, with a K_s of 34.5 ± 5.4 mM at pH 7.0.[65] From the pH dependence of NEM inhibition it was observed that the enzyme titrates itself at pH 9.3 into a form which can then react with NEM. However, NEM was found not to ionise in the pH range of this study, indicating that an acid with a pKa of 9.3 must be deprotonated in order to react with NEM. Magnesium was found to be an activator and increased the rate of NEM inactivation by ~ 10-fold (K_s = 2.67 ± 0.37 mM). It was suggested that the increased rate of inactivation in the presence of magnesium resulted from an increase in affinity for the enzyme and not from an increase in the rate of alkylation.[65]

In order to determine the sites of modification by NEM, methylapartase was protected with substrate and then treated with unlabelled NEM.[65] Excess unreacted substrate and NEM were removed prior to incubation with *N*-[2-^{3}H]-ethylmaleimide. The inactive enzyme was digested with trypsin and analysed by HPLC. Edman degradation analysis, highlighted the presence of one major peptide with the sequence ^{350}ANGMGAYXGGTZNETNR^{366}.[65] Residue 8 was shown not be a cysteine residue.

However, residue 361 contained radioactivity and further analysis suggested the presence of a modified amino acid. The peptide was shown to possess two cysteine residues, Cys-357, which was not radiolabelled and Cys-361, which had been radiolabelled.[65]

Thus it was concluded that in the presence of magnesium, NEM binds to the enzyme-Mg^{2+} complex and this results in alkylation of one of the catalytically essential acid-base groups. It was proposed that this was Cys-361, which attacks NEM at a position analogous to the C-3 position of the substrate.[65]

1.3.5.2 Active-site dehydroalanine residue of methylaspartase

A deduced amino acid sequence for the protein was obtained from the sequence of the *mal* gene and this was used to map the peptide, which had been isolated in the studies with NEM.[46]

The total amino acid content of the radiolabelled peptide, was matched against the deduced amino acid sequence of the enzyme. There appeared to be no correlation with peptides containing cysteine residues.[46] However, an excellent match was obtained with a 37-mer peptide Lys-147 to Lys-183, which contained a serine at position 173. It was proposed that this serine or a derivative was the reactive species with respect to NEM. It was suggested that in order for Ser-173 to undergo reaction with NEM the residue must first undergo post-translational dehydration to afford a dehydroalanine residue. Reaction of this intermediate with NEM could then occur by two mechanisms outlined in Scheme 1.16.[65]

The first involving electrophilic attack of the imine form of dehydroalanine onto the double bond of NEM (mechanism A, Scheme 1.16). The second reaction involves initial addition of ammonia to the double bond of dehydroalanine to form lysine (R = -$(CH_2)_4NH_2$), which can then attack NEM (mechanism B, Scheme 1.16).[65]

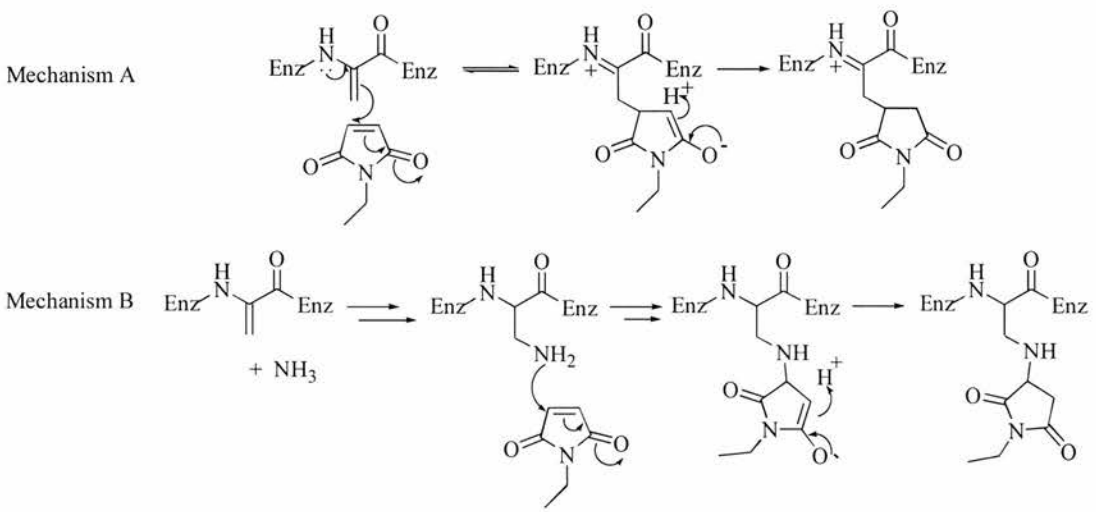

Scheme 1.16: *Proposed mechanisms for the reaction of dehydroalanine residue with NEM*

The peptide containing the SGD motif of amino acids, which was proposed to have been modified by NEM was also observed in HAL[66, 67] and PAL.[22] In both these enzymes (see Sections 1.4 and 1.5) a dehydroalanine residue derived from serine has been implicated in the mechanism of the reaction and it was suggested that the serine from the SGD motif was a probable candidate for dehydration.

In order to probe the reaction of dehydroalanine with N-nucleophiles such as various amines, a series of chemical model studies were carried out using a range of synthetically prepared dehydroalanine containing peptides (Scheme 1.17).[68] In each case, a dehydroalanine model was incubated with propylamine. The results showed that by altering the electron withdrawing and donating properties of the neighbouring groups

(protecting groups on the C- and N-termini of the model peptide) and thus the electronic properties of the dehydroalanine residue, the regioselectivity of addition of the amine could be controlled, with addition occurring at either the α or β-position of the imine group (Scheme 1.17).[68]

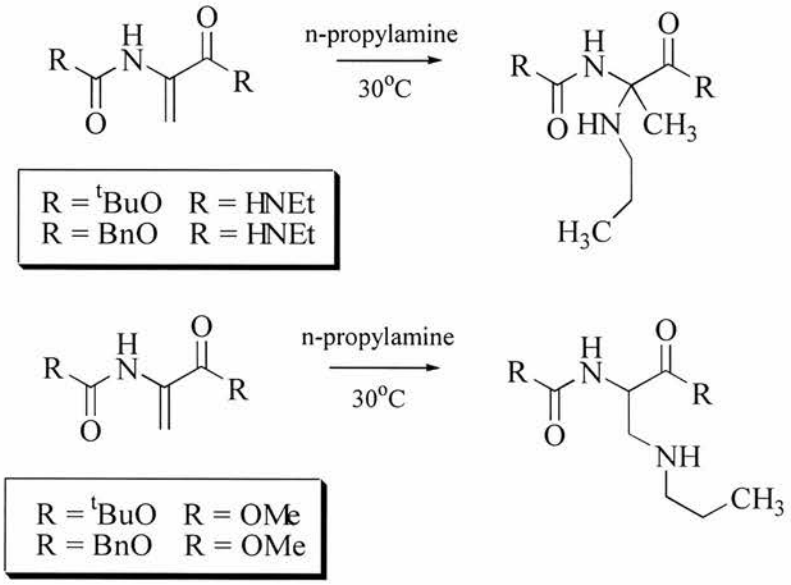

Scheme 1.17: *Reaction of synthetic peptides with n-propylamine*

1.3.6 Recent studies on the mechanism of methylaspartase

Recent investigations into the mechanism of methylaspartase have focused extensively on the use of kinetic isotope effects. In complete contrast to previous findings, a deuterium isotope effect of 1.7 on V and V/K was observed with (2*S*,3*S*)-[^{2}H]-3-methylaspartic acid at pH 9.[54] This result therefore indicated that C-H bond cleavage is at least partially rate limiting. Two possible explanations for the previous lack of an observed primary kinetic isotope effect were proposed. The first was that the C-3 deuterated substrate which was used in the early studies, may have contained only 87%

deuterium at C-3.[54] However, this explanation alone was not sufficient to explain the total masking of the isotope effect. The second explanation concerned the conditions under which the original experiment was carried out. Although the precise conditions had not been reported by previous workers, it seemed most likely that the experiment had been conducted at a potassium ion concentration of at least 50 mM.[69]

The influence of potassium ion concentration was then studied and it was demonstrated that at high concentrations the kinetic isotope effect was completely suppressed (V and $V/K = 1$).[69] Table 1.5 shows the dependence of the primary deuterium isotope effect upon K^+ ion concentration.

Table 1.5: *Potassium ion dependence on primary deuterium isotope effects*

KCl (mM)	$^{D}(V/K)$
0.2	1.27
1.6	1.68
4.0	1.21
50.0	1.00

These results suggested that potassium ion in its action as an activator of methylaspartase, was able to increase the commitments to the isotopically sensitive step (C_f is the forward commitment and C_r is the reverse commitment). Having established the existence of a significant primary isotope effect, the stepwise carbanionic mechanism was challenged and the effect of C-N bond cleavage on the kinetic profile of the reaction was

studied.[70] The ^{15}N isotope effect for (2*S*,3*S*)-3-methylaspartic acid was determined by measuring the ratio of $^{15}N/^{14}N$ in the substrate and in the ammonia product after ~ 17% of the deamination reaction had proceeded. The ^{15}V (^{15}N-isotope effect on *V*) at pH 6.5 and pH 9.0 were 1.0255 ± 0.0011 and 1.0246 ± 0.0013, respectively. These significant values of ^{15}V suggested that C-N bond cleavage was at least partially rate-limiting.[70] However, both a balanced step-wise and a concerted mechanism would be expected to show an isotope effect on V/K for both C-H and C-N bond cleavage steps.

In order to distinguish between the two possible mechanisms, the ^{15}N-isotope effect for C-N bond cleavage was measured in the presence and absence of deuterium at C-3 of the substrate (double fractionation studies).[70] In both deuterium oxide and water at pH 6.5, the deuterated substrate showed a value for $^{15}(V/K)$ of 1.0417 ± 0.0009 compared to the value for the non-deuterated substrate ($^{15}(V/K)$ = 1.0225 ± 0.0011).[70] It was therefore concluded that the presence of a deuterium atom at C-3 increased the significance of C-N bond cleavage in a manner consistent with a concerted mechanism where both the C-H and C-N bonds are broken in the same step.[70]

Scheme 1.18 shows the proposed mechanism for methylaspartase on the basis of this kinetic data.

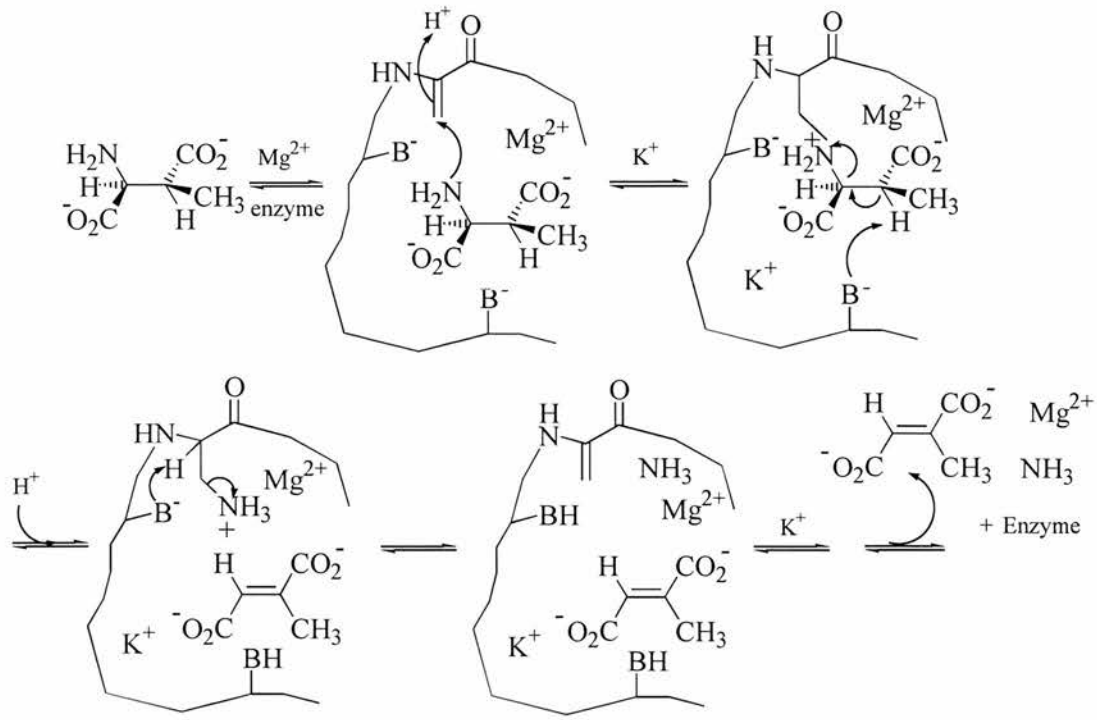

Scheme1.18: *Proposed mechanism for the concerted reaction of methylaspartase*

The first step following binding of the substrate and both metal ion co-factors involves conjugate addition of the amine moiety of the substrate to the dehydroalanine residue. An active-site base then abstracts the C-3 proton and concerted cleavage of the C-N bond takes place to form mesaconic acid and the covalent amino-enzyme adduct. In the subsequent steps, the amino-enzyme is protonated and deaminated to afford the product complex. The products of the reaction are then released to regenerate the free enzyme (Scheme 1.18).[69]

1.3.7 Inhibitors of methylaspartase

A range of 1-substituted cyclopropane 1,2-dicarboxylic acids were incubated with methylaspartase and all were found to be inhibitors of the enzyme.[71] The most potent inhibitor (1*S*,2*S*)-1-methylcyclopropane 1,2-dicarboxylic acid (**49**) (Fig. 1.3) (K_i = 20 μM) was thought to act as a transition state analogue for the deamination reaction step as it is able to mimic the geometry and bond hybridisation expected for the transition state of a concerted elimination mechanism. This finding is in accord with the proposed concerted elimination mechanism.[71]

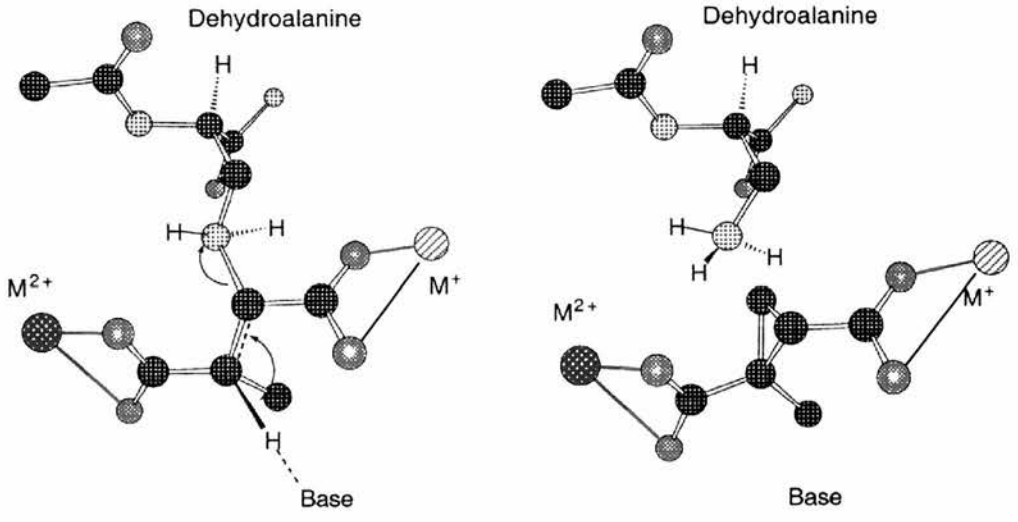

49

Figure 1.3: *A) Expected transition state for C-N bond cleavage of substrate. B)Possible interaction of (1*S*,2*S*)-1-methyl-1,2-cyclopropanedioic acid with methylaspartase*

1.3.8 Alternative sources of methylaspartase

Methylaspartase from three different strains of facultative anaerobes from soil, *Citrobacter strain sp.* YG-0504, *Morganella morganii* YG-0601[72] and *Citrobacter amalonaticus* YG-1002 [73, 74] have been isolated, characterised and compared to the wild-type enzyme from *Clostridium tetanomorphum*.[57] All three enzymes were reported to be homo-dimers with a sub-unit mass of 40 kDa, 44 kDa and 42 kDa respectively.

All three enzymes are very similar to the *Clostridial* enzyme[74] and share greater than 60% sequence identity.[72] The biochemical properties of the enzymes from *Citrobacter sp.* and *Morganella morganii* have been studied in some detail and the results are presented in Table 1.6.[72]

Table 1.6: *Biochemical properties of methylaspartase from various soil bacteria*

Property	*Citrobacter sp.*	*Morganella*	*C. tetanomorphum*
Sub-unit weight	40,000	44,000	45,539
No. sub-units	2	2	2
pH optimum :			
deamination	9.7	9.7	9.7
amination	8.0	8.5	9.0
K_m (mM) :			
(2S,3S)-3-Measp **(2)**	1.0	2.95	2.37
Mesaconic acid **(3)**	0.61	0.60	1.24

The enzymes shown in Table 1.6 have similar metal ion co-factor requirements and substrate specificity, with one exception. The enzymes from *Citrobacter* and *Morganella* were able to catalyse the reversible amination-deamination of (2*R*,3*S*)-3-

chloroaspartic acid to chlorofumaric acid, however they could only catalyse the amination of fumaric acid and not the deamination of aspartic acid.[72]

The *Clostridial* enzyme on the other hand is able to catalyse the amination of chlorofumaric acid[57] and the reversible deamination of (2*S*)-aspartic acid to fumaric acid.[72] This suggests that whilst the enzymes from other bacterial sources are extremely similar, there are subtle differences in the active site structure, allowing for changes in the substrate specificity.

1.4 Histidine ammonia-lyase

The enzyme Histidine ammonia-lyase (Histidase, HAL) (EC 4.3.1.3),[26] catalyses the first step in the non-oxidative metabolism of (2*S*)-histidine (**50**) to (2*S*)-glutamic acid (**1**) and formamide (Scheme 1.19).[4] Histidase has been isolated from bacterial systems including *Pseudomonas putida*[75] *P. fluorescens,*[76, 77], *P. acidovorans,*[75] *Bacillus subtilis*[78, 79], *Streptomyces griseus*[80, 78] and also from mammalian sources.[80]

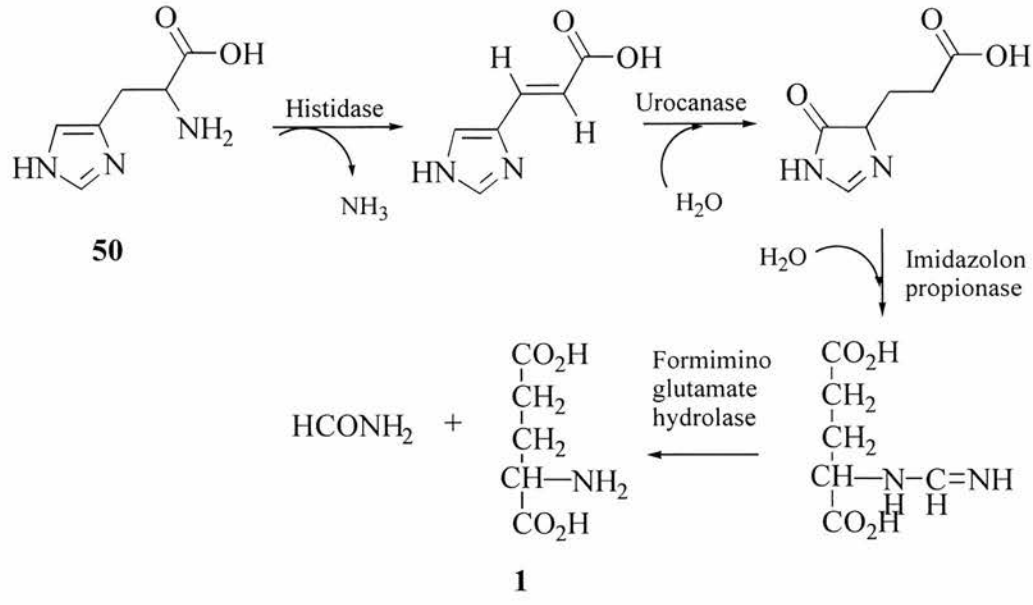

50 **1**

Scheme 1.19: *Pathway for histidine degradation*

The human genetic disease histidinemia[81] is characterised by a hereditary absence of this enzyme from both the liver and the epidermis and as a consequence, the plasma concentration of (2*S*)-histidine (**50**) becomes abnormally high.[81] This is accompanied by urinary excretion of the amino acid, imidazolylpyruvic acid and other metabolites.[81, 82] Long-term studies into the disorder have shown that in the majority of cases it is a benign metabolic disease which does not require treatment.

The enzymes isolated from both mammalian and bacterial sources all appear to have a homo-tetrameric structure with a sub-unit mass of ~ 53,000 Da. Comparison of the inferred amino acid sequence of histidase isolated from *P. putida* and *B. subtilis* show 41% and 43% amino acid identity with that isolated from rat liver (Table 1.7).[83]

Table 1.7: *Percent amino acid identity in pairwise comparisons of histidase sequence*[80]

	S. griseus	*P. putida*	*B. subtilis*	*Rat*
S. griseus	100%	38%	38%	37%
P. putida		100%	42%	42%
B. subtilis			100%	42%
Rat				100%

The high level of sequence identity observed between histidase isolated from various bacteria indicates that the enzyme is well conserved.[75]

1.4.1 Mechanism of Histidase

Initial mechanistic studies of histidase involved incubation of (2*S*)-histidine (**50**) with histidase in tritiated water (Scheme 1.19).[24] Both the product urocanic acid and the remaining substrate were isolated and the ^{3}H incorporation determined. It was found that ^{3}H had only been incorporated into the substrate pool.[24]

Subsequent chemical degradation of the radiolabelled (2*S*)-histidine showed that the ^{3}H was bound to the C-3 atom of the substrate. Incubation of this labelled substrate (2*S*)-([3-^{3}H]-histidine) with histidase and analysis of the reaction products for radiolabel incorporation showed that the urocanic acid product was unlabelled. These results strongly supported the stereoselective abstraction of the pro R hydrogen at C-3, resulting in either ammonia elimination to afford urocanic acid or hydrogen exchange with the bulk solvent.[24]

In an independent study it was shown that the reaction equilibrium favored the forward reaction very strongly as only with very long incubations could any amination of urocanic acid be observed.

In order to determine whether the mechanism of the elimination reaction catalysed by histidase was concerted or stepwise, analogues of (2*S*)-histidine labelled with deuterium were tested as substrates. Incubation of (2*S*)-[3,3,5'-$^2H_3$]-histidine (**51**) with histidase resulted in loss of 44% of the C-5' deuterium label.[76]

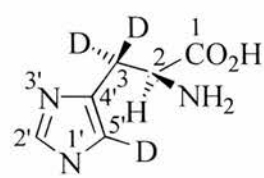

(51)

(2S)-[3,3,5'-$^2H_3$]-histidine

When unlabelled (2*S*)-histidine was incubated with histidase in deuterium oxide, only 20% incorporation of deuterium at C-5' was observed. The observation that exchange occurred at C-5' led to the proposal that histidase is unlikely to operate *via* a concerted mechanism.[76] From these studies a step-wise $E1_{cb}$ mechanism for the elimination of ammonia from (2*S*)-histidine was proposed (Scheme 1.20).[76] The stereospecific abstraction of the C-3 proton results in a carbanion on C-3, which can be delocalised onto the imidazole ring.[76]

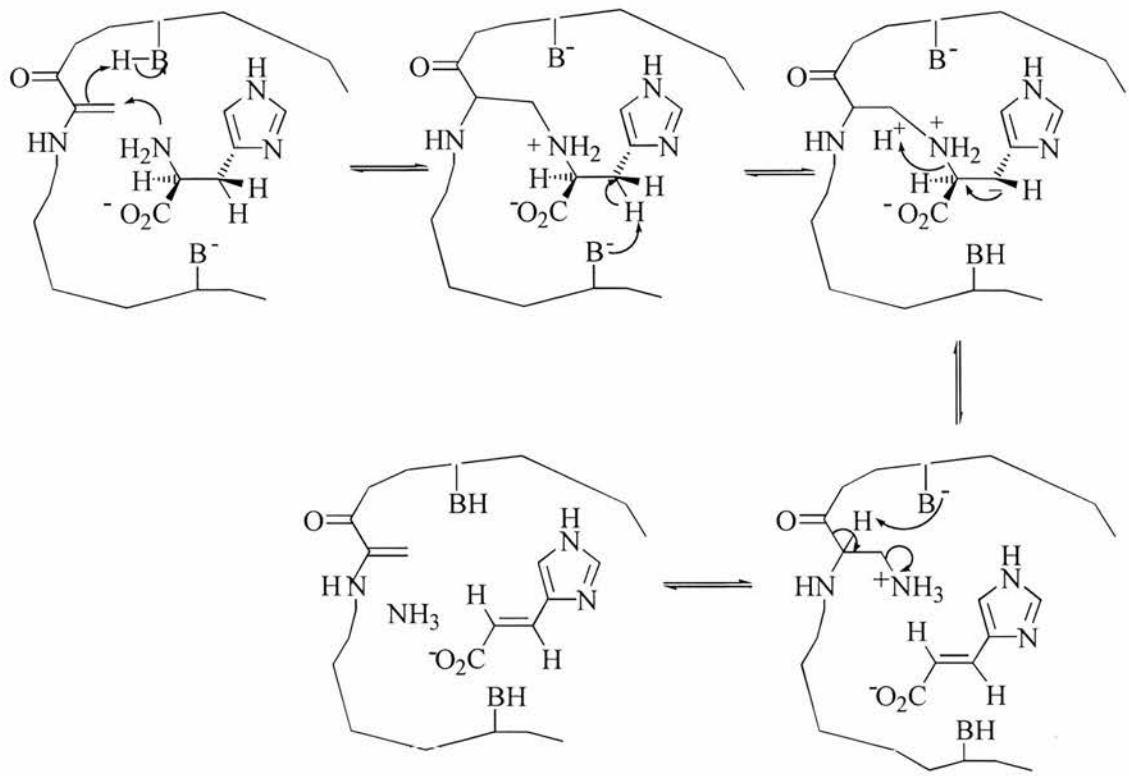

Scheme 1.20: *$E1_{cb}$ mechansim for histidine ammonia-lyase*

1.4.2 Inhibitors of Histidase

In support of the proposed mechanism it was found that (2*S*)-cysteine in the presence of dioxygen, at pH 10 or greater, resulted in complete inactivation of histidase.[84] Under these conditions the inactive enzyme was shown to generate a strong UV chromophore with λ_{max} of 340 nm. However, enzyme, which had been treated with substrate, sodium borohydride, potassium cyanide or sodium sulfite, followed by (2*S*)-cysteine and dioxygen was inhibited but failed to show an absorbance at 340 nm by UV spectroscopy.[84] This indicated that modification by the two sets of inhibitors was taking place at the same position in the active site.

The peptide containing the chromophore was isolated from a digestion of modified protein treated with trypsin and the endoproteinase Glu-C. The amino acid sequence of the peptide was found to be Gly-Ser-Val-Gly-Ala-Xaa-Gly-Asp (mapped to position 138-145). The modified residue was shown by comparison with the inferred amino acid sequence to be Ser-143.[84]

In a series of experiments designed to monitor the effects of site specific chemical modifying agents on the activity of histidase, it was discovered that nucleophiles such as nitromethane,[25] ^{14}C-potassium cyanide and tritiated sodium borohydride were capable of irreversibly inactivating the enzyme.[66] In order to rationalise this observation, it was suggested that the active site contained an electrophilic residue and it was proposed that this was a dehydroalanine derived from dehydration of a serine.[67, 85]

Evidence to support this observation was obtained from studies on the mutant S143A and the double mutant A142S/S143A. Both mutants were found to have lost all activity (S143A K_m = 7.5 mM, V_{max} = 0.0214 IU/ mg).[86, 87]) V_{max} for the S143A mutant was 110-fold less than for the wild-type enzyme. It was proposed that the lack of observed activity was due to the inability of the enzyme to produce the dehydroalanine residue at position 143.[67, 87] However, in the mutant S143C, full catalytic activity was observed (V_{max} = 22.2 mol dm^{-3} min^{-1}, K_m = 5.4 mM) and the mutant enzyme had similar kinetic properties to the wild-type enzyme *from P. putida* (V_{max} = 28.0 mol dm^{-3} min^{-1}, K_m = 4.0 mM). The results indicated that cysteine was able to eliminate (hydrogen sulfide) in order to generate the catalytically essential dehydroalanine residue in an analogous manner to serine dehydration.[88]

To test this hypothesis, a series of histidase mutants, S143G and S143T, were prepared. The mutant enzymes were tested with (2*S*)-histidine as the substrate and showed similar K_m values to the wild-type enzyme, but V_{max} values were 5310 and 53,100 times lower, respectively (Table 1.8).[86]

Table 1.8: *Kinetic values for histidase mutants with (2S)-histidine*

Histidase	*K_m (mM)*	*V_{max} (IU/ mg)*
Wild-type *(P. putida)*	5.3	25
mutant S143G	5.3	<0.01%
mutant S143T	not accesible	<0.01%

Interestingly, however, the substrate analogue 5'-nitrohistidine (**52**) was processed at the same rate by the two mutants as observed for the wild-type enzyme (K_m = 7.7 mM, V_{max} = 0.85 [IU/ mg]).[86]

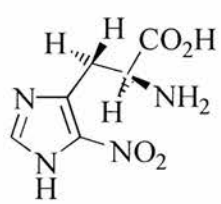

52 *(2S)-5'-nitrohistidine*

The reason for the observed activity was attributed to the lowered pK_a of the C-3 proton in the (2*S*)-5'-nitro-histidine analogue (**52**). In this case the pK_a at C-3 is lowered sufficiently for the active site base to be able to remove the proton without the additional

activation obtained by alkylation of the imidazole ring.[86] This was further supported by the observation that (2*S*)-histidine showed competitive inhibition against the 5' nitro analogue (K_i 5.3 ± 0.4 mM) with the S143G mutant.[86]

In the light of these results a novel mechanism was proposed for the histidase reaction (Scheme 1.21).[89, 90, 91] Following binding of the histidine substrate at the active site of the enzyme the C-5 carbon atom of the imidazole ring attacks the dehydroalanine residue in a conjugate Michael style mechanism. The resulting intermediate (**53**) involves the formation of a positive charge on the 3'-nitrogen of the imidazole ring. Inductive effects, which act to stabilise this positive charge, result in the build up of a partial positive charge at the C-β carbon atom which leads to an increase in acidity of the C-3 proton. An active site base is then able to remove the acidic proton which in a subsequent step allows release of the α-amino group to afford the deaminated product.[86, 90]

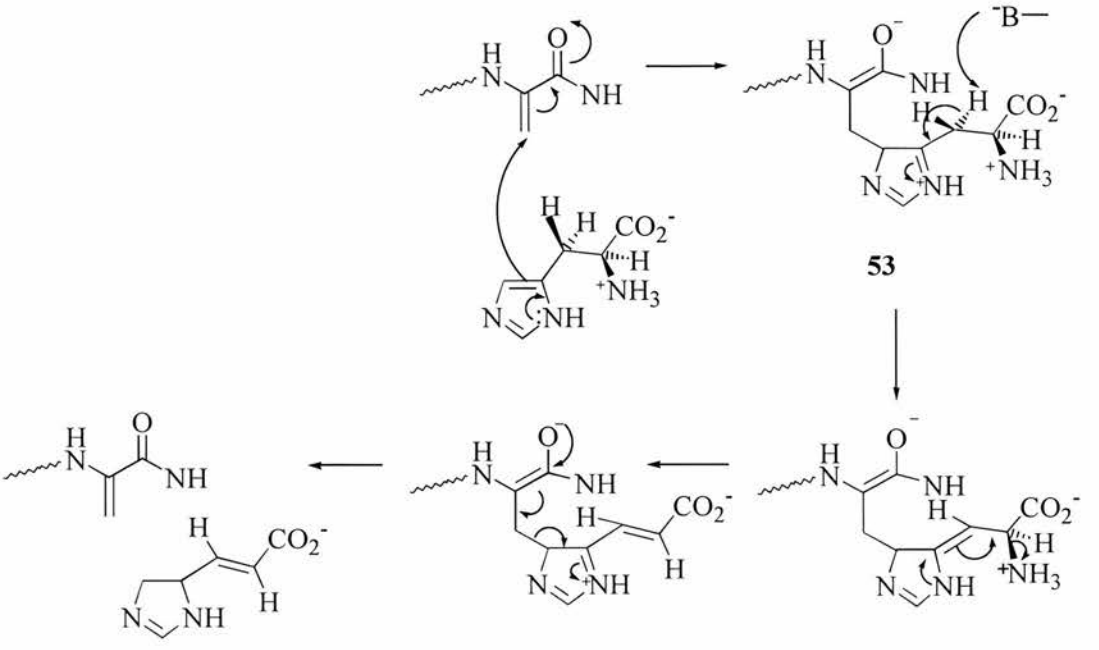

Scheme 1.21: *Proposed mechanism of HAL involving attack of imidazole on dehydroalanine*

1.4.3 Crystal structure of histidase

Preliminary attempts to crystallise the wild-type histidase from *Pseudomonas putida* were unsuccessful due to problems associated with protein precipitation at low pH and non-specific aggrcgation.[92] However, the C273A mutant was shown to be homogenous and not susceptible to precipitation or aggregation and hence high quality crystals of the mutant were prepared.[92]

The crystal structure of histidase was subsequently determined to 2.1 Å resolution. Each of the sub-units was found to be composed of two domains, an N-terminal domain consisting of, eight α-helices and four short β-strands and a C-terminal domain predominantly composed of 11 α-helices.[92]

All of the mechanistic studies including numerous mutagenesis studies and inhibitor studies have suggested the involvement of a dehydroalanine residue in the mechanism of elimination (see Section 1.4.2). An inspection of the electron density map for the active site revealed that it was not consistent with a dehydroalanine residue at position 143. However, an unusual heterocycle was observed (**55**) (4-methylidene-imidazole-5-one, MIO) which contained an olefinic group (Scheme 1.22). It was proposed that the formation of this residue occurs through the elimination of two water molecules from an internal tripeptide Ala-Ser- Gly (142-144) (**54**).[92]

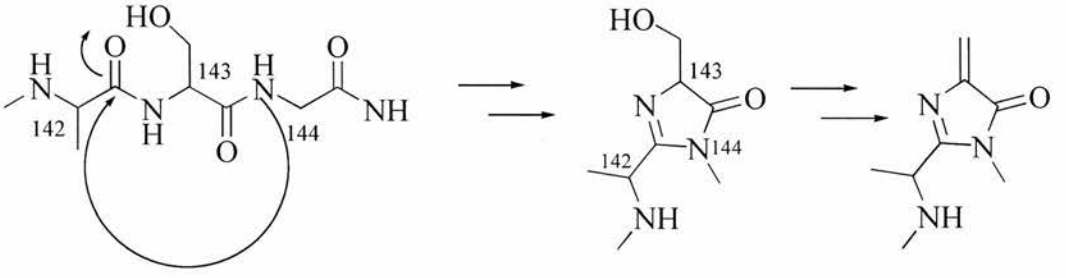

54 **55**

Scheme 1.22: *Proposed formation of 4-methylidene-imidazole-5-one residue at the active-site of histidase*

The presence of an unsaturated heterocyclic catalytic residue is consistent with all of the results described above and does not contradict the mechanism shown in Fig. 1.21. The olefin in the new catalytic heterocycle can behave in a chemically similar manner to that of the previously proposed dehydroalanine residue.[92, 93]

The observation that mutants S143G and S143A resulted in inactive enzyme has subsequently been attributed to their inability to undergo transformation to the MIO group (**55**) (Scheme 1.22). In contrast, mutation of Ser-143 to cysteine afforded an

enzyme which retained all catalytic activity, since the MIO group can be formed in this case through desulfuration of cysteine.

In labelling studies with both [^{3}H]-sodium borohydride and [^{14}C]-potassium cyanide (followed by acid hydrolysis) [^{3}H]-alanine and [^{14}C]-aspartic acid were isolated respectively.[86] Despite being originally attributed to reaction with dehydroalanine, these results were also consistent with an MIO group. It was expected that the modified MIO heterocycle would also degrade, upon acid hydrolysis to give aspartic acid. Scheme 1.23 shows a modified mechanism for histidase including a role for the alternative unsaturated catalytic residue active-site residue.[92]

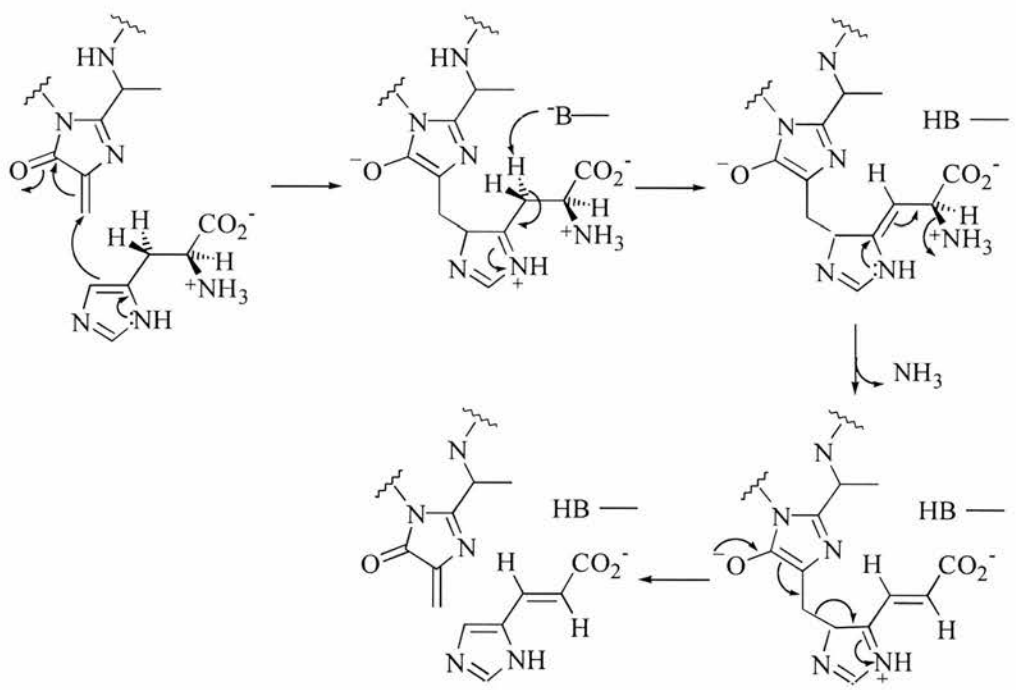

Scheme 1.23: *Proposed catalytic mechanism for histidase incorporating the MIO catalytic residue*

1.5 Phenylalanine ammonia-lyase

Phenylalanine ammonia-lyase (PAL) (EC 4.3.1.5) catalyses the reversible elimination of ammonia from (2*S*)-phenylalanine (Scheme 1.24, **(56)**) to give *trans*-cinnamic acid (**57**) (Scheme 1.24).[23, 94]

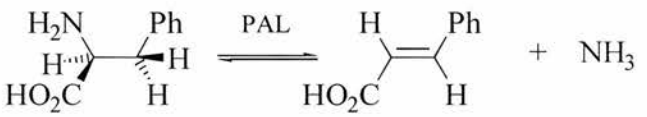

56 **57**

Scheme 1.24: *Reaction catalysed by phenylalanine ammonia-lyase*

The enzyme has been observed in potato, sweet potatoes,[21] maize, [95] wheat shoots,[23] yeasts such as *Rhodotorula glutinis*,[96] fungi, certain algae such as *Dunaliella marina* and *E. coli* [97, 98] There are no reports of PAL activity in mammalian systems and only one study of the enzyme from a prokaryotic organism, *Streptomyces verticillatus* has been reported.[94]

PAL plays a major role in the biosynthesis of polyphenol compounds such as flavonoids and phenylpropanoids in plants.[94, 99] In sweet potato roots this activity is induced in response to various stimulii, such as light, wounding or fungal infection.[100] PAL activity reaches a maximum after external stimulation and then declines as a result of an inactivation. However, this system is not clearly understood.[100]

In mammals phenylalanine, which is obtained from exogenous sources, is essential for neoplastic cell growth.[21] PAL metabolises phenylalanine and as a result has been observed to inhibit the growth of neoplastic cells in mice, which have been inoculated with leukemia.[21, 101, 102] The therapeutic benefits of PAL have also found

applications as a biosensor for detecting levels of phenylalanine in human serum.[98] Phenylketonuria (PKU) a human genetic disease, results in the accumulation of phenylpyruvate in the urine and if the condition remains untreated it can result in impaired cognitive development in infants.[103, 104] Treatment from birth with a low phenylalanine diet is often effective in preventing the disease. PAL offers an efficient way of monitoring the levels of phenylalanine in the blood, thus allowing treatment to be carried out when necessary.

PAL from yeast, maize and potato was shown to have a homo-tetrameric structure with a sub-unit molecular mass of 83 kDa.[105] Labelling experiments with ^{14}C-nitromethane indicated that there are two active sites per tetramer.[94]

1.5.1 Substrate specificity of phenylalanine ammonia-lyase

The enzyme isolated from potato, was found to be specific for (2*S*)-phenylalanine (K_m = 0.17 mM, V_{max} 0.63 IU/ mg) whereas, those from maize and the yeast, *Rhodotorula glutinis*, were shown to have a broader substrate specificity and as such could accept alternative substrates, such as 3-(1,4-cyclohexadienyl)-*(2S)*-alanine (**58**) with a K_m of 0.55 mM with PAL from yeast.[106]

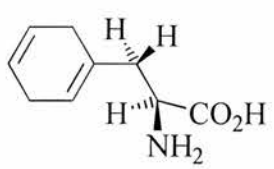

58 *3-(1,4-cyclohexadienyl)-(2S)-alanine*

Wheat shoots containing PAL were found to be able to convert a number of ring-substituted phenylalanine analogues such as *p*-fluorophenylalanine (**59**), *p*-hydroxyphenylalanine (**60**) and *p*-methylphenylalanine (**61**) to the corresponding cinnamic acid (Table 1.9).[23]

Table 1.9: *Alternative substrates for phenylalanine ammonia-lyase*

Substrate	*Relative Conversion (%)*
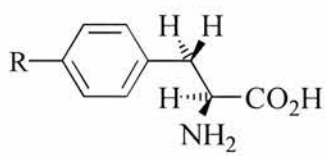	
56; R = H	100
59; R = F	94
60; R = OH	16
61; R = CH_3	6

The amino acid (2*S*)-tyrosine (**60**) was shown to act as a substrate for the enzymes from *Rhodotorula glutinis*[107] and maize[108] *with a* K_m of 0.03 mM at pH 8.7 in both cases.

Cyclooctatetraenyl-acrylic acid (**62**) was tested as a substrate for phenylalanine ammonia-lyase in the reverse amination direction.[109] V_{max} was found to be extremely low at 0.0038 IU/ mg (0.6% of that for (2*S*)-phenylalanine) and the value of K_m at 22.6 mM was almost 30 times higher than for the natural substrate, (2*S*)-phenylalanine (K_m = 1.0 mM). This suggested that both binding and turn-over were affected by increased size of

the side-chain ring. It was proposed that this was due to the puckered nature of the cyclooctatetraenyl (COT) ring (**62**) as opposed to the flat structure of the phenyl ring for the natural substrate.[109]

62 *Cyclooctatetraenyl-acrylic acid*

It was suggested that in order for the COT ring to bind in the phenyl pocket the substrate analogue would be forced into a geometry that would disfavour electrophilic attack at the dehydroalanine residue.[109]

Three isomers of pyridyl-(2*S*)-alanine (**63**), (**64**) and (**65**) were also prepared and found to be excellent substrates for PAL with kinetic parameters as reported in Table 1.10.[109]

Table 1.10: *Pyridyl-(2S)-alanine analogues, substrates for PAL*

Substrate	$V_{max}/ V_{max(2S)\text{-}Phe}$	$K_m/ K_{m\ (2S)\text{-}Phe}$
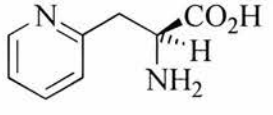 **63**	0.8	22.0
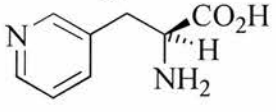 **64**	2.4	41.6
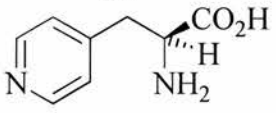 **65**	1.8	12.1

The pyridyl isomers were found to have higher K_m values than the natural substrate (K_m = 1.0). This was attributed to the increased polarity of the pyridine ring compared to the phenyl ring of the natural substrate, which results in a decrease in the hydrophobic interactions thought to be important in substrate binding.[109]

1.5.2 Inhibitors of phenylalanine ammonia-lyase

The substrate analogues, 2-aminoindan-2-phosphonic acid (**66**) and (2*S*)-2-oxyamino-phenylalanine (**67**) and which were both found to act as competitive inhibitors of PAL with K_i's of 1.4 nM and 80 μM, respectively (Table 1.11).[110] In blocking phenylpropanoid synthesis in plant cells and tissues these inhibitors have potential applications as pesticides.[111]

Table 1.11: *Inhibitors of phenylalanine ammonia-lyase*

Inhibitor	K_i (mM)
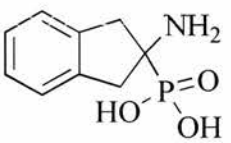 **66**	0.08
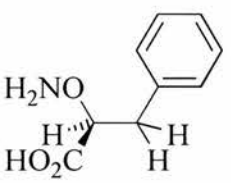 **67**	1.4×10^5

In a recent study metacreosol (**68**) and glycine (**69**) were tested as potential inhibitors of PAL. Independently both metacreosol with a K_i of 17 mM and glycine with a K_i of 20 mM proved to be weak inhibitors of PAL.[109] However, simultaneous addition of these two components to the enzyme led to synergistic inhibition and an increased K_i of 0.89 mM was observed (Scheme 1.25). It was proposed that the two molecules co-occupy the active site of PAL mimicking 3-hydroxphenylalanine (*m*-tyrosine), a known inhibitor of the enzyme.[109]

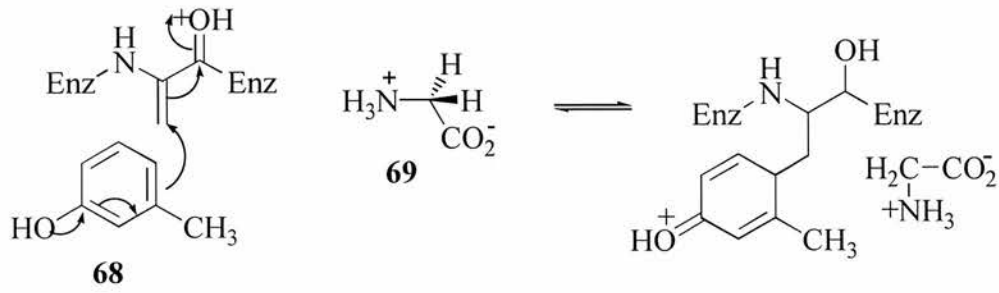

Scheme 1.25: *Synergistic inhibition of PAL by metacreosol and glycine*

1.5.3 Kinetics of the phenylalanine ammonia-lyase reaction

Preliminary kinetic evaluation of the PAL catalysed reaction showed that the value of K_m and V_{max} were dependent upon the concentration of the substrate, (2*S*)-phenylalanine. The K_m increased from 0.038 mM to 0.26 mM and the apparent V_{max} doubled, with concentrations of substrate ranging from 0.01 mM to 6.7 mM.[112] From this study it was concluded that the kinetics of the PAL reaction with (2*S*)-phenylalanine could not be described by the Michaelis-Menten equation.[112] However, Michaelis-Menten kinetics were observed with (2*R*)-phenylalanine, which was shown to act as a competitive inhibitor of PAL.[112]

In order to determine whether the reaction catalysed by PAL was concerted or step-wise kinetic studies were carried out using [3-$^2H_2$]-phenylalanine and (2*S*)-phenylalanine.[105] A small deuterium isotope effect (product of primary (*pro-S* hydrogen) and secondary (*pro-R* hydrogen) isotope effects) of 1.15 was observed on V and V/K with [3-$^2H_2$]-phenylalanine between pH 7.5 and 10.5. This result suggested that the isotope effect on V and V/K was pH independent.[105]

A small ^{15}N-isotope effect of 1.0146 ± 0.0005 on V/K was also observed with (2*S*)-phenylalanine containing natural abundance ^{15}N.[105]

As a result of the small deuterium isotope effect observed with (2*S*)-phenylalanine, it was suggested that the C-3 proton was highly acidic and this led to high commitments to the proton removal step. An alternative substrate, with a less acidic C-3 proton, was sought. The partially ring-saturated analogue, dihydrophenylalanine (**70**) was chosen since the K_m was 122 ± 4 μM (Phenylalanine K_m = 216 μM) and the V_{max} only 7% relative to (2*S*)-phenylalanine.[105]

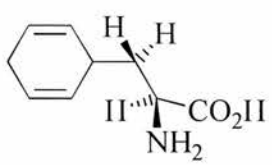

70 *Dihydrophenylalanine*

The deuterium isotope effect for [3-$^2H_2$]-dihydrophenylalanine was 2.0 on V and V/K. This suggested that the proton abstraction was more rate limiting than for (2*S*)-phenylalanine. The isotope effect was also shown to be independent of the pH.

The ^{15}N-isotope effect for dihydrophenylalanine at pH 8.55 was also increased to 1.0195 ± 0.0002 showing that C-N bond cleavage is partially rate determining.[105]

However, primary deuterium isotope effects on elimination reactions are usually 5-7. Thus, a value of 2.0 on V/K for [3-$^2H_2$]-dihydrophenylalanine, suggested that steps slower than C-H bond cleavage may be partially rate limiting.[105]

The mechanism was further examined by measuring the ^{15}N-isotope effect for dihydrophenylalanine and [3-$^2H_2$]-dihydrophenylalanine.[105, 110] For both the labelled and

unlabelled substrate the ^{15}(V/K) isotope effect was seen to decrease at higher pH. At pH 9.5 the value of ^{15}(V/K) of dideutrated dihydrophenylalanine (0.9921) was lower than that for dihydrophenylalanine (1.0047), suggesting that the C-N bond cleavage step is not deuterium sensitive.[105, 110] As a result the concerted and carbonium ion mechanisms were ruled out and it was suggested that PAL operated *via* a carbanion intermediate. In addition it was proposed that the intermediate is stabilised by delocalisation of the electrons with the aromatic ring of phenylalanine or in the case of dihydrophenylalanine, by the single bond of the ring.[105]

1.5.4 Active site residues involved in the phenylalanine ammonia-lyase reaction

The nature and identity of amino acids at the active site of PAL were investigated by a series of site specific modification experiments. PAL from barley and *R. glutinis* was irreversibly inactivated by the cysteine specific reagents *p*-CMB, NEM and iodoacetic acid.[94] However, the enzyme from potato and maize was unaffected by any of these reagents.[94] From these results it was suggested that the lack of inhibition observed, in some of these systems, indicated that the thiol groups were most probably involved in either substrate binding or maintaining the structure of the protein as opposed to playing a catalytic role in the mechanism.[94]

The enzyme was also inhibited by nucleophilic reagents such as potassium cyanide, phenylhydrazine[113] and nitromethane[108] and irreversibly inactivated by sodium borohydride.[108] In all cases complete protection from inhibition was afforded by

including the substrate, or cinnamic acid, in the incubation mixture; thus indicating that the inhibitors were directed at the active site of the enzyme.

In order to identify the site of chemical modification, the experiments were repeated using [$^{3}H_4$]-sodium borohydride.[107] Complete acid hydrolysis of the intact protein and analysis of the products highlighted the presence of [3-^{3}H]-alanine. The levels of tritium incorporation indicated that only one modification per active site had been made, presumably to an electrophilic site. A similar experiment in which PAL was inactivated with [^{14}C]-potassium cyanide and subsequently hydrolysed under acid conditions led to the isolation of [^{14}C]-aspartic acid.[107] These observations indicated that the electrophile, which had been modified, was most probably a dehydroalanine residue.[112]

As a result of the kinetic and inhibition studies a mechanism for the PAL catalysed reaction was proposed (Scheme 1.26). The first step involves nucleophilic attack of the substrate amino group at the dehydroalanine residue[90] to form an intermediate Michael adduct. Subsequent abstraction of the C-3 proton gives the carbanion intermediate. This then collapses to eliminate ammonia, affording cinnamic acid and the aminated form of the enzyme. Subsequent protonation and elimination of ammonia from the active site regenerates the enzyme prosthetic group (Scheme 1.26).[90]

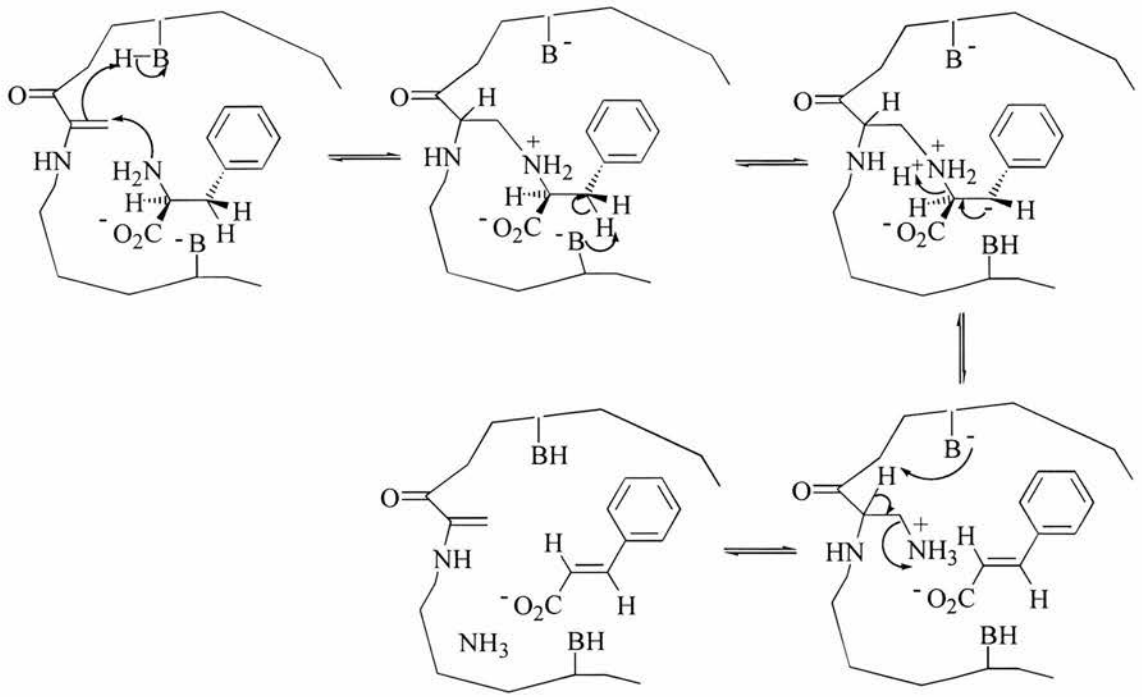

Scheme 1.26: *$E1_{cb}$ mechanism of the PAL reaction*

1.6 Aspartate ammonia-lyase

Aspartate ammonia-lyase (Aspartase, EC 4.3.1.1) catalyses the reversible elimination of ammonia from (2*S*)-aspartic acid (Scheme 1.27, **(10)**) to afford fumaric acid (**12**) (Scheme 1.27).[114, 115] The enzyme was first observed in plants[116] and bacteria,[114] and subsequently in mammalian tissues[117, 118] where very little is known. Aspartase from micro-organisms such as *Pseudomonas fluorescens*,[119] *Bacterium cadaveris*[19] and *Hafnia alvei*[116] have been partially purified, however, the most extensively characterised sources of the enzyme are those from *E. coli,*[117] and *P. fluorescens.*[118]

Examination of the physiological role of aspartase suggests that the enzyme plays an essential role in the metabolism of glutamate and therefore has a role which is analogous to methylaspartase.[44]

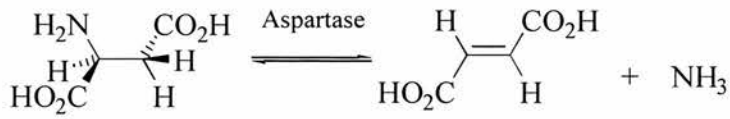

10 **12**

Scheme 1.27: *Reaction catalysed by aspartase*

1.6.1 Biochemical properties of Aspartase

The gene from *E. coli* has been shown to encode for 477 amino acids[120] with a sub-unit mass of 52 kDa. The morphology of the native protein being homo-tetrameric.[117]

Various analogues of aspartic acid such as β-alanine, (2*R*)-aspartic acid and (2*S*)-aspartatic acid ester[115] have been tested as substrates for the enzyme from *E. coli*. However, only (2*S*)-aspartic acid was able to serve as a substrate with a K_m calculated to be 1.0 mM.[115]

1.6.2 Metal ion cofactor requirements

Early studies on the metal ion dependency of aspartase suggested that the enzyme had a strong requirement for a divalent metal ion.[20, 115] Divalent metal ions including those shown in Table 1.12 were found to be capable of re-activating the apoenzyme at neutral pH or above.[115] The Michaelis constant for each metal ion is also shown in the Table 1.12.

Table 1.12: *Activation of aspartase by divalent metal ions*

Metal ion	K_m *(μM)*
Zn^{2+}	0.21 ± 0.04
Cd^{2+}	0.7 ± 0.5
Mn^{2+}	0.8 ± 0.4
Co^{2+}	2.0 ± 0.3

The pH optimum for the reaction was found to be 8.7 in the presence of 2 mM magnesium ion.[121] At high pH the enzyme requires divalent metal ion for activity, whilst at low pH, metal ions are not necessary.[115] This observation led to the proposal that aspartase exists in a pH-dependent equilibrium between two forms.[122]

1.6.3 Substrate specificity

The K_m for wild-type aspartase with the natural substrate, (2*S*)-aspartic acid is 1.0 mM at pH 7.0.[121] A range of substrate analogues was tested for inhibition properties by incubation with the enzyme. Table 1.13 lists some of the compounds, which were found to be competitive inhibitors with respect to (2*S*)-aspartic acid. Values were found to range from 0.2 to 36 mM.[115]

Analogues such as (2*S*)-alanine and (2*S*)-serine, which lack a C-3 carboxylate group, were found to act as neither an inhibitor nor a substrate. However, when the C -3 carboxylic acid group was replaced with a phosphate group (**71**), a phosphonate group (**72**) or a nitro group (**73**), the resulting analogues were all shown to be competitive inhibitors (Table 1.13). The presence of a carboxylate at the 1- position was found to be an absolute requirement. It was thus concluded that binding at the active site of aspartase requires a carboxylate group or the functional equivalent in the 1- and 4-position.[115, 123]

Table 1.13: *Substrate analogues as inhibitors of aspartase*

Inhibitor	K_i *(mM)*
(2*S*)-aspartic acid **10**	1.0[a]
O-phospho-(2*S*)-serine **71**	0.2
(2*S*)-2-amino-4-phosphono-butyrate **72**	2.4
3-nitropropionate **73**	0.83
Succinate**74**	24
(3-aminopropyl)-phosphonate **75**	36
3-nitro-2-amino-propionate **76**	0.0045

a) K_m for aspartic acid

A second but less rigorous requirement for inhibitor binding was the presence of an amino group in the C-2 position. Succinate (**74**) was shown to act as a weak competitive inhibitor with a K_i of only 24 mM.[115] Substitution of the amino group with a halogen as in bromo-(2*S*)-aspartic acid or chloro-(2*S*)-aspartic acid resulted in significant inhibition with K_i's of 2.3 mM and 1.7 mM, respectively.[115] 3-Nitro-2-aminopropionate (**76**) was found to be the most potent competitive inhibitor with a K_i of 4.5 μM, three orders of magnitude lower that the K_m value for the natural substrate (K_m = 1.0 mM), suggestive of a structure similar to the transition state for the natural substrate. It was proposed that formation of a carbanion species (**77**) at C-3 of the inhibitor, mimics the build-up of negative charge which would occur in the proposed transition state for the enzyme catalysed reaction, as shown in scheme 1.28.[115]

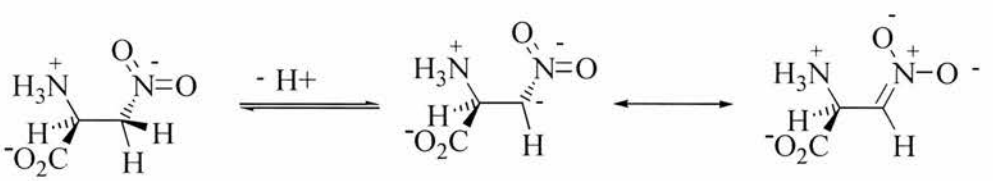

76 **77**

Scheme 1.28: *3-Nitro-2-aminopropionate as a mimic of the enzyme-catalysed transition state*

1.6.4 Mechanism of aspartase

(2*S*,3*R*)-^{2}H]-aspartic acid was incubated with the enzyme and the kinetics of the reaction determined.[18] However, no primary isotope effect was observed on V or V/K. This suggested that C-H bond cleavage was not rate determining. In a second experiment (2*S*)-[2-^{2}H]aspartate was incubated with aspartase and in this case a small isotope effect

of 1.11 ± 0.02 was observed on V, consistent with a secondary isotope effect.[116] This would arise as a result of a change in hybridisation of the carbon to which the 2*S* proton is attached (from sp^3 to sp^2). A significant ^{15}N-isotope effect of 1.0239 ± 0.0014 on V/K was observed for (2*S*)-[^{15}N]-aspartic acid. These kinetic results suggested the operation of a step-wise $E1_{cb}$ mechanism involving the formation of an intermediate carbanion, where the rate-determining step is cleavage of the C-N bond.[116]

1.6.5 Active site residues involved in the aspartase reaction

Incubation of the cysteine modifying agents *p*-mercuribenzoate and NEM with aspartase resulted in complete loss of activity, consistent with the involvement of a cysteine in the catalytic mechanism of the enzyme.[17]

Subsequent peptide mapping experiments were conducted using the fluorescent cysteine modifying agent *N*-(7-dimethylamino-4-methylcoumarynyl) maleimide (DACM) in an attempt to identify the cysteine residues at the active site of the enzyme.[124] Aspartase which had been inactivated with DACM was subjected to tryptic digestion and purified by reversed-phase HPLC. Isolation and analysis of the modified peptide showed that two residues, Cys-140 and Cys-430, had been modified.[124] When the same experiment was repeated in the presence of magnesium ion or substrate, none of the cysteine residues were modified. This indicated that two cysteine residues Cys-140 and Cys-430 were located at the substrate binding site.[124]

In a separate experiment the substrate analogue (2S)-aspartate β-semialdehyde (L-ASA) (**78**) was found to act as a moderate inhibitor of aspartase with a K_i of 0.71 mM

(Scheme 1.29).[125] The proposed mechanism of inactivation involved enzyme catalysed elimination of ammonia from L-ASA (**78**) to afford fumaric acid semialdehyde (FAA) (**79**) still bound at the active site (Scheme 1.28). The newly generated olefin (Scheme 1.28, **(80)**) is then susceptible to attack by an active site nucleophilic residue such as a cysteine or lysine to give adduct (**81**), which it was proposed was the inactive form of the enzyme (Scheme 1.29).[125]

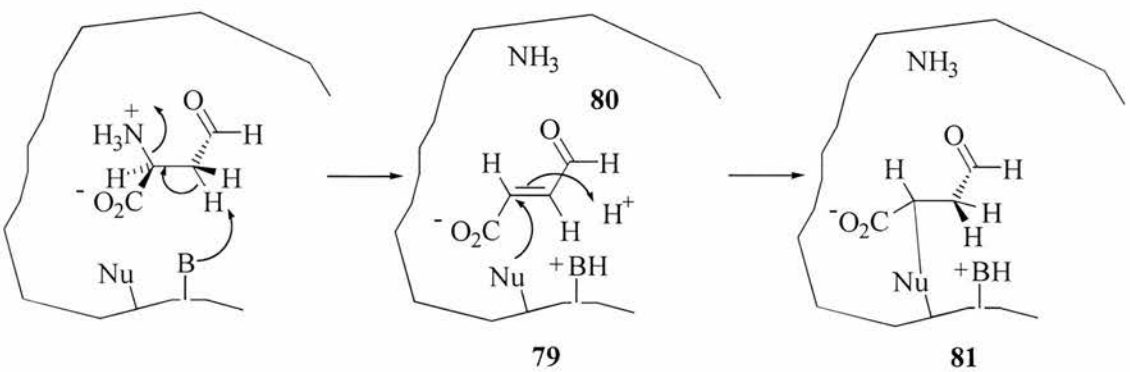

Scheme 1.29: *Mechansim of inactivation of aspartase with* L-*aspartate β-semialdehyde*

After tryptic digestion of the inactive enzyme a single peptide containing the covalently modified residue was isolated and characterised. The results of Edman degradation of the peptide showed the site of modification to be Cys-273.[125] Mutagenesis experiments were carried out in an attempt to further probe the involvement of Cys-140, 273 and 430. The mutant C430W was tested with the natural substrate and was found to possess 3-fold greater activity than the wild-type enzyme, indicating that Cys-430 was not essential for catalysis.[126]

Two mutants C273S and C273A were shown to possess kinetic parameters similar to the wild-type enzyme, however, both were found to have lower but still

appreciable rates of inactivation with respect to L-ASA. From this, it was proposed that Cys-273 had no direct role in catalysis (Table 1.14).[127]

Table 1.14: *Kinetic parameters for aspartase mutants*

Enzyme	K_m *(mM)*	k_{cat}/K_m
Wild-type	1.2 ± 0.1	150 ± 10
C273S	1.3 ± 0.1	160 ± 10
C273A	0.54 ± 0.04	340 ± 20

An analogue of L-ASA (**82**) (Scheme 1.30) was tested with the enzyme with the aim of stabilising the enzyme-FAA intermediate. Analysis of the intact protein showed an additional modification involving a cross-link between the previously identified Cys-140 and Lys-139 (adjacent) (Scheme 1.29).[125] Mutation of Cys-140 to serine had no effect on the kinetic parameters for the natural substrate and suggested that Cys-140 is not essential for catalysis.[125] This information led to the proposal that Cys-140 is important for the enzyme, perhaps for substrate binding. The mutant K139I showed a 10-fold increase in K_m for (2S)-aspartic acid, indicating that this residue is also important in substrate binding. This mutant was also rapidly inactivated by L-ASA, which suggested that the initial modification by the stabilised L-ASA analogue occurs at Cys-140 which is then followed by cross-linking to Lys-139.[125]

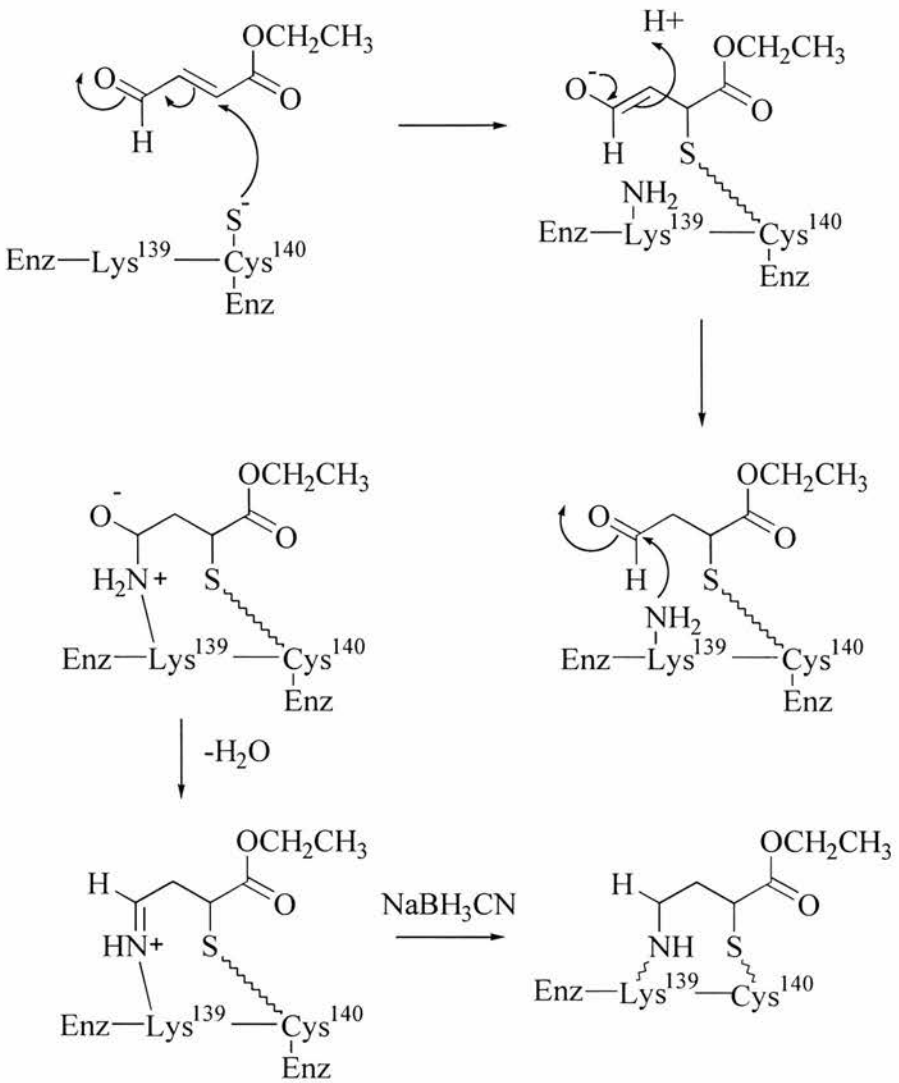

Scheme 1.30: *Mechansim of inactivation of aspartase with an analogue of L-aspartateβ-semialdehyde*

The chemical modifying agent diethylpyrocarbonate (DEP), specific to histidine side chains was found to irreversibly inactivate the enzyme.[114] The ability of the substrate to protect the enzyme from inhibition directed the site of modification to be in the active site of the protein. Inspection of the deduced amino acid sequence for the protein, highlighted the presence of eight histidine residues, only one of which, corresponding to His-123 was retained throughout the family of histidase enzymes.[114]

The mutant H123L was prepared and a kinetic analysis showed that V_{max}/ E_t for the natural substrate had decreased to 50.7 ± 0.1 min^{-1} for the natural substrate ((2*S*)-aspartic acid = 61.4 ± 2.2 min^{-1}), however, DEP was still able to inactivate the mutant. This suggested that His-123 was unlikely to be the site of modification by DEP, in the native enzyme and consequently was not a catalytically essential residue.[120]

Aspartase contains 27 lysine residues, however, only Lys-54 and Lys-327 are conserved within the fumarase-aspartase family of enzymes.[120] Lys-327 occurs within a region of high sequence identity, which serves as a signature sequence for the members of this family of enzymes.[120]

When Lys-327 was mutated to arginine, the resulting mutant had low catalytic activity (V_{max}/ E_t = 0.20 ± 0.02 min^{-1}) and the K_m for (2*S*)-aspartic acid increased by a factor of 5 (K_m = 23.8 ± 6.0 mM, wild-type K_m = 4.3 ± 0.6 mM).[120] This result suggested that Lys-327 had an important role in substrate orientation and binding.[128, 120]

Lys-54 was also mutated to an arginine residue and the mutant enzyme was found to be devoid of all enzymic activity. This result suggested that Lys-54 was essential for enzyme activity.[120]

Despite the determination of the X-ray crystal structure of the apoenzyme form of aspartase to 2.8 Å resolution,[129] the identity of the catalytic residues involved in the deamination reaction remains undetermined. Unlike the other ammonia-lyase enzymes discussed above a dehydroalanine or equivalent electrophile was not observed in the X-ray structure.

1.7 Dehydroalanine and unsaturated amino acids

The ammonia-lyase enzymes HAL[86] and PAL (see preceeding sections) have both been shown to contain the unsaturated amino acid dehydroalanine. Indeed, this same residue has also been implicated in the mechanism of methylaspartase. Although relatively rare, unsaturated amino acids such as dehydrocysteine, dehydrovaline, dehydrobutyrine and dehydroalanine, have been observed in a range of biologically relevant peptides.[130] The antibiotics subtilin, from *Bacillus subtilis,*[131] and nisin, from *Streptococcus lactis*,[132] are known to contain at least one dehydroalanine residue. The dehydroalanine group also occurs in several more highly modified peptides such as Berninamycin A (**83**) [133] and Nosiheptide (**84**),[134, 135] a polypeptide antibiotic, which has been shown to inhibit ribosomal protein synthesis (Fig. 1.4).

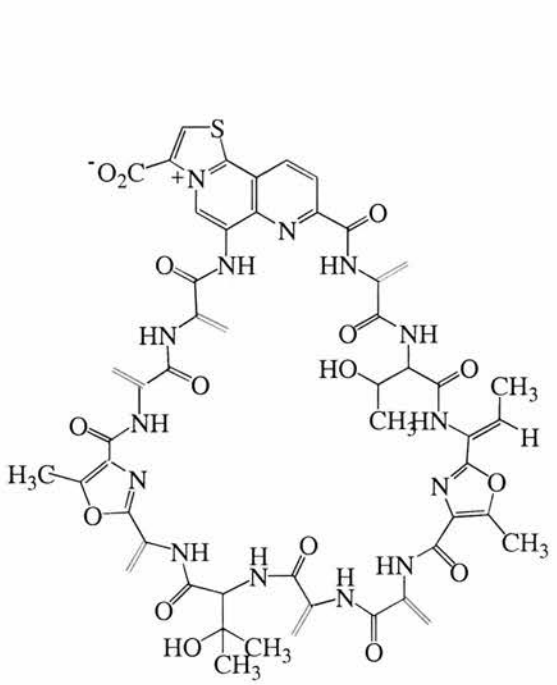

83

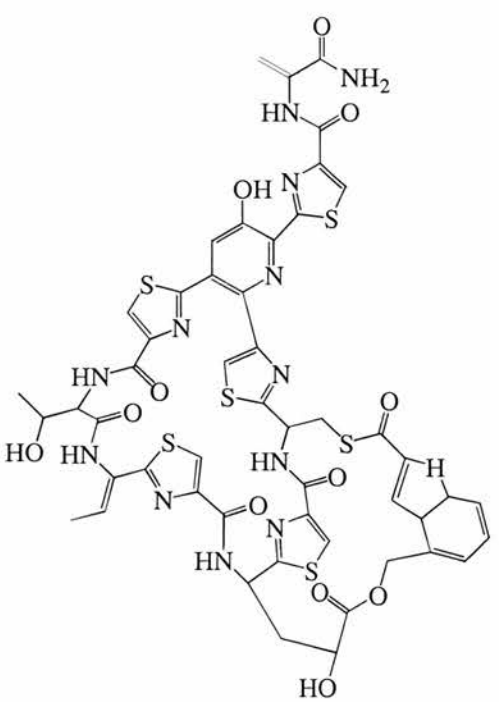

84

Figure 1.4: *Dehydroalanine-containing polypeptides Berninamycin A (**83**) and Nosiheptide (**84**)*

In addition dehydroalanines have been implicated as biochemical reaction intermediates in both cephalosporin and penicillin biosynthesis.[133] It is also incorporated into naturally occuring peptide hormones such as enkephalin and lutenizing hormone-releasing hormone[135] which leads to analogues displaying more potent agonist and anatagonist activity and increased selectivity.[136] Dehydroalanine has been shown to be derived from amino acids such as serine, cysteine or alanine through a post-translational dehydration, dethiolation, or dehydrogenation respectively.[133]

Formation of dehydroalanine has also been observed as a result of the degradation of cysteine residues in proteins during treatment with alkali[137] and in particular the cleavage of disulfide bonds in insulin and oxidised glutathione under basic conditions (Scheme 1.31).[138]

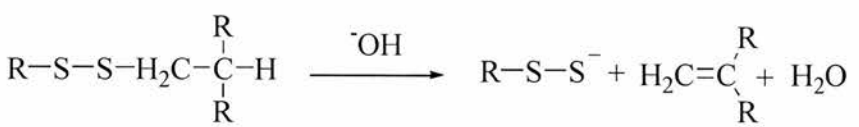

Scheme 1.31: *Lysis of disulfide bonds to generate a dehydroalanine residue*

In both cases the mechanism involves β-elimination to give a dehydroalanine-containing product.

Although it has been postulated that biosynthesis of dehydroalanine residues is a consequence of either the dehydration of serine, dehydrogenation of alanine or dethiolation of cysteine, very little experimental evidence exists to indicate which of these is the most likely route. Indeed for HAL and PAL, although it was assumed that a serine was the precursor, only very recently with the advent of the crystal structure has it

been shown that Ser-143 is dehydrated to afford the unsaturated amino acid. In the case of the antibiotic Berninamycin (Fig. 1.11),[133] the biochemical origin of the dehydroalanine residue was investigated by growing up the organism in the presence of ^{14}C-serine and ^{14}C-alanine. The natural product was isolated and it was shown that 100 times more ^{14}C-serine had been incorporated into the peptide than ^{14}C-alanine. Thus providing compelling evidence to suggest that, in this case, ^{14}C-alanine is not an effective precursor to dehydroalanine.[133]

1.7.1 Chemical properties of dehydroalanine residues

The α,β-double bond in a dehydroamino acid represents a chemically reactive site which also has interesting conformational and electronic features.[139] The chemical properties of dehydroalanine deserve specific comment as dehydroalanine residues possess the ability to react with nucleophiles,[68] electrophiles and radical species.[140]

When the double bond of a dehydroalanine residue, which has been incorporated into a peptide is co-planar with the carbonyl group or the peptide backbone, the system becomes susceptible to attack by nucleophiles in a conjugate manner, to afford β-adducts as shown in Scheme 1.32.[68] In addition nucleophiles can attack the double bond at the α-position in a manner similar to that for nucleophilic addition to imines (α-imine capture). In this case α-adducts are formed as shown in Scheme 1.32.[68]

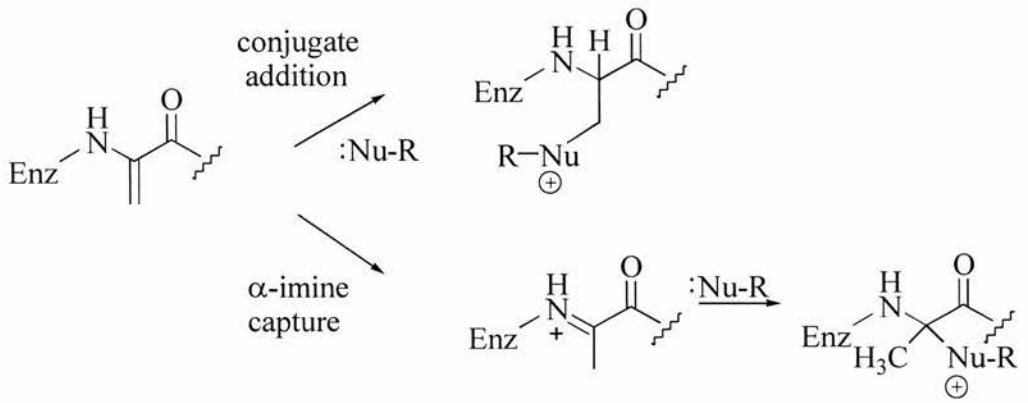

Scheme 1.32: *Addition of a nucleophile to dehydroalanine*

In the presence of electrophiles and with sufficient overlap of the lone pair of electrons on the adjacent nitrogen atom with the π electrons of the double bond, dehydroalanine can act as a nucleophile produce acetylated enamines (Scheme 1.33).[68]

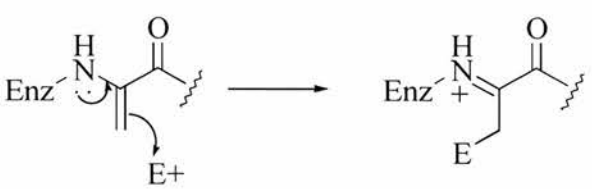

Scheme 1.33: *Attack of dehydroalanine on an electrophile*

The reaction of dehydroalanine with radical species is very much dependent upon the electron withdrawing and donating properties of the neighbouring functional groups. When electron-withdrawing species such as a carbonyl containing group are adjacent to the dehydroalanine residue, the system becomes electron deficient and hence activated toward attack by a radical, thus making the reaction facile.[141]

The reaction of dehydroalanine with certain radical species constitutes an important method for carbon-carbon bond formation[142] and has been used to generate saturated dipeptides and tri-peptides from dehydroalanine containing peptides (Scheme 1.34).[143]

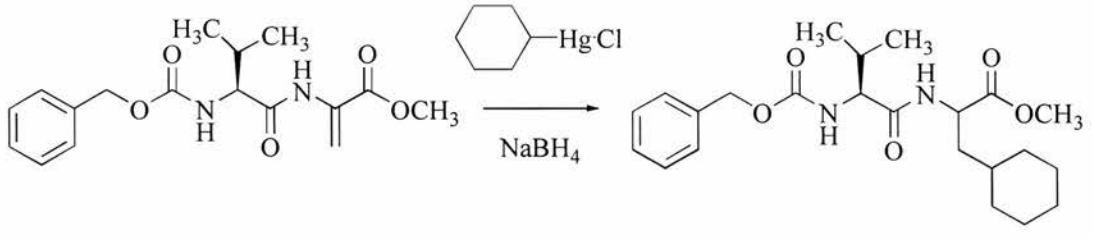

Scheme 1.34: *Radical reaction of dehydroalanine containing di-peptide*

In the majority of cases however, the dehydroalanine is flanked by both electron withdrawing and donating species (denoted as a captodative system), under these conditions the details of the reaction are less easy to predict.[141, 144, 140]

1.7.2 Conformational analysis of dehydroalanine

α,β-Unsaturated amino acids, such as dehydroalanine, have a significant role to play in certain natural peptides.[135, 145] In order to understand the structure-activity relationships of these compounds, a knowledge of the conformation and electronic characteristics of these residues is necessary. This in turn may assist the design of more biologically potent analogues, containing dehydroamino acids.[136]

The conformation of peptides containing a dehydoalanine residue is thought to be affected by the backbone sp^2 carbon atom, the extended conjugation of the π-system and the geometrical rigidity (resulting from the double bond).[136]

In order to explore the likely conformational consequences of replacing a saturated amino acid by a dehydroamino acid, conformational analysis was carried out on N-acetyl-dehydrophenylalanyl-(2*S*)-proline (Fig. 1.5).[130]

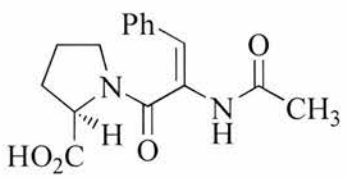

Figure 1.5: *N-acetyl-dehydrophenylalanyl-(2*S*)-proline*

Investigation of the system by a range of techniques found that the molecules with an unsaturated amino acid residue do not adopt a planar conformation in the crystalline state and can have greater conformational flexibility than the corresponding analogue containing the saturated residue.[130, 145]

Model peptides containing a dehydroalanine residue have also been prepared and their solution conformations determined by NMR spectroscopy. These studies indicated that dehydroalanine favours an inverse γ-turn.[136] This behaviour was not observed with the corresponding saturated analogue, alanine, which suggests that dehydroalanine may act as a γ-turn inducer. In contrast to this, the incorporation of a dehydrophenylalanine or dehydroleucine residue has been shown to stabilise β-turn conformations in peptides.[135]

These studies suggest that it may be possible to constrain a chosen conformation of a peptide by introducing a suitable dehydroamino acid.[136]

1.7.3 Synthesis of dehydroamino acids

In order to study the properties of dehydro-peptides and to generate chemical models of these peptides, it has been necessary to prepare synthetic dehydroalanine containing peptides.[146]

Peptides containing dehydroamino acids have traditionally been synthesised by the dehydration of serine (Route A; **85**, R = H), *N*-chlorination and subsequent dehydrochlorination of an amino acid (Route B) or alternatively by Wittig-Horner olefination using an α-phosphonylated glycine precursor (Route C, Scheme 1.35).[146]

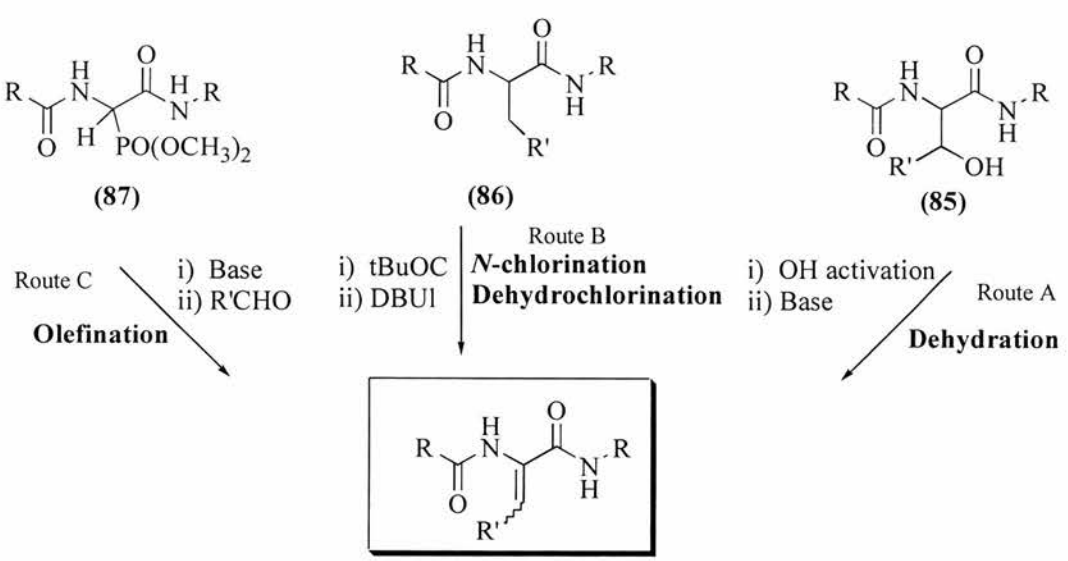

Scheme 1.35: *Routes to the chemical synthesis of dehydroalanine*

In a model reaction dehydration of serine was achieved in a number of synthetic peptides by acylation of the serine hydroxyl group, followed by treatment with DBU, in the presence of lithium perchlorate (Scheme 1.36).[146]

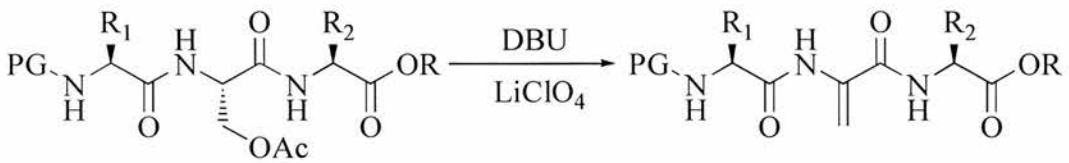

Scheme 1.36: *Preparation of dehydroalanine from O-acylated serine*

Dehydroalanine moieties are also important intermediates in the synthesis of many unusual amino acids.[143] However, dehydroalanine containing monomers have been shown to readily undergo free radical polymerisation in organic solvent, to give polymers of varying molecular weight.[144] They can also decompose to pyruvate and the corresponding amide.[143]

Dehydroalanine has been artificially incorporated into biological molecules using solid-phase peptide synthesis. In one method the synthesis of a dehydroalanine residue was achieved from a saturated precursor which was introduced as an asparagine residue. The final product was generated *via* a Hofmann type degradation, followed by elimination (Scheme 1.37).[147]

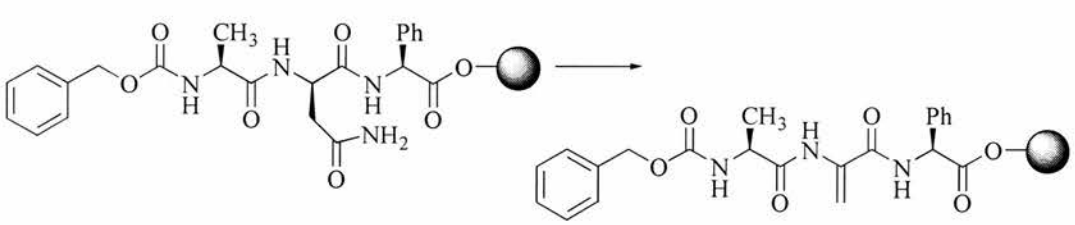

Scheme 1.37: *Solid-phase synthesis of dehydroalanine from asparagine*

In an alternative method, the same dehydro group was introduced as a cysteine residue (**88**), which was subsequently oxidised to the corresponding sulfone (**89**) (Scheme 1.37). The dehydration product was obtained by base-promoted β-elimination of the sulfone (**89**) and simultaneous release of the product (**90**) from the solid support (Scheme 1.38).[132]

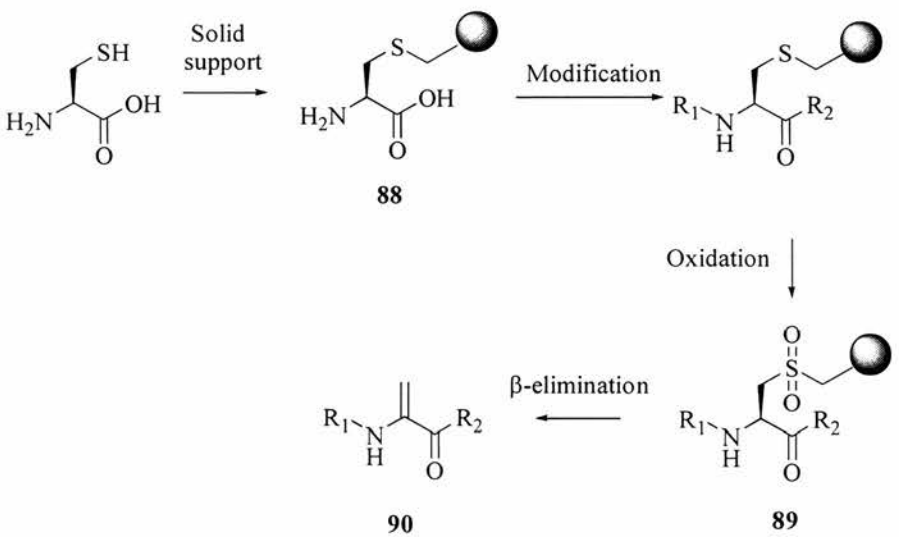

Scheme 1.38: *Solid-phase synthesis of dehydroalanine using sulfone chemistry*

More recently dehydroalanines have been synthesised by incorporating an S-methyl cysteine residue into a peptide during synthesis (Scheme 1.39). This was subsequently oxidised to the sulfoxide (**92**) and eliminated to afford the desired residue (93) (Scheme 1.39).[143]

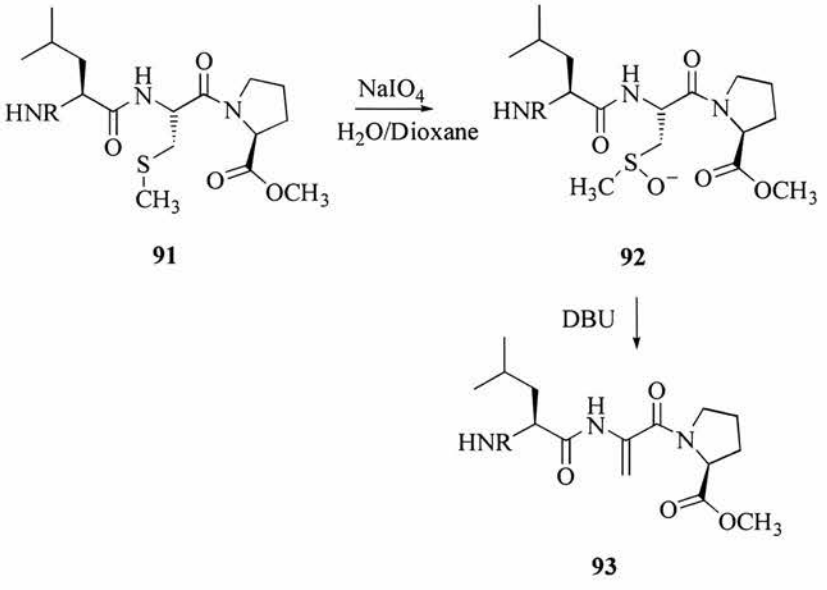

91 **92** **93**

Scheme 1.39: Preparation of dehydroalanine from S-methyl cysteine

Chapter 2 : Cloning and Purification of His-tagged Methylaspartase

2.1 Isolation and purification of methylaspartase from pSG4

Methylaspartase was purified from cultures of *E. coli* pSG4 based on a method established by Goda *et al.*[46]

A 3-litre culture was grown and the cells were harvested by centrifugation.[46] The crude extract was prepared by sonication of a suspension of the cells in 50 mM potassium phosphate buffer at pH 7.6 containing 1 mM β-mercaptoethanol and the protease inhibitor PMSF (2 mM), followed by centrifugation to remove the cellular debris. The crude extract was then subjected to an acetone fractionation and methylaspartase activity was located in the precipitate afforded at 55% to 78% acetone.

The resulting pellet was resuspended in 50 mM potassium phosphate buffer at pH 7.6 and further purified by gel filtration size exclusion chromatography on Sephadex G-150. Methylaspartase activity was eluted in fractions corresponding to between 1.2 and 1.6 column volumes. The active fractions were pooled and concentrated by ultrafiltration and then applied to an FPLC anion-exchange column. The column was eluted with an increasing potassium chloride gradient (0-1000 mM), and activity eluted in fractions corresponding to 80 mM salt concentration. The pooled active fractions were found to possess a specific activity of 150 units/ mg, corresponding to a 11-fold increase in purification when compared to crude extract (Table 2.1).

Table 2.1: *Purification of recombinant methylaspartase*

	Volume (cm^3)	*Total Activity* ($\mu mol\ min^{-1}$)	*Specific Activity* ($\mu mol\ min^{-1} mg^{-1}$)	*Total Protein* (*mg*)	*Purification* (*-fold*)
Crude Extract	8.0	2681	13.8	194	1.0
Acetone Pellet	3.0	2571	29.8	86	2.1
G-150 pool	2.8	1741	42.9	40.5	3.1
FPLC pool	3.0	588	158.9	3.7	11.5

The enzyme extract from each step in the purification was analysed by 12% SDS-polyacrylamide gel electrophoresis and was visualised with Coomassie blue stain. Following FPLC anion-exchange the enzyme was judged to be 80-85% homogeneous.

2.2 Expression of His-tagged methylaspartase

In parallel experiments within our laboratory the *mal* gene was sub-cloned into a pET vector containing the nucleotide sequence for an N-terminal deca-tag.[148] This was carried out in order to increase protein yield and to simplify the purification of the protein through the use of a nickel chelate affinity column.

2.3 Isolation of His-tagged methylaspartase

Crude extracts were prepared for each of four constructs (pMASM 1-4) from 500 cm^3 cultures induced with IPTG at an OD_{600} of 0.6-0.9. The buffer used contained 50 mM sodium phosphate at pH 8 and 300 mM sodium chloride. Phenyl methylsulfonyl fluoride (PMSF) and β-mercaptoethanol were both added to a final concentration of 1 mM.

Clones 2 and 3 showed 2-fold and 1.5-fold higher levels of activity and consequently were selected for further studies.[46]

2.3.1 Optimisation of IPTG induction

The optimum conditions for induction with IPTG were investigated by growing 1-litre cultures of clones 2 and 3. The OD_{600} of both cultures was monitored and once mid-log phase had been reached an aliquot of cells was removed, centrifuged and the cell pellet frozen at –80 °C. IPTG was then added to the remaining culture to a final concentration of 1 mM and further aliquots of the culture were removed after 3, 6 and 16 hours and then treated as before. Crude extracts of the frozen cell pellets were prepared in 50 mM sodium phosphate buffer at pH 8 containing 350 mM sodium chloride and 50 mM imidazole and the methylaspartase activity determined as shown in Table 2.2.

Table 2.2: *Optimisation of IPTG induction period*

Induction Period (h)	*Activity of clone 2 ($\mu mol\ min^{-1}\ cm^{-3}$)*	*Activity of clone 3 ($\mu mol\ min^{-1}\ cm^{-3}$)*
0	0.432	0.438
3	14.76	25.8
6	7.84	9.72
16	6.24	9.12

These results show that the yield of enzyme activity increased to a maximum with a 3 hour induction period and then decreased.

2.3.2 Plasmid stability test

Attempts to produce second generation cultures of either pMASM 2 or 3 all resulted in crude extracts with very low levels of methylaspartase activity. This indicated that the plasmid was probably unstable and prompted a series of experiments to be carried out in order to determine the proportion of *E. coli* cells which still retained intact pMASM plasmid.

The pET-16b Vector used as the host for the *mal* gene contains the ampicillin resistance gene, consequently all cells containing the circular plasmid will express ampicillin resistance, allowing growth on LB-amp media. In addition, the plasmid also contains the T7 promoter, which is absent from the *E. coli* chromosome.

When IPTG is added to the growing cell culture, it promotes expression of the genetic material on the *lac* operon which is located on the *E. coli* chromosome. This in

turn leads to overexpression of T7 RNA polymerase (the gene for which has been previously engineered into the recombinant *E. coli* chromosome) which subsequently binds to the T7 promoter on the pET plasmid, which in turn induces expression of the downstream DNA, which includes the *mal* gene. As a consequence even lower numbers of cells will be expected to grow on LB-amp medium which contains IPTG.

A 5 cm^3 culture of pMASM clone 3 was prepared and grown to mid log phase. An aliquot of the cells was removed immediately prior to the addition of IPTG and the remaining cells subsequently plated out onto four separate LB-agar plates which contained a) ampicillin, b) IPTG, c) ampicillin and IPTG and d) a control with no additives. The results and expected results (made with the assumption that all cells contain the intact plasmid) are shown in Table 2.3.

Table 2.3: *Plasmid stability test*

Plate Additives	*Expected Results*	*Results Obtained*
No additives	Most cells form colonies	Most cells formed colonies
Ampicillin	>90% of cells form colonies	<1% of cells formed colonies
IPTG	<2% of cells form colonies	>60% of cells formed colonies
IPTG + Ampicillin	<0.01% of cells form colonies	<0.01% of cells formed colonies

Less than 1% of the cells formed a colony on the plate containing ampicillin (when compared to the control plate) indicating that most of the cells did not retain intact plasmid.

2.4 Cloning of His-tagged methylaspartase

Having established that the pET-16b plasmid containing the *mal* gene was unstable, co-workers in the laboratory sub-cloned the gene into the pET-5b vector using the restriction enzymes *Nde* I and *Bam*H I.[148] The *Nde* I and *Bam*H I restriction sites are located at the new N-terminus (ie. including the His-tag) and the C-terminus respectively of the *mal* gene. The entire *mal* construct was then ligated into the new host plasmid. The resulting plasmid was then transformed into *E. coli* BL21 (DE3) competent cells.[148]

2.5 Purification of His-tagged methylaspartase

Methylaspartase from the pET-5b vector is expressed with a histidine affinity tag (His-tag) at the N-terminus, which comprises ten consecutive histidine residues. It was anticipated that the introduction of a His-tag would allow methylaspartase to be purified by immobilised metal chelate chromatography.

This technique is based upon the selective affinity of a nickel charged nitrilotriacetic acid matrix (Ni-NTA) for a protein, which has been tagged with high levels of sequential histidine residues at either the C- or the N-terminus. The protein is

then eluted from the column with an increasing concentration of imidazole, which competes with the protein for the nickel ion binding sites.

2.5.1 Purification of His-tagged methylaspartase by affinity chromatography

Purification of his-tagged methylaspartase by metal ion affinity chromatography was developed with Ni-NTA agarose resin. The crude enzyme extract was added to a suspension of Ni-NTA resin in 50 mM potassium phosphate buffer at pH 8 containing 350 mM sodium chloride and 20 mM imidazole.

After 1 hour the supernatant was assayed for methylaspartase activity and was shown to contain less than 0.1% of the original activity of the extract. This result demonstrated that methylaspartase was binding efficiently to the Ni-NTA resin. The resin was centrifuged and washed several times with the above buffer containing 50 mM imidazole prior to elution of methylaspartase by an increasing stepped concentration of imidazole (50-250 mM, 50 mM in increments). Methylaspartase activity eluted between 200 and 250 mM imidazole. Analysis of the purified enzyme by SDS-polyacrylamide gel electrophoresis developed using silver stain showed it to be >90% homogeneous as determined by eye.

2.5.2 Adaptation of purification of his-tagged MAL for HPLC

Having established that methylaspartase activity could be purified using Ni-NTA resin, an HPLC purification method was developped.

A 3-litre culture of *E.coli* BL21 DE(3) cells was grown at 37 °C to an OD_{600} 0.6-0.9 prior to induction with 1mM IPTG and then grown for a further 3-4 hours at 37 °C. The crude extract was prepared as before by sonication and centrifugation to remove cellular debris.

This was then applied to a column of Ni-NTA superflow resin (1.6 cm x 10 cm) which had been pre-equilibrated with 50 mM potassium phosphate buffer at pH 8.0 containing 350 mM sodium chloride and 50 mM imidazole. The column was washed with the same buffer until the absorbance at 280 nm was less than 0.05 absorbance units. A linear imidazole concentration from 50 mM to 1 M over 5 column volumes was applied at a flow rate of 2.5 cm^3/ min. Methylaspartase activity was eluted in fractions 11-15, corresponding to an imidazole concentration of 210 mM. All fractions containing enzyme activity were pooled and then were concentrated by ultrafiltration to afford extract with a specific activity of 201.8 units/ mg. This corresponds to a 6.5-fold purification over the crude extract (Table 2.5). The purified extract was analysed by 12% SDS-polyacrylamide gel electrophoresis developed using silver stain. The electrophoretogram showed the presence of a single major band with a mass of 45kDa, consistent with the expected mass for methylaspartase.

The protein was further purified by a second HPLC step using a Bio-Cad HQ Poros 20 column (4.6 mmD x 100 mmL). The partially purified protein was loaded onto the column and washed with 3 column volumes of Tris buffer at pH 9 containing 100 mM sodium chloride. The protein was then eluted with an increasing sodium chloride concentration gradient from 100 mM to 500 mM over 25 column volumes. Methylaspartase activity was found in those fractions corresponding to a 200 mM sodium

chloride concentration (Fig. 2.1). The active fractions were pooled and concentrated by ultrafiltration to yield an extract with a specific activity of 218 units/ mg, affording a 7-fold purification when compared to the crude extract (Table 2.4). Analysis by 12% SDS-polyacrylamide gel electrophoresis showed the presence of a single band at 45 kDa, corresponding to the expected mass of methylaspartase.

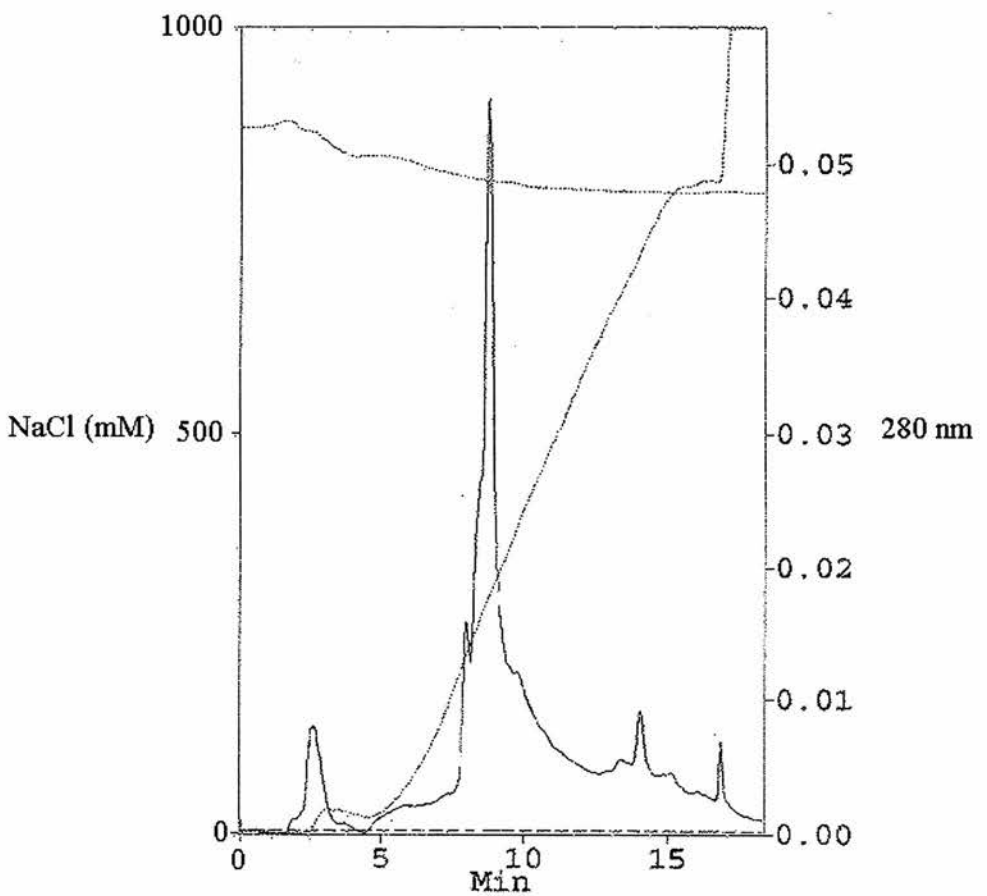

Figure 2.1: *Anion-exchange column profile for purification of methylaspartase*

Table 2.4: *Purification table for his-tagged recombinant methylaspartase*

	Volume (cm^3)	*Total Activity* ($\mu mol\ min^{-1}$)	*Spec. Activity* ($\mu mol\ min^{-1}\ mg^{-1}$)	*Total Protein* (*mg*)	*Purification* (*-fold*)
Crude extract	30	12840	31.2	411	1.0
Ni-NTA Pool	16	10656	201.8	52.8	6.5
Anion-exchange pool	20	9483	218	43.5	7.0

Fig 2.2 shows an SDS-gel of methylaspartase at each stage of the purification.

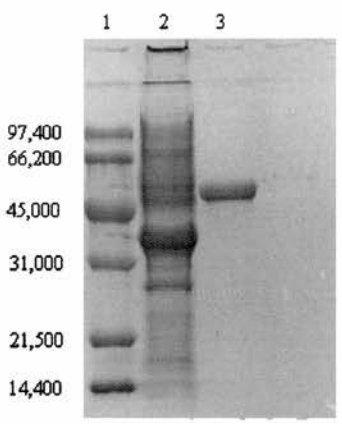

Figure 2.2: *SDS gel (Coomassie stain) of samples of 10 x his-tagged methylaspartase during purification. Lane 1: Molecular weight markers, Lane2:Crude extract, Lane 3: Nickel affinity chromatography pool*

2.6 Kinetic characterisation of his-tagged methylaspartase

The kinetic parameters K_m and V_{max} for the His-tagged recombinant protein were determined with (2*S*,3*S*)-3-methylaspartic acid and (2*S*,3*S*)-[3-^{2}H]-3-methylaspartic acid at pH 9.0, pH 7.6 and pH 6.5. The values at each pH were determined in triplicate and

then compared to those for the wild-type enzyme isolated from *Clostridium tetanomorphum*. The kinetic parameters K_m and V_{max} were determined from lineweaver-Burk plots of the initial rate data for the deamination reaction and are shown in Table 2.5.

Table 2.5: *Kinetic parameters for deamination of proteo- and deutero substrates at pH 9.0, 7.6 and 6.5. Values in parentheses are those for the wild-type enzyme*

Substrate	*pH*	K_M *(mM)*	V_{max} *(x 10^{-6} mol dm^{-3} min^{-1})*	$^{D}(V/K)$
(2*S*,3*S*)-3-Measp acid	9.0	2.57 ± 0.064 (2.37 ± 0.2)	696 (680)	
(2*S*,3*S*)-[3-^{2}H]-3-Measp acid	9.0	2.22 ± 0.049 (2.35 ± 0.3)	692 (396)	1.15 (1.7)
(2*S*,3*S*)-3-Measp acid	7.6	5.54 ± 0.23	665 (576)	
(2*S*,3*S*)-[3-^{2}H]-3-Measp acid	7.6	5.07 ± 0.36	625 (358)	1.16 (1.6)
(2*S*,3*S*)-3-Measp acid	6.5	5.10 ± 0.63	187 (294)	
(2*S*,3*S*)-[3-^{2}H]-3-Measp acid	6.5	5.04 ± 0.59	166 (216)	1.11 (1.4)

The results show that at all of the three pH values, the primary isotope effect on V/K was determined to be ~ 1.6 for the wild-type enzyme. However, with the His-tagged recombinant protein the values for V/K were all about 1.13-1.16. This suggests that the inclusion of the His-tag may have an effect on the rate of the C-H bond cleavage reaction.

The recombinant protein differed from the wild-type enzyme by possessing additional residues (MGHHHHHHHHHHSSGHIEGRHMLEDP) upstream at the N-

terminus and additionally it was later discovered that the protein also contained five extra amino acids (YGSGC) at the C-terminus.[65], [149] These resulted from a mutation in the stop codon of the DNA.[46]

2.7 Conclusion

The use of modern recombinant DNA techniques permitted the over-expression of methylaspartase with a histidine affinity-tag. As a result the enzyme was rapidly purified *via* a two step process to greater than 95% homogeneity with an 11-fold increase in yield of purified enzyme compared to the existing protocol.

Chapter 3 : Labelling the Active Site of Methylaspartase

3.1 Introduction

With the enzymes HAL and PAL, the presence of an electrophilic dehydro amino acid has been proven by the determination of X-ray crystal structures.[92] In the case of methylaspartase, however, the overwhelming evidence for the involvement of an electrophilic Michael acceptor in the mechanism of the enzyme has been gained from kinetic studies with labelled substrates[54] and inhibitors,[71] in the absence of any structural information (for a detailed discussion see chapter 1).

Attempts to produce crystals of methylaspartase of sufficient integrity to obtain X-ray diffraction data, has to date proven unsuccessful.

In order then to gain some detailed information on the structure of the active site of the enzyme and in particular the environment of the catalytic olefin a series of spectroscopic experiments were designed.

It was anticipated that enrichment of Ser-173, the proposed precursor for dehydroalanine,[11] with a ^{13}C-label would facilitate a detailed NMR spectroscopic analysis of the enriched amino acid and the local environment of the residue.

3.2 Supplementation of culture medium with (2*S*)-serine

The incorporation of a ^{13}C-label into the active site of methylaspartase could potentially be achieved by supplementing the culture medium with ^{13}C-serine. As the enzyme is transcribed, the enriched amino acid would be incorporated throughout the

protein, at all serine sites. However, our concern was that supplementing the culture medium (LB medium) with an increased concentration of (2*S*)-serine would alter the balance of amino acids significantly, leading to an adverse effect on the activity of the enzyme. This could result as a consequence of altering the metabolic balance within the growing cell culture, perhaps by amplifying a serine degradation pathway, directing the cellular machinery away from the production of methylaspartase.

A trial experiment was conducted in order to determine the effect on enzyme activity of supplementing the growth medium with (2*S*)-serine, at various times during cell growth. Five cultures (5 cm^3) were prepared in LB medium and the cells grown as described in chapter two (section 2.2). At pre-determined points during culture growth, additional (shown in Table 3.1) (2*S*)-serine was added to each of the five cultures. In addition a control culture was prepared which was not supplemented with additional serine. Table 3.1 shows the times at which serine was added and in each case the relative activity of the isolated enzyme compared to MAL isolated under standard conditions.

Table 3.1: *Supplementation of culture medium with (2S)-serine*

Culture	*Time of serine addition to main culture*	*Activity* ($\mu mol\ min^{-1}$)	*Rel. Activity* ($\mu mol\ min^{-1}$)
1	Control	0.14	1.0
2	Start of mid-log phase growth	0.18	1.29
3	During mid-log phase growth	0.34	2.43
4	Before IPTG addition	0.23	1.64
5	After IPTG addition	0.46	3.29

The results indicated that in all cases higher levels of methylaspartase activity were observed compared to enzyme isolated under standard conditions. However the highest level of enzyme activity was obtained when serine was introduced immediately after induction with IPTG.

It was proposed that the increased yield of protein activity was as a result of the anticipated amplification of a serine degradation pathway which would result in an increase in primary metabolites and subsequently an increase in the yield and rate of cell growth.

3.3 Supplementation of culture medium with [UL-^{14}C]-(2*S*)-serine

Having established that supplementing the LB growth media with additional serine had no adverse effect on the protein yield, similar experiments were carried out with [UL-^{14}C]-(2*S*)-serine. It was anticipated that the incorporation of serine into methylaspartase could be monitored during growth by analysing the ^{14}C-content of the isolated enzyme, and subsequently conditions for maximal ^{14}C incorporation could be optimised.

In a preliminary experiment, radiolabelled serine (specific activity (141 mCi/ mmol, 0.05 μCi total ^{14}C content) was added to both the overnight culture (5 cm^3) and the main culture (1 dm^{-3}, 10.0 μCi total ^{14}C content). The radioactivity incorporation into the cell paste was measured by scintillation counting an aliquot (1 cm^3) of the residual supernatant, following centrifugation of the cell pellet. The ^{14}C incorporation was then subtracted from the total amount of radioactivity added at the beginning of the

experiment. It was found that 48% (4.8 μCi) of the total radioactivity (10.05 μCi) had been taken up by the cells, however, after disruption of the cells by sonication, only 3.3% (0.33 μCi) of the total radioactivity was found to have remained in the crude extract. This showed that despite a large percentage of the radiolabel being incorporated into the cell paste, 93% of this was being retained in the cellular debris.

As the preliminary experiment had resulted in low overall incorporation of radiolabelled serine into the crude extract, a series of experiments were carried out to determine if the composition of the culture medium had an affect on the incorporation of radiolabelled serine into the crude extract.

E. coli BL21(DE3) was cultured in Davis minimal broth (DMB). Under these conditions the cells required 14 hours to reach mid-log phase (3-4 hours for LB media) and the resulting cell pellet was found to be significantly less than with LB. A comparison of the MAL activity in crude extracts from both LB and DMB is shown in Table 3.2.

Table 3.2: *Comparison of methylaspartase grown in LB and DMB*

Culture medium	*Pellet weight (g)*	*Total activity ($\mu mol\ min^{-1}$)*	*Specific activity ($\mu mol\ min^{-1}mg^{-1}$)*
LB	5.3	2131	31.2
DMB	1.2	59.7	4.0

The results show that under minimal media conditions methylaspartase is isolated in a very low yield, ~ 3% of LB. For this reason, the effect of adding LB to DMB was investigated.

A series of cultures were prepared with varying proportions of LB and DMB as shown in Table 3.3. Cells were grown from overnight cultures (5 cm^3) which were used to induce 1L cultures. Radiolabelled serine (0.5-5.0 μCi) was added at the beginning of the induction period, shown previously to afford the highest levels of enzyme activity. Incorporation was determined for both the cell paste and crude lysate for each culture and the MAL activity determined (Table 3.3). In all cases results were compared with those for methylaspartase isolated using 100% LB as a control.

Table 3.3: *Effect of varying medium composition on radio-label incorporation and MAL activity*

o/n culture %LB / %DMB	*main culture %LB/ %DMB*	*% Inc. cell paste*	*% Inc. crude lysate*	*Activity (μmol min^{-1})*
12.5 / 87.5	12.5 / 87.5	64.2	4.0	413
25.0 / 75.0	25.0 / 75.0	61.5	2.4	2332
100 / 0	25.0 / 75.0	60.8	13.7	1957
100 / 0	100 / 0	47.5	3.0	6166

The results show that maximum enzyme activity was obtained with a 3:1 mixture of DMB and LB in both the overnight culture and the main culture. However, interestingly, the maximum incorporation of ^{14}C into the crude extract was obtained with an overnight culture composed of 100% LB. Under these conditions, significant enzyme

activity was still observed (31% cf. 100% LB) and three times more ^{14}C were incorporated, compared to all other conditions tested.

Methylaspartase which was isolated under these conditions was purified and shown to contain 0.8% of the total radioactivity. These studies suggest that a fully enriched medium (100% LB) is required during the initial stage of cell growth, after which the use of a less nutrient rich medium leads to an increased level of ^{14}C incorporation. Despite these findings, the levels of ^{14}C observed in purified methylaspartase was still disappointing. In order then to increase the ^{14}C a defined media was used in which a pre-determined quantity of nutrients such as amino acids and sugars can be controlled.

Preparation of the alternative medium was based upon the commercially available synthetic medium 'Celtone' which is made up of all the amino acids required for protein biosynthesis. The mixture was sonicated to improve the dissolution of insoluble components and centrifuged to remove the remaining insoluble precipitate. Inorganic salts such as phosphate and glycerol, the main carbon source, were also added (see Appendix 1).

The cells were cultured under identical conditions as for that described using LB. Details of the total protein yield and methylaspartase activity are shown in Table 3.4. The values are compared to those for methylaspartase isolated under standard condition with 100% LB.

Table 3.4: *Comparison of protein expression and activity isolated under defined and un-defined conditions*

Medium	*Weight of cell paste (g)*	*Total activity ($\mu mol\ min^{-1}$)*	*Total protein (mg)*	*Spec. Activity ($\mu mol\ min^{-1}\ mg^{-1}$)*
LB	10.8	6330	202.8	31.2
'Defined'	10.5	13,640	437.2	31.1

The results show a marked increase in protein expression levels with the cells cultured in defined medium as opposed to LB. This is perhaps due to an improved availability of the amino acid primary metabolites required for protein synthesis. In undefined media (LB) certain amino acids required for protein synthesis may be deficient and consequently must be synthesised within the cell. This process may limit the rate of intracellular protein synthesis, resulting in a decreased expression level of cellular proteins, including methylaspartase.

The incorporation of ^{14}C into the enzyme was then studied using half the quantity of serine that had been used in previous studies. This was done in order to reduce the dilution of radiolabelled serine. ^{14}C-Serine was added to both the overnight culture (5 cm^3) (0.25 μCi) and the main culture (1dm^3) (5.0 μCi). Isolation of the cell pellet showed that 51% of the label had been retained in the cell paste, with 9.4% radioactivity incorporation into the crude extract. As such a two-fold improvement was observed when compared to protein isolated using LB as the culture medium. However, methylaspartase activity under these conditions was ~50% of that observed when the culture medium contained 100% serine. As a result, we were reluctant to further decrease the amount of

serine due to the effect that this could be expected to have on the activity of the expressed protein.

3.3.1 Time of radio-label addition after IPTG

Previous studies discussed above have shown that the timing of serine addition to the culture medium had a profound effect on the yield of methylaspartase activity. In a similar study, the effect on ^{14}C-incorporation into the enzyme with ^{14}C-serine was investigated.

Cultures were prepared in medium which contained serine at 50% of the levels of the remaining amino acids. ^{14}C-Serine (5.0 μCi) was then added at pre-determined times following induction with IPTG. Cells were harvested in the usual manner and ^{14}C incorporation in both the pellet and the crude extract are reported in Table 3.5.

Table 3.5: *Radioactivity incorporation after different times of label addition (defined medium)*

Time of ^{14}C addition after IPTG	*Weight of cell paste from 2 litres (g)*	*% Inc. into cell paste*	*% Inc. into lysate*
1	14.5	80	4.1
2	11.5	48	8.7
3	13.5	30	6.3

The results of the study showed that the highest percentage radioactivity incorporation into the crude extract was achieved when radiolabelled serine was added 2 hours after IPTG induction. However, purification of the enzyme from the cell pellet obtained under these conditions and analysis for ^{14}C-content, showed that despite 8.7% of the label being present in the cell paste, only 1.0% of the label has been incorporated into the enzyme. This suggests that the majority of the radiolabel has been incorporated into alternative proteins. These studies showed that only a slight improvement of ^{14}C-incorporation into methylaspartase was observed under the conditions discussed here with respect to the isolation of ^{14}C-methylaspartase using 1:3 LB/ DMB culture media.

3.3.2 Further improvement of radio-label incorporation

In an attempt to increase the ^{14}C-incorporation into the enzyme a thorough search of the literature was initiated. A procedure was discovered in which the cells were washed with a physiological buffer before the simultaneous addition of the radiolabelled amino acid and IPTG.[150] This procedure was adapted for use in our radiolabelling studies. Overnight cultures (5 cm^3) were prepared in LB media. The cultures were then transferred into fresh defined media (1L). The cells were grown to mid-log phase and centrifuged at 8000 rpm for 20 minutes. The cell pellet was washed with 59 mM sodium phosphate buffer at pH 7.6 containing 0.8% v/v saline solution. The cells were then re-suspended in defined media and shaken at 110 rpm at 37 °C. After 20 minutes ^{14}C- serine (0.5 μCi) was added along with IPTG (1 mM) and shaken for a further 3 hours, prior to harvesting by centrifugation.

Analysis of the ^{14}C-incorporation into the cell paste and crude extract showed that no increase had been achieved with this method. However, analysis of purified methylaspartase showed that the ^{14}C-incorporation had increased from 1% (from previous experiments) to 2.5%.

This result suggests that rinsing of the cells to remove excess unlabelled serine prior to addition of the radiolabelled material does result in a significant increase in the levels of ^{14}C incorporation into purified methylaspartase.

In conclusion, these studies have shown that a maximum incorporation of ^{14}C into pure methylaspartase of 2.5% was achieved by using LB media for the overnight culture (5 cm^3) and a defined media containing half equivalent of serine (Appendix 1) for the main culture (1L). Removal of excess unlabelled serine by rinsing the cells immediately prior to the addition of ^{14}C-serine 2 hours after induction with IPTG, increased the incorporation of the radiolabel.

3.4 ^{13}C-Labelling of the active-site of methylaspartase

Having established the optimal conditions for the incorporation of labelled serine into purified methylaspartase, ^{14}C-serine was exchanged with [1-^{13}C]-(2*S*)-serine in preparation for ^{13}C NMR studies.

^{13}C-Labelled methylaspartase was prepared under the conditions described above using [1-^{13}C]- (2*S*)-serine. A 1L culture afforded 7 grams of wet cell paste, which after purification by nickel chelation chromatography gave 5 mg of >90% homogeneous

methylaspartase (judged by SDS-PAGE analysis) with a specific activity of 206 units/ mg.

3.5 Analysis of ^{13}C-labelled methylaspartase by NMR spectroscopy

The purified, labelled enzyme was prepared for NMR analysis by adding 10% deuterium oxide to the buffered solution (50 mM potassium phosphate, 10 mM potassium chloride, 1 mM magnesium chloride hexahydrate, pH 7.0).

Trypsin was added to the NMR sample and a ^{1}H-NMR time-course profile of the digestion was recorded over 2 hours. Figure 3.1 shows the ^{1}H-NMR spectra at various time intervals during the digestion period.

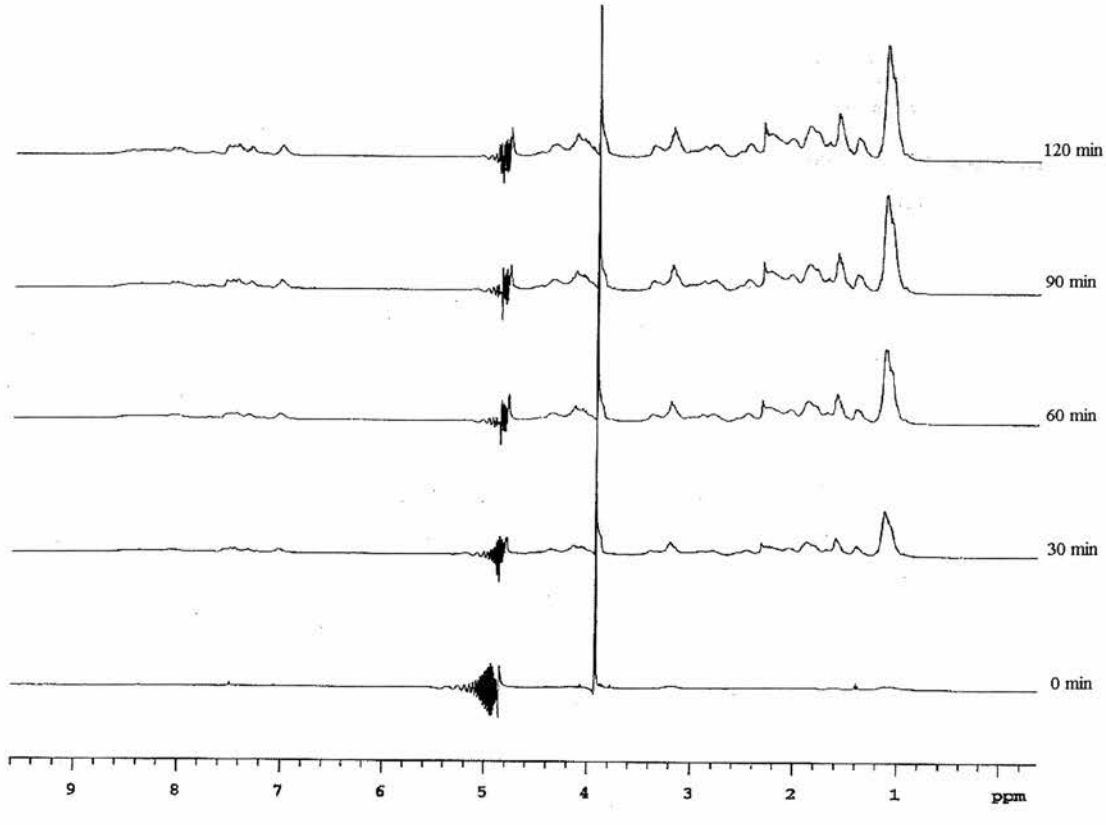

Figure 3.1: *Stacked ^{1}H-NMR spectra at time intervals during digestion of ^{13}C-labelled methylapartase*

An improvement in spectral resolution and band sharpening was observed over the time course of the experiment. However, the complicated nature of the spectrum and signal overlap precluded a detailed analysis of the digest mixture by ^{1}H- NMR spectroscopy. Consequently a two-dimensional HMQC (heteronuclear multiple-quantum resonance experiment with ^{1}H detection) spectrum was performed with the intention of establishing which hydrogen atoms were attached to specific ^{13}C-atoms (Fig. 3.2). This can be achieved since a spin coupling system exists between ^{1}H protons and ^{13}C atoms through a covalent bond. The magnetisation which is applied to the adjacent protons, can then be coupled to the ^{13}C-nuclei and subsequently back to the protons. Alternative heteronuclear correlation experiments exist. However, in many cases, a limitation is observed which is associated with the reduced sensitivity of ^{13}C detection (50 times less sensitive than for proton). An HMQC experiment avoids the problems with sensitivity since both excitation and detection are carried out on protons, maintaining maximal sensitivity throughout the experiment, despite transfer of the magnetisation onto an adjacent ^{13}C-nucleus. This sensitivity could be further increased by using specifically enriched protein, which would result in highlighting the proton environment of the ^{13}C-label, in the case of methylaspartase, serine and dehydroalanine.

Since the residue of interest was an unsaturated dehydroalanine residue, the ^{1}H resonance would be in the 5-6 ppm range and the ^{13}C resonance in the 100-120 ppm region of the spectrum.

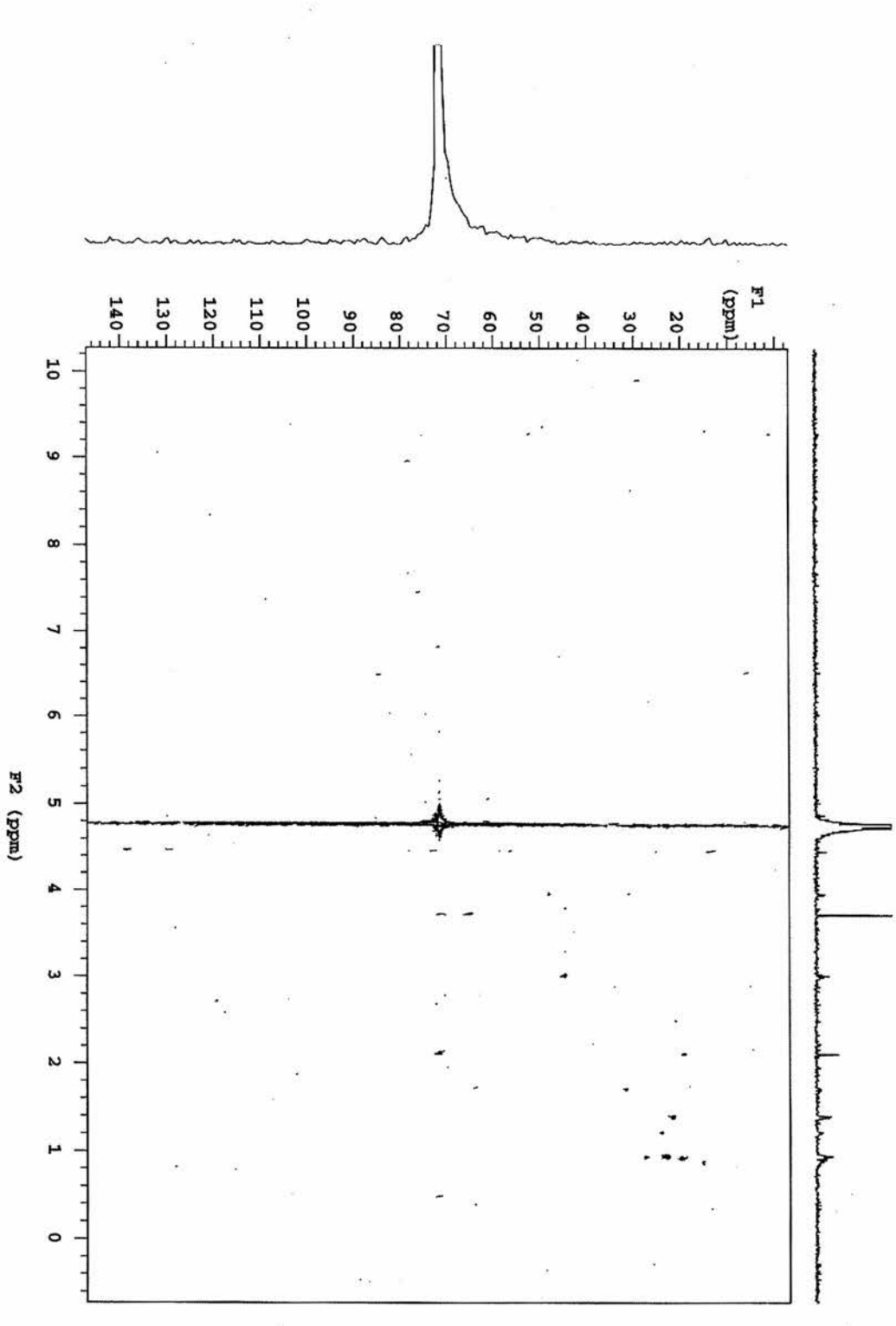

Figure 3.2: *Heteronuclear HMQC of tryptic digest of ^{13}C-labelled methylaspartase*

The HMQC spectrum was acquired and analysis of the 2D-spectrum showed that the majority of signals were observed in the high field region of the spectrum (< 4 ppm in ^{1}H dimension and < 70 ppm in the ^{13}C dimension). These were attributed to the chemical shifts for the α-protons and α-carbon atoms of saturated residues such as alanine, valine, leucine, isoleucine, methionine and serine.

This result suggested that the ^{13}C-label had been incorporated into a range of amino acids, most probably derived from the *in vivo* metabolism of ^{13}C-serine. The primary labelled metabolites are then introduced into the bio-synthetic pathways for a number of amino acids. In addition signals corresponding to the double bond of a dehydroalanine, which were expected to appear between 5-6 ppm in the ^{1}H spectrum, were not observed. This may be explained by insufficient ^{13}C-labelling at the dehydroalanine residue, resulting in a low sensitivity. Secondly, over the time course of the experiment the dehydroalanine residue may have undergone rehydration to afford ^{13}C-serine. If this were the case then the labelled residue would give rise to ^{1}H-chemical shifts in the high field region of the 2D-NMR spectrum (5-6 ppm). This would make it extremely difficult to differentiate between the active site serine residue and the other six serine residues which are known to occur in the primary sequence of the enzyme.

3.6 Conclusions

These studies have shown that it has not been possible to selectively enrich a specific amino acid by incorporating the label into the growth media. Consequent NMR spectroscopic analysis of digested labelled protein, has not been successful in establishing the presence of a dehydroalanine residue.

Chapter 4 : Application of Solid-Phase-Specific Inhibitors to Probe the Active Site of Methylaspartase

The ammonia-lyase enzymes HAL and PAL, are both known to be inactivated by a variety of nucleophiles including cyanide and borohydride.[66, 75, 107] Analysis of the site of modification by Edman degradation has provided compelling evidence for the involvement of the postulated dehydroalanine residue in the mechanism of ammonia elimination. With methylaspartase, both cyanide and borohydride are known to have no effect on the enzyme, however, a range of hydrazine analogues, have been shown to act as irreversible inhibitors.[61] Furthermore, inhibition was directed towards the active site, since the presence of substrate in the inactivation experiment lead to the protection of the enzyme. Table 4.1 shows the kinetic properties of hydrazine inhibition.

Table 4.1: *Kinetics of hydrazine inhibition of methylaspartase*

Substrate/ Inhibitor	K_i / K_m
(2*S*,3*S*)-3-methylaspartic acid	2.3 mM
Hydrazine	23.1 mM

The mode of inhibition was thought to be nucleophilic addition of the primary amine nitrogen of the hydrazine to either the β-carbon of the postulated dehydroalanine in a conjugate, Michael type addition, or at the α-carbon in a 1,2-addition mechanism (Scheme 4.1).

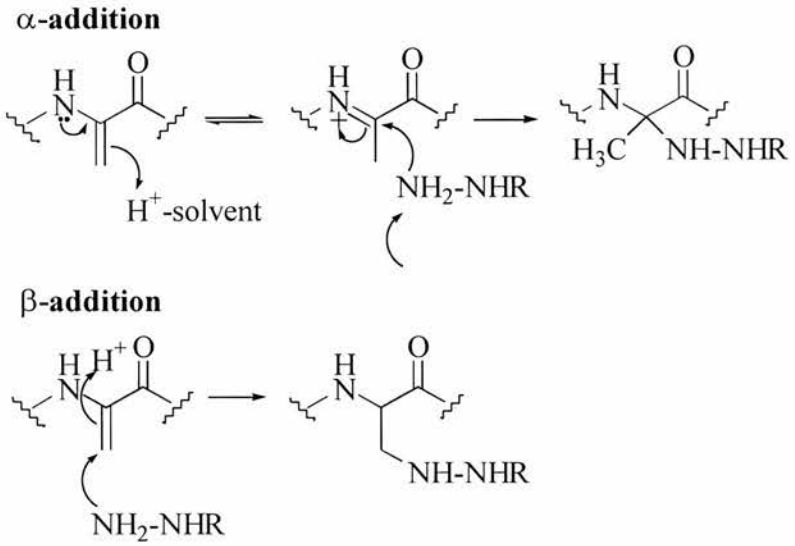

Scheme 4.1: *Proposed mechanisms of addition of hydrazines to the putative active site dehydroalanine residue of methylaspartase*

Attempts to characterise the site of modification, using radiolabelled phenylhydrazine or phenylhydrazine containing a ^{15}N-NMR label, gave rise to results which were difficult to understand and rationalise, given the compelling kinetic evidence in support of a dehydroalanine and the observation of irreversible inhibition with both of the labelled hydrazines (For a full discussion see chapter 5).

In an attempt to isolate and characterise the modified amino acid, a strategy was designed in which an analogue of the hydrazine would be attached to a solid support; effectively resulting in an affinity resin. Enzyme bound to the solid support could then be subjected to digestion with a protease to strip away the bulk of the protein, leaving a single peptide, covalently attached to the resin *via* the site of modification by the hydrazine analogue.

4.1 Design of a solid phase inhibitor

The skeleton for the desired inhibitor, which is shown in Figure 4.1, comprises a solid polymeric support attached to a hydrazide analogue *via* an intermediary linker.

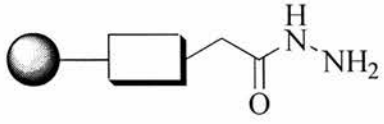

Figure 4.1: *Solid support for hydrazide analogue*

The role of the linker would be to allow the hydrazide functionality to gain access to the active site of the enzyme.

As such, it was anticipated that the linker should fix the hydrazide at a significant distance from the bulky resin support and have the appropriate steric bulk and flexibility to allow the hydrazide to access the active site dehydroalanine residue.

Previous studies with substrate analogues used to probe the specificity and spatial geometry of the active site, concluded that the enzyme could accommodate un-branched, alkyl substituents such as ethyl and n-propyl.[56] However, groups such as iso-propyl were not accepted. Consequently, it was anticipated that the most appropriate linker structure would be a simple alkyl chain. As the reaction between the solid phase inhibitor and the enzyme was to be carried out under aqueous conditions, the linker structure was adopted to incorporate a polyethylene glycol chain, with the aim of avoiding aggregation of the linker, which may well occur with a large hydrophobic alkyl chain. The hydrazide functionality was then attached to the solid support *via* an activated carboxylic acid, resulting in a hydrazide group.

The desired properties of the solid support resin were to include good swelling across a wide range of solvents, including water in which the inhibition reaction would be carried out, in addition to organic solvents, thus allowing the simple preparation of the resin bound hydrazide. Consequently, Tentagel resin was selected which possesses a polyethylene glycol linker unit (PEG). The linker is soluble in almost, all organic solvents which leads to a high degree of mobility of the PEG chain and consequently the attached inhibitor.[151] Due to such properties, which are not common in resins, tentagel has reported uses in combinatorial synthesis of compound libraries, where organic solvents are used, followed by assays in aqueous media (Scheme 4.2, **96**).[152]

Before embarking on the solid phase synthesis of the PEG hydrazide, the inhibition properties of a solution phase equivalent (3,6-dioxaoctanedioate hydrazide; **96**) were assessed (Scheme 4.2).

4.1.1 Synthesis of a solution phase mimic

3,6-Dioxaoctanedioic acid (**94**) was esterified with diazomethane to afford a pale yellow oil (**95**) in 63% yield, which upon treatment with hydrazine hydrate in methanol gave the hydrazide (**96**) as a white crystalline solid in 40% yield (mp 132-133 °C) (Scheme 4.2). This compound displayed the expected ^{1}H and ^{13}C NMR spectra for the desired 3,6-dioxaoctanedioic acid hydrazide (**96**).

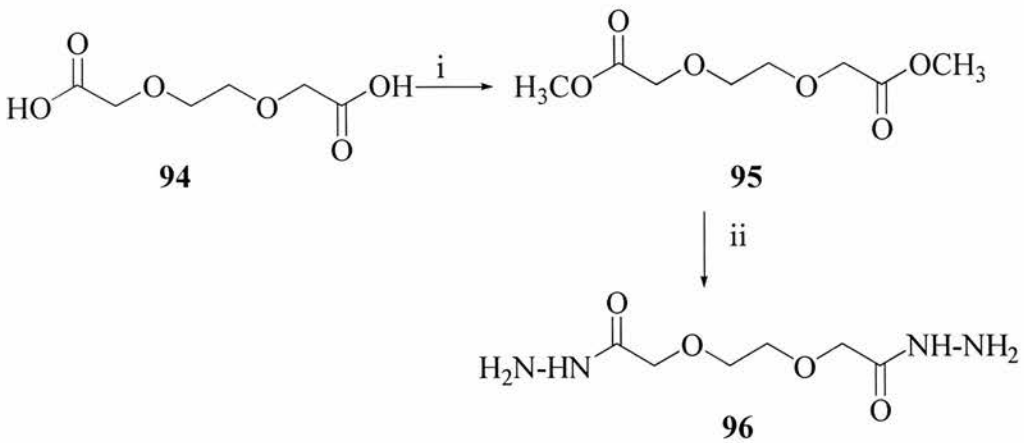

Reagents: i CH_2N_2, THF; ii NH_2-NH_2.H_2O, MeOH

Scheme 4.2: *Synthesis of the solution phase hydrazide*

Methylaspartase was incubated with the potential irreversible inhibitor at a final concentration of 1 mM and aliquots were removed with time, to determine the amount of enzyme activity remaining. The results show that all activity was lost within 75 hours (Fig. 4.2). Dialysis of the inhibited protein failed to restore activity, consistent with 3,6-dioxaoctanedioic acid hydrazide acting as a slow, time-dependent, irreversible inhibitor. Inclusion of 0.5M substrate in the inhibition incubation, completely protected the enzyme from inactivation, indicating that the inhibitor was directed to the active site of the enzyme.

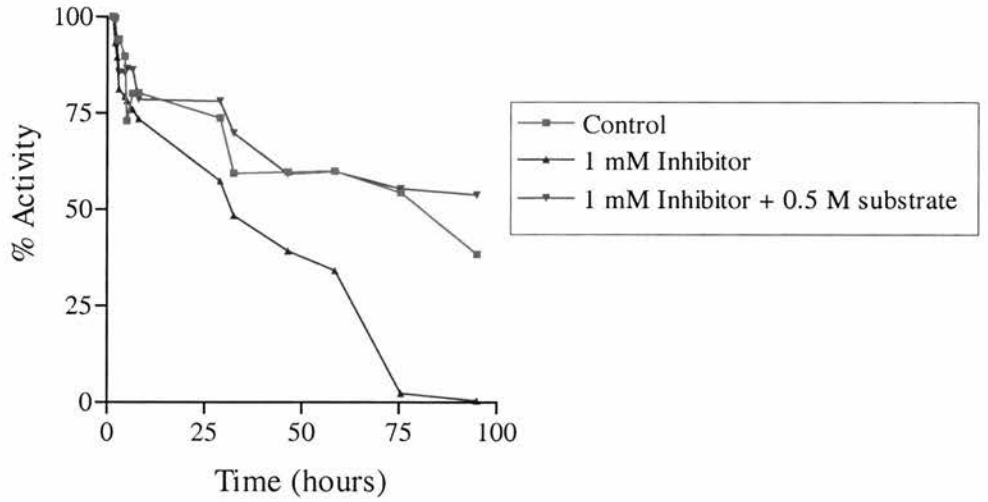

Figure 4.2: *Substrate protection of MAL inhibition by hydrazide inhibitor (**96**)*

4.1.2 Synthesis of a solid phase inhibitor

Having established that 3,6-dioxaoctanedioic acid hydrazide (**96**) acted as an active site directed, irreversible inhibitor, we decided to prepare its solid-phase analogue.

Tentagel resin (**97**) with the terminal acid functionality was pre-treated with a solution of trifluoroacetic acid (0.5%), in order to remove any traces of base remaining from preparation of the acid functionalised resin.

The carboxylic acid resin (**97**) was then stirred overnight in a solution of diazomethane in THF and ether (Scheme 4.3). The carboxy ester resin was analysed by ^{1}H-NMR spectroscopy and showed a broad signal between 3-4 ppm, which is due to the more solvent accessible PEG side chains of the matrix.[151] Unfortunately if a ^{1}H-signal corresponding to the OCH_3 group of the intermediate ester was present at ~3.7 ppm, it was completely masked (**95**, Scheme 4.2). Analysis of the solid phase ester by ^{13}C-NMR spectroscopy did not yield any further information. The ^{13}C-NMR spectrum of both the

acid and the ester showed only a sharp signal at 70.77 ppm which was due to the polyethylene glycol back bone of the resin.[152] In addition we were unable to observe signals between 160-180 ppm corresponding to the carbonyl group of the ester. This was attributed to the low loading of the resin (0.26 mmole gram) coupled with the inherent insensitivity of detecting ^{13}C-nuclei.[153]

As infrared spectroscopy has been used successfully to characterise functionalised resins [154, 155] we decided to analyse the solid phase ester using this technique. IR analyses was performed using potassium bromide discs and the spectrum was recorded immediately after pressing as decompaction was seen to have a negative effect on the resolution of the spectrum obtained. Figure 4.3 shows the infrared spectra of the tentagel carboxy resin and the ester resin. A small increase in the frequency of the carbonyl band was observed after esterification (1700 cm^{-1}) compared to the carboxylic acid precursor (1625 cm^{-1}).

Treatment of the ester (**98**) with hydrazine hydrate in methanol under reflux resulted in the desired hydrazide resin (**99**).

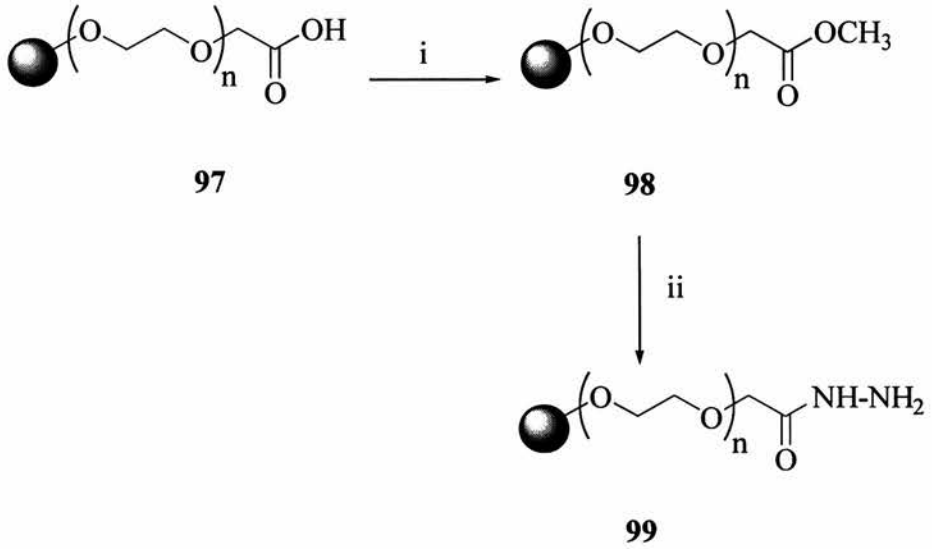

97 **98** **99**

Reagents: i CH_2N_2, THF/ ether, 12h, ii NH_2-$NH_2.H_2O$, MeOH, 60°C

Scheme 4.3: *Synthesis of the solid phase hydrazide inhibitor*

Analysis of the resin after hydrazinolysis showed that the carbonyl band had shifted to a lower frequency than that of the ester (1701 cm^{-1}) (Fig. 4.3).

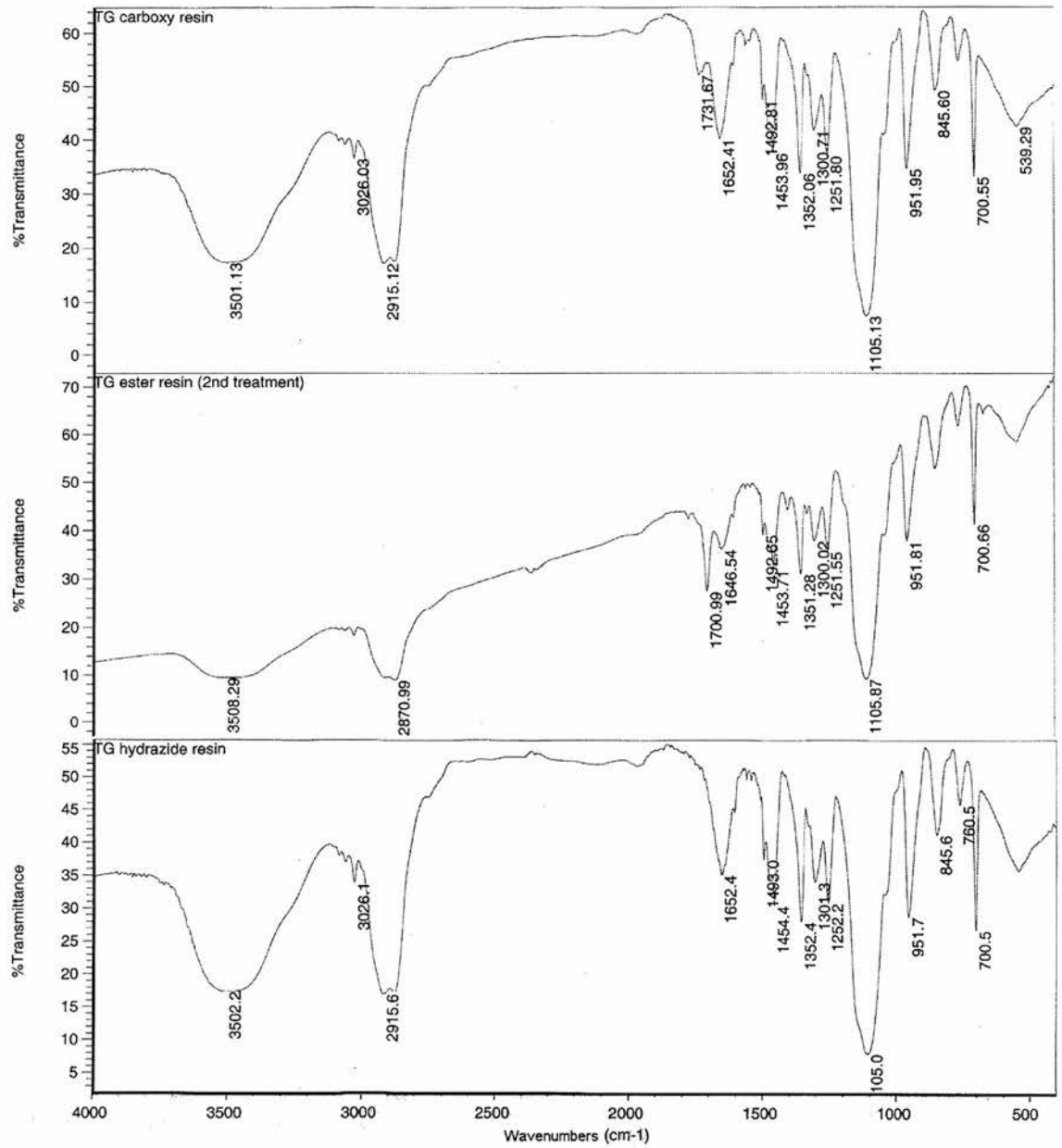

Figure 4.3: *Infrared spectra for solid phase acid (**97**), ester (**98**) and hydrazide (**99**)*

Further evidence for the hydrazide functionalised resin was obtained by microanalysis, which showed that nitrogen had been incorporated into the functionalised resin. Calculations based on this analysis gave an estimated resin loading of 0.24 mmol/g.

4.1.3 Characterisation of the solution phase and solid phase inhibitor

The inhibition properties of the solid phase hydrazide were determined by incubating methylaspartase with a 50 mM final concentration of hydrazide inhibitor (based on 0.24 mmol/ g loading). Aliquots of the enzyme were removed at regular intervals and methylaspartase activity was determined. In order to directly compare the effects of the solid phase versus the solution phase hydrazide, the experiment was repeated in the absence of any inhibitor (control) and with 50 mM 3,6-dioxaoctanedioic acid hydrazide (Fig. 4.4).

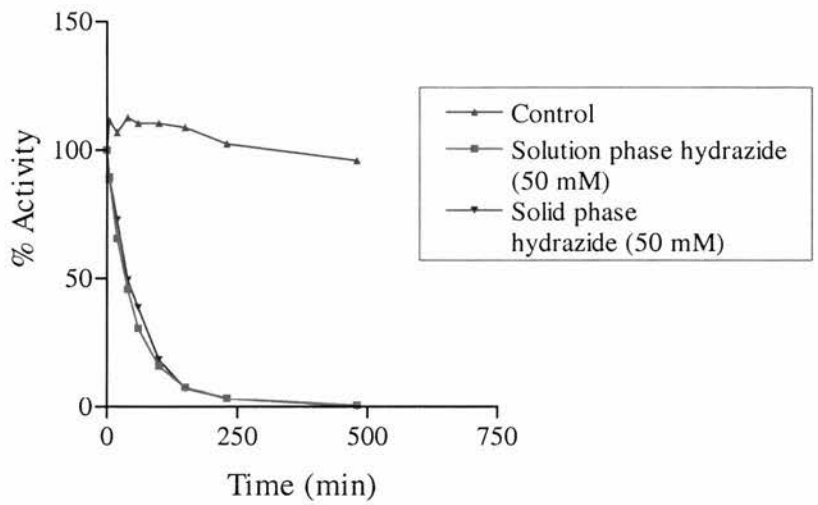

Figure 4.4: *Comparison of inhibition profile of solution phase and solid phase hydrazide with methylaspartase*

The results, which are shown in Figure 4.4, show that both the solution phase and solid phase versions of the hydrazide inhibitor effect 90% inhibition at 250 minutes. This suggests that the presence of the PEG linker and solid support have no adverse effect on the inhibition process and consequently that the hydrazide was still able to access the active site of the enzyme.

In a repeat experiment, methylaspartase (5 mg) was incubated with the solid phase hydrazide (**99**) (200 mg, 0.24 mmol/ g final conc). After 24 hours a 90% decrease in activity had been observed and the solid support was subsequently rinsed with 50 mM Tris buffer at pH 9 in order to remove excess unbound protein from the resin. In order to determine the amount of methylaspartase immobilised onto the solid support, the washings were pooled, analysed by Bradford assay and compared to the protein concentration at the beginning of the experiment (Table 4.2).

Table 4.2: *Typical loadings of methylaspartase onto solid support*

Weight of resin (mg)	*Total protein immobilised) (mg)*	*Concentration (mmole/ g)*
100	1.20	1.3×10^{-8}
250	3.10	1.3×10^{-8}

The results showed that 12 mg of protein/ g of resin had bound, corresponding to about 0.05% of the hydrazide binding sites being occupied. This probably reflects the steric bulk of protein, which binds to the functionalised resin.

In order to determine whether methylaspartase had been irreversibly attached to the solid support, the resin was then suspended in a solution of ammonium chloride (0.4 M) in 50 mM Tris buffer at pH 9. It was anticipated that if reversible inhibition was occurring, then high concentrations of ammonia should displace the enzyme from the support. After 24 hours the protein concentration in the buffer was determined by the method of Bradford and was found to be less than 0.1% of the total protein concentration

at the beginning of the experiment.[156] This indicated that under these conditions, no bound protein was removed from the resin.

4.2 Peptide mapping studies of immobilised methylaspartase

Having irreversibly bound the protein to the solid support, attempts were made to strip away the bulk of the protein with the protease enzyme trypsin. It was anticipated that this would leave the active site peptide, containing the dehydroalanine residue bound to the support. Comparisons between the unbound protein bulk could then be made with non-inhibited protein digests in an attempt to identify the bound peptide.

Immobilised methylaspartase was denatured by heating to 100 °C for 15 minutes and subjected to digestion with the protease enzyme trypsin at 2.5% w/w which is known to hydrolyse the amide bond at the C-terminus of the basic residues, lysine and arginine. After 6 hours, the resin was washed thoroughly with water to remove the unbound tryptic peptides.

The unbound tryptic peptide mixture was analysed by reversed-phase C18 HPLC and the elution profile compared to a tryptic digest of native methylaspartase (Fig. 4.5).

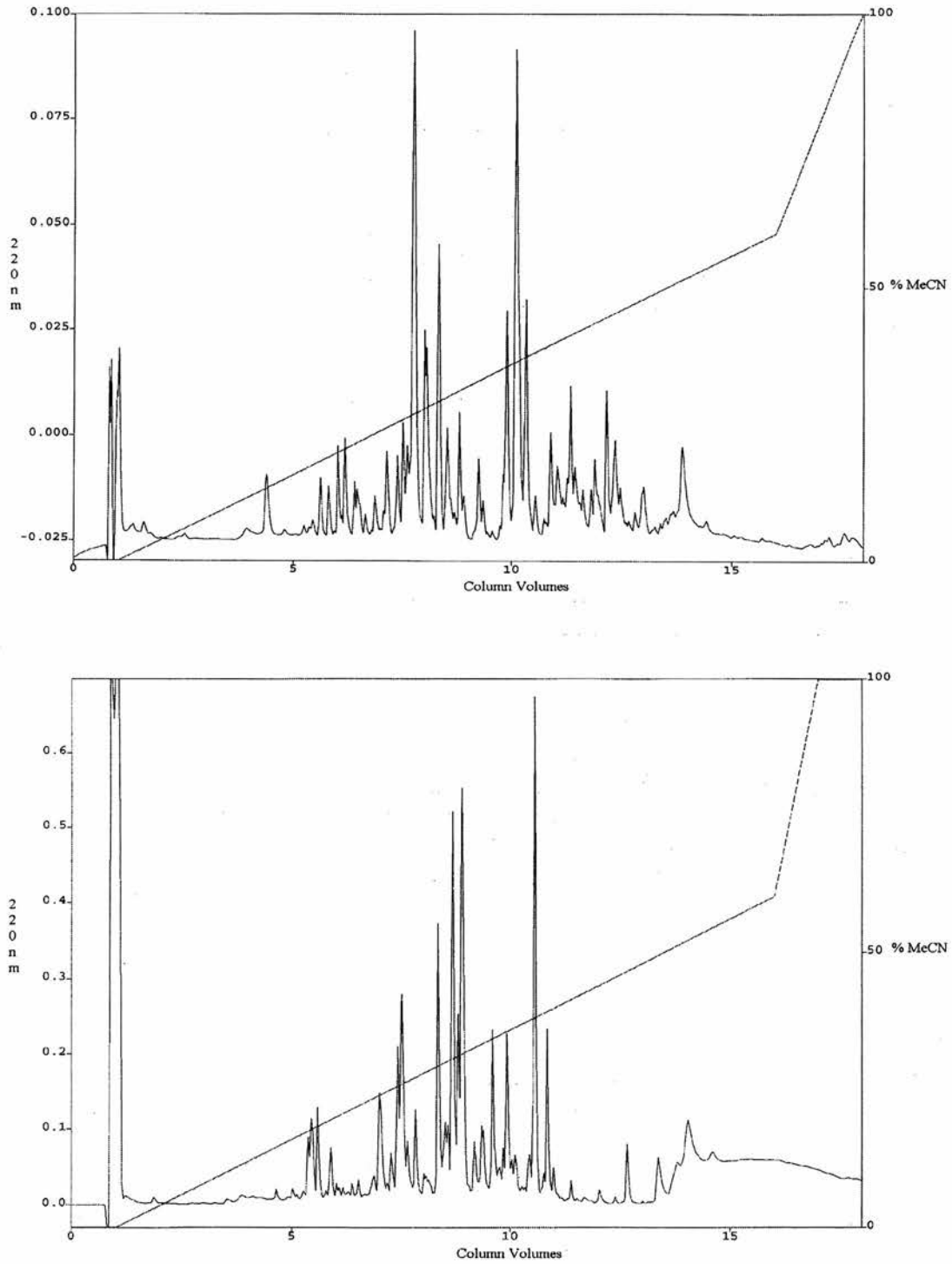

Figure 4.5: *Reversed-Phase HPLC trace (220 nm) for tryptic digest of native methylaspartase (upper profile) and immobilised methylaspartase (lower profile)*

Whilst it was hoped that a comparison of the two elution profiles would highlight a missing peak from the solid-phase inhibited protein, in reality the results show that the profiles are extremely complex and different throughout the elution. In addition, it has been shown within the group, that elution profiles from different digest experiments of the same protein are never identical.[65] This most probably occurs either as a result of incomplete digestion or the presence of additional proteases such as chymotrypsin. Therefore, practically identifying a single peak proved to be too difficult.

4.2.1 Digestion of immobilised methylaspartase with V8 protease

In an attempt to simplify the elution profile of digested protein, the alternative protease V8 was used. This protease from *Staphylococcus aureus* is known to cleave specifically at the C-terminus of glutamic acid at pH 4. Native methylaspartase was treated with the protease and the HPLC elution profile obtained. The results show the presence of about 30 peaks and not the 26 anticipated (based on number of glutamic acid residues) (Fig. 4.6).

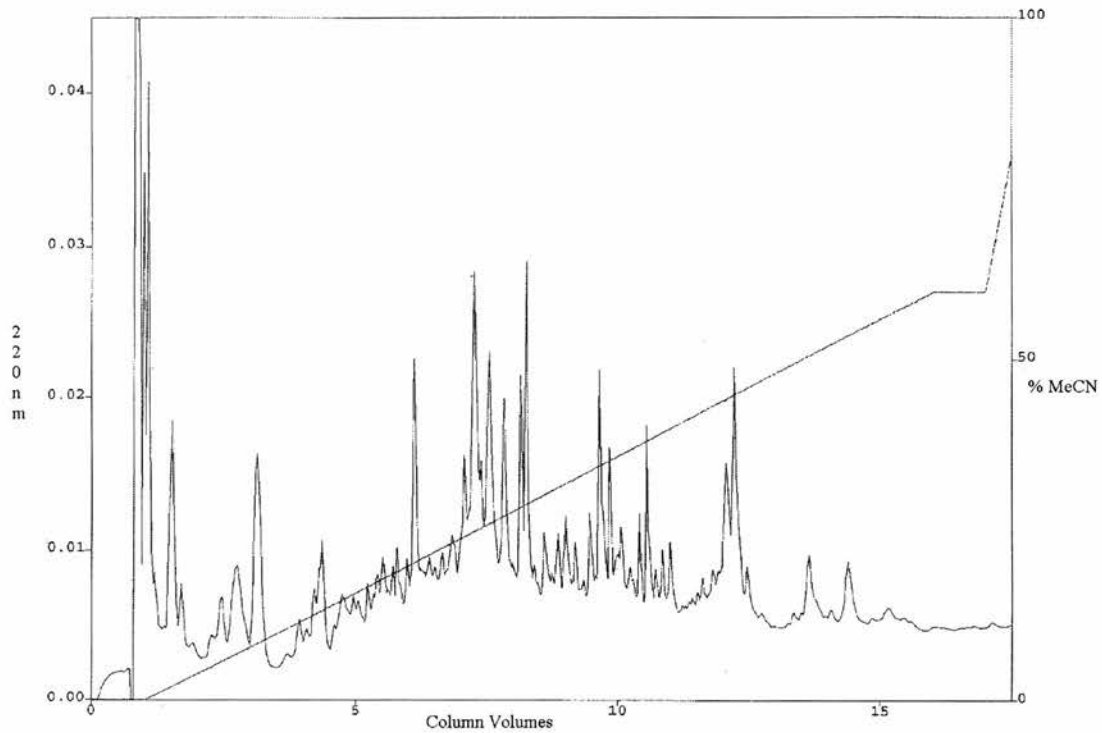

Figure 4.6: *C18-RP-HPLC profile of V8 digest of immobilised methylaspartase*

This may be due to a lack of protease specificity or the presence of a second protease activity in the sample or auto-proteolysis of V8 itself. Further attempts to simplify the HPLC profile by limited tryptic digestion also proved unsuccessful.

4.3 Cleavage of the immobilised active site derived peptide

Having established that intact methylaspartase was bound irreversibly to the resin and that treatment with a protease resulted in removal of the bulk protein, it was assumed that the active site peptide was still attached to the resin. Although it had not been possible to observe the absence of this peptide from tryptic digests, it was anticipated that

a chemical cleavage of the hydrazide bound peptide from the resin would afford the free peptide, which could be visualised and characterised by HPLC.

4.3.1 Cleavage using sodium hydroxide

In the proposed catalytic mechanism of methylaspartase, following elimination of ammonia from methylaspartic acid, regeneration of the putative dehydroalanine residue is initiated with a deprotonation of the polypeptide backbone and concerted elimination of ammonia (Scheme 1.18). It was anticipated that in an analogous mechanism aqueous sodium hydroxide would catalyse the removal of the same backbone proton resulting in concerted cleavage of the C-N peptide-hydrazide bond.

Resin which had been treated with methylaspartase and digested with trypsin was added to an aqueous solution of sodium hydroxide (1 M) and left at room temperature for 2-3 hours and washed with water. The combined washings were analysed by C18 RP-HPLC. The resulting elution profile showed one major peak with a retention volume of 11.0 CV, which was isolated and upon treatment with ninhydrin gave rise to a pink spot consistent with the presence of a peptide (Fig. 4.7).

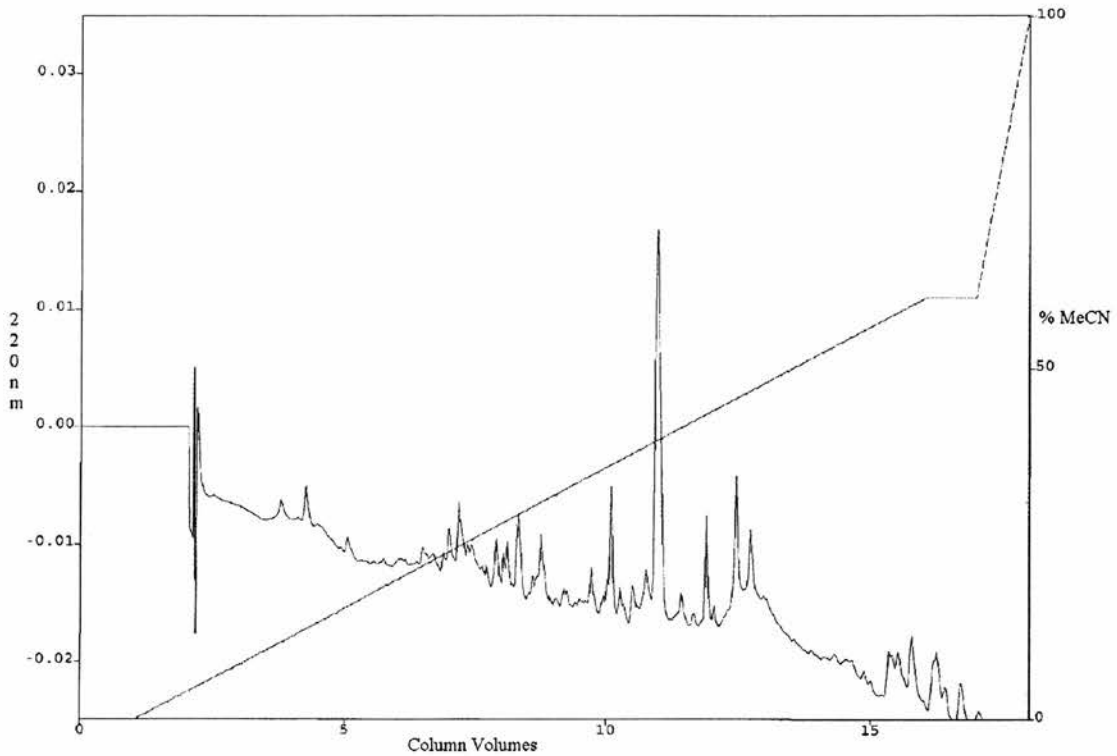

Figure 4.7: *C18 RP-HPLC elution profile for cleavage of peptide using sodium hydroxide*

The sample was submitted for N-terminal amino acid sequencing and was found to contain only minor impurities.

Alternative methods of removing the peptide from the resin were associated with reductive cleavage of the N-N hydrazide bond as shown in Figure 4.8 in blue.

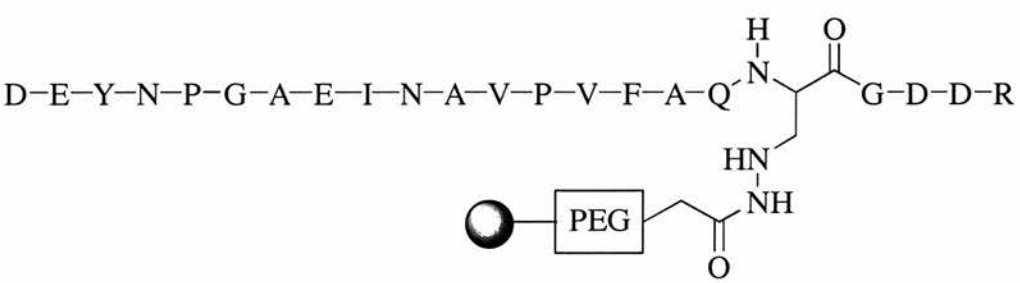

100

Figure 4.8: *Active-site derived peptide attached to the solid support*

Dissolving metal reduction: A sample of resin (**100**) (200 mg) which had been treated with methylaspartase and trypsin was stirred for 1 hour in liquid ammonia whilst sodium metal was added and a dark blue colour persisted. The reaction was quenched by the addition of methanol and water. The mixture was neutralised by adding hydrochloric acid and then lyophilised overnight, prior to analysis by C18 RP-HPLC. The presence of one major peak was observed with a retention volume of 13.69 CV. Again this gave rise to a pink spot on treatment with ninhydrin, however, no peptide was observed by Edman degradation.

Catalytic hydrogenation: For this application palladium on charcoal was selected as the catalyst, as it is known that a simple filtration will remove it from the reaction mixture. It was anticipated that problems with solid/solid reactions between the catalyst and the resin might affect the efficiency of the reaction. These interactions at the catalyst/substrate interface were minimised by the use of the highly soluble PEG linker, which renders the bound peptide susbtrate more solvent accessible. In addition an excess of the catalyst was used.

Resin (25 mg) which had been treated with methylaspartase and trypsin was stirred overnight in the presence of the catalyst and hydrogen gas. The catalyst was removed by filtration and the supernatant liquor lyophilised and analysed by C18 RP-HPLC (Fig. 4.9).

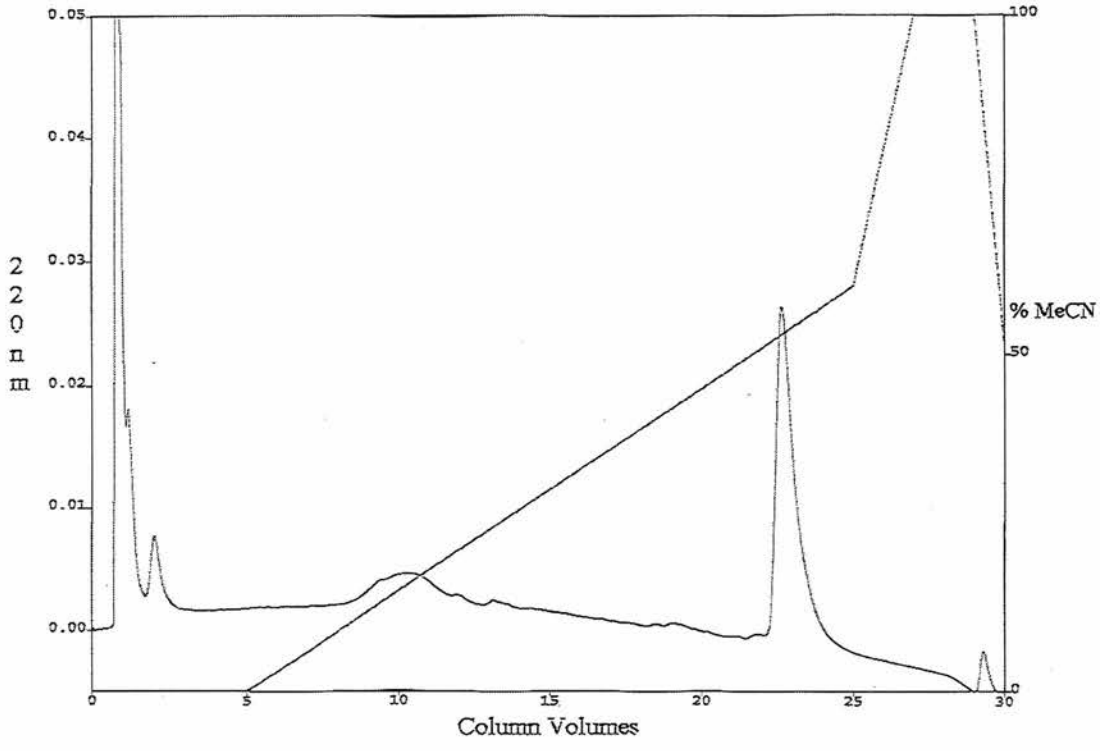

Figure 4.9: *HPLC profile of peptide cleaved from solid support by catalytic hydrogenation*

One major peak was observed in the resulting HPLC profile with a retention volume of 22.75 CV, however, analysis by Edman degradation failed to show the presence of a cleaved peptide.

4.3.2 Cleavage using an alternative catalyst ($(PPh_3)_3Rh(I)Cl$)

Although its application in the cleavage of N-N bonds had not been reported, it was thought that this catalyst would be able to effect the reduction.

In order to establish whether these conditions were capable of cleaving an N-N bond, a preliminary test reaction was carried out using the solution phase hydrazide. A

sample of 3,6-dioxaoctanedioic acid hydrazide (**96**) (25 mg) was stirred overnight in the presence of the catalyst and under an atmosphere of hydrogen gas. The catalyst was removed by filtration and lyophilised. Analysis of the reaction mixture by ^{1}H-NMR showed the appearance of new signals in the range 3.6-3.9 ppm which were not observed in the ^{1}H-NMR spectrum of the solution phase hydrazide at the beginning of the reaction. However, due to the complexity of the reaction mixture it was not possible to determine whether the N-N bond had in fact been cleaved.

A sample of the resin (25 mg) which had been treated with methylaspartase and trypsin was stirred overnight in the presence of Wilkinsons catalyst under an atmosphere of hydrogen gas. Analysis of the cleavage mixture by C18 RP-HPLC failed to show any peak in the elution profile and therefore suggested that no peptide was present.

4.3.3 Cleavage using V8 protease

An alternative method of identifying the peptide bound to the resin was investigated, which involved cleaving the peptide mid-way through the sequence with a second specific protease, V8 from *Staphylococcus aureus.* This was chosen as the protease specifically hydrolyses amide bonds at the C-terminus of glutamic acid residues (pH 4) and as such, it was anticipated that the immobilised peptide would be cleaved into two short peptides as shown in Fig. 4.10. These could then be separated by C18 RP-HPLC and analysed by Edman degradation.

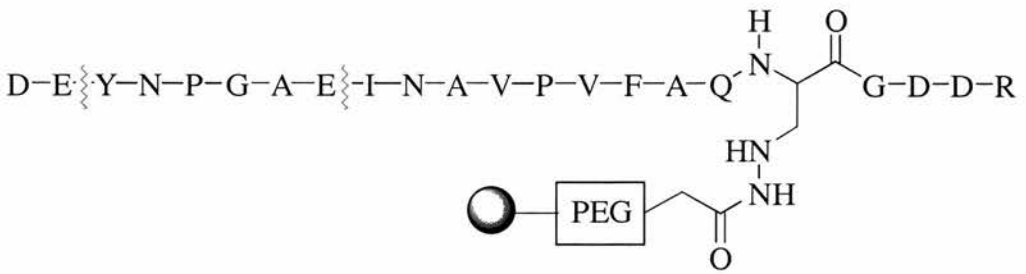

Figure 4.10: *Cleavage of the immobilised peptide by V8 protease*

A sample of solid phase hydrazide (**99**) (200 mg), which had been treated with methylaspartase and trypsin was suspended in a solution of ammonium acetate (100 mM) in 50 mM Tris buffer at pH 4.0. V8 protease (Staphylococcus aureus) was then added (in equal amounts to 2.0 % by weight of peptide). After 18 hours the enzyme was denatured by addition of hydrochloric acid and the sample lyophilised.

Analysis of the cleavage mixture by C18 RP-HPLC gave rise to two major peaks with retention volumes of 12.37 CV and 12.84 CV. However, sequence analysis by Edman degradation failed to identify the presence of any peptides.

Having shown that methylaspartase was irreversibly binding to the resin, all attempts to isolate and identify a single peptide attached to the resin following tryptic cleavage proved unsuccessful.

It was proposed that failure to cleave a peptide from the resin, might be a result of premature release of the peptide during proteolysis. This could arise as a result of loss of the tertiary structure of the protein bulk, allowing water to access the scissile N-N bond. A plausible mechanism for elimination of the peptide is shown in Scheme 4.4 (see also section 5.3, schemes 5.2, 5.3a and 5.3b).

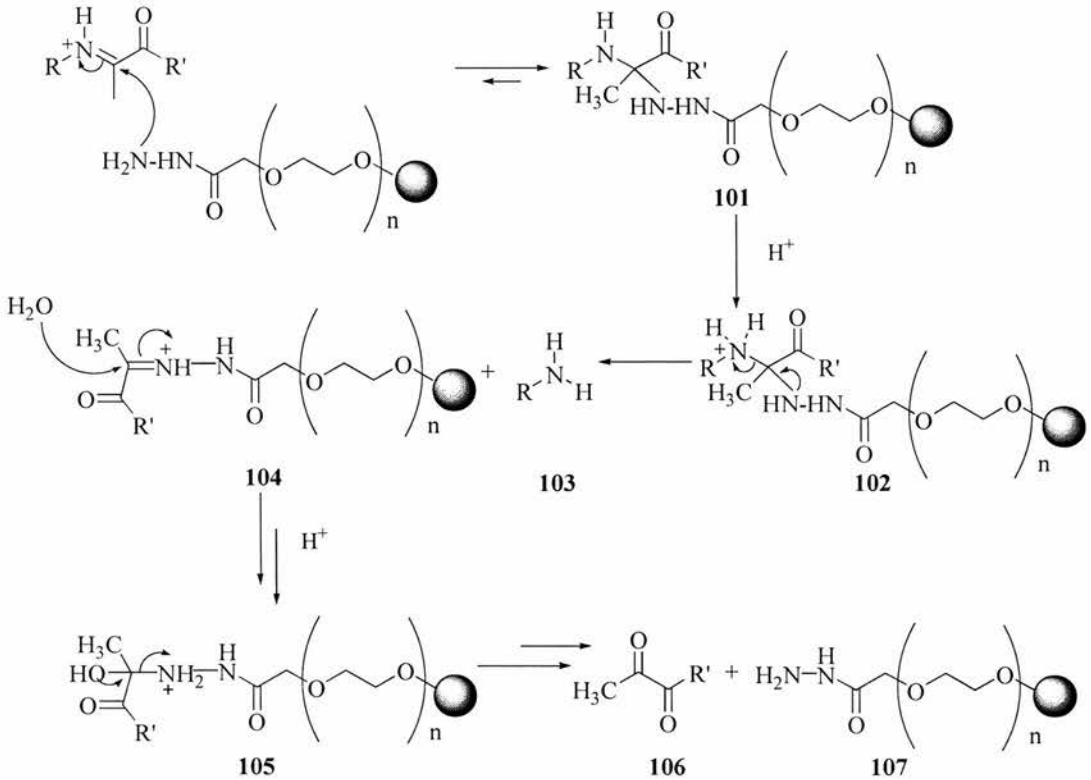

Scheme 4.4: *Mechanism for proposed active-site ketone formation*

1,2-Addition of the solid phase hydrazide proceeds with α-addition to the dehydroalanine residue (Scheme 4.4). Protonation of the backbone nitrogen enables the lone pair of electrons on what was the primary nitrogen of the free hydrazide to feed into the system, cleaving the peptide backbone, to give the corresponding amine (**103**) and an iminium intermediate (**104**). The iminium ion can then undergo hydrolysis to afford the α-hydroxy hydrazine (**105**), which dissociates to afford the β-diketone (**106**) and the original resin bound hydrazide (**107**) (Scheme 4.4).

4.4 Conclusions

Evidence has been obtained which supports the involvement of an electrophilic residue at the active-site of methylaspartase. However, attempts to probe the nature of the residue, using a solid-phase inhibitor designed specifically to target the active site have failed to shed any light on the identity of the amino acid.

Chapter 5 : Probing the Active Site of Methylaspartase with Irreversible Inhibitors

Previous studies described in Chapter 4 have shown that methylaspartase can be irreversibly bound to a solid phase supported alkyl hydrazide. Following digestion with trypsin, however, no solid phase bound peptide could be detected.

In order to understand the mechanism of this seemingly reversible covalent bond formation between the enzyme and the solid phase inhibitor, a series of detailed studies were initiated in order to characterise the inhibition of methylaspartase by a series of simple hydrazine and hydrazide inhibitors.

5.1 Acetyl hydrazide as a potential inhibitor of methylaspartase

The simplest mimic of the solid phase hydrazide inhibitor was acetyl hydrazide and as such the concentration dependence of inhibition of methylaspartase by acetyl hydrazide was studied in Tris buffer at pH 9.0 and at 30 °C (Fig. 5.1a).

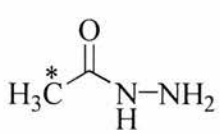

108 *Acetyl hydrazide*

The results which are shown in Figure 5.1, show that the rate of inhibition is concentration dependent.

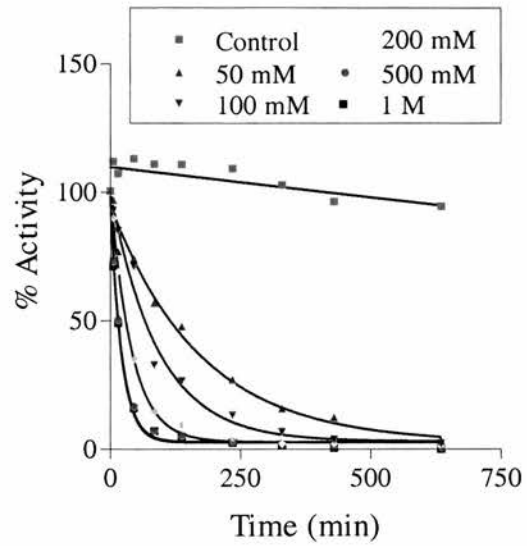

Figure 5.1: *Concentration dependence of inhibition of methylaspartase by acetyl hydrazide*

Incubation of methylaspartase with the natural substrate (2*S*,3*S*)-3-methylaspartic acid at a concentration of 0.5 M prior to addition of 200 mM acetyl hydrazide afforded complete protection of methylaspartase from inhibition (Fig. 5.2). This observation of substrate protection, supports the proposal that inhibition by acetyl hydrazide is directed at or near the active site of the enzyme, presumably in a mechanism similar to the solid phase inhibitor, potentially involving the postulated active site dehydroalanine residue.

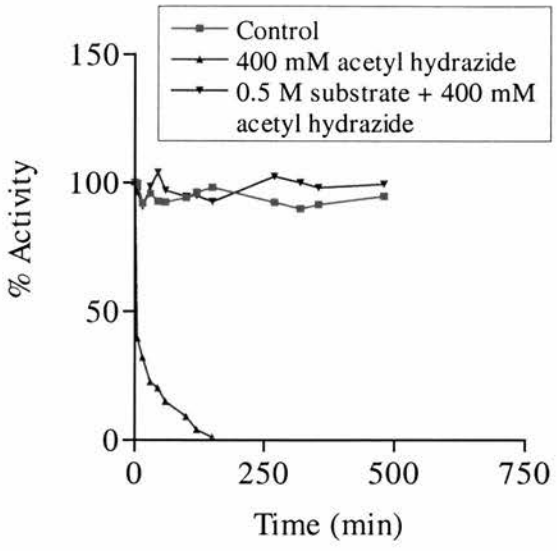

Figure 5.2: *Substrate protection of methylaspartase from inhibition by acetyl hydrazide*

A simple pH inhibition rate study was carried out over the pH range 6.0-9.0. The results displayed in Fig 5.2, show that the rate of inhibition rises markedly as the pH increases above pH 7.0. Above pH 7.0 presumably the majority of the inhibitor exists as the free amine and is able to undergo nucleophilic attack on the dehydroalanine residue.

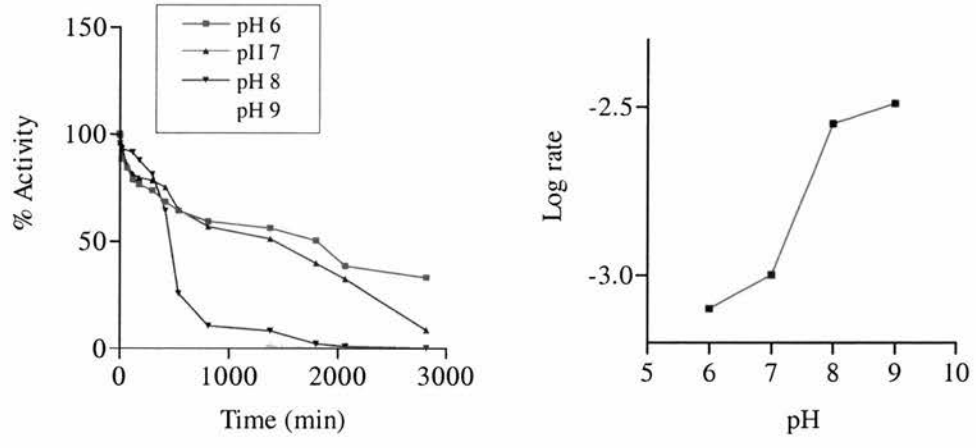

Figure 5.3: *pH profile for inhibition of methylaspartase by acetyl hydrazide*

The plot of the log of initial rate of inhibition versus pH of the buffer shows an inflection at pH 7.5, thus reflecting the involvement of an ionisable group with a pK_a of about 7.5

Finally methylaspartase was inhibited with 500 mM acetyl hydrazide at pH 9.0 in 50 mM Tris buffer and the inactive enzyme was dialysed extensively against the same buffer. Following dialysis no enzyme activity was observed, confirming that inhibition is irreversible.

In an attempt to map the site of irreversible inhibition, the synthesis of [UL-^{14}C]-acetyl hydrazide was carried out. It was intended that inhibition of methylaspartase by [^{14}C]-acetyl hydrazide followed by digestion with trypsin and HPLC purification of the resulting peptides, would enable isolation and characterisation of any radio-labelled peptides.

[UL-^{14}C]-Acetyl hydrazide was synthesised in one step from [UL-^{14}C]-acetic anhydride (specific activity 2.3 mCi/ mmol) and hydrazine hydrate (100%) by slowly adding hydrazine hydrate to an ice cold solution of acetic anhydride in THF, to afford the desired compound as the acetate salt (**109**) in 60% yield (m.p 65-68 °C, specific activity 0.5 mCi/ mmol) (Scheme 5.1).

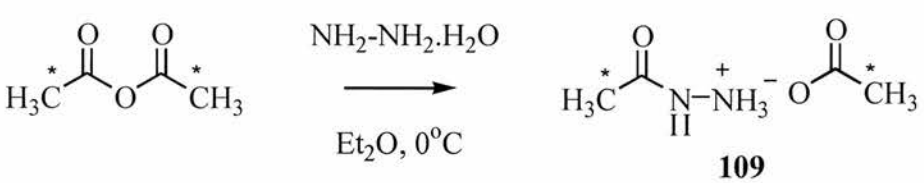

Scheme 5.1: *Synthesis of ^{14}C-acetyl hydrazide*

Methylaspartase was incubated with 200 mM ^{14}C-acetyl hydrazide (specific activity 0.5 mCi/ mmole). Complete inactivation was observed within 24 hours and

excess unreacted radioactive material removed by dialysis against 50 mM Tris buffer at pH 9.0. The levels of radioactivity in the dialysis buffer were measured by scintillation counting and dialysis continued until the detection levels were similar to background.

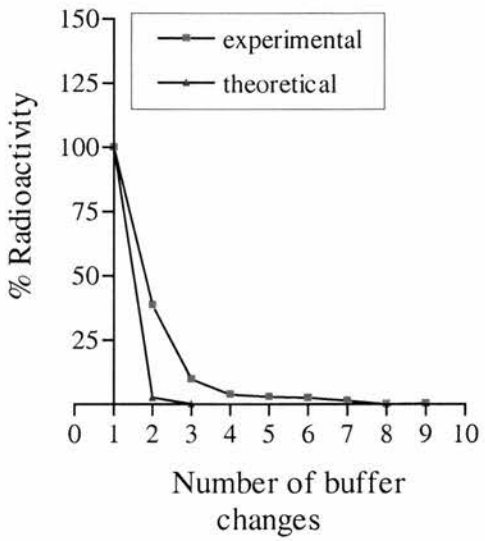

Figure 5.4: *Dialysis of methylaspartase after inhibition with ^{14}C-acetyl hydrazide*

The results shown in Fig 5.4 indicate that significant levels of ^{14}C were leaching into the dialysis buffer following 3-4 changes of buffer. This unexpected behaviour indicated that during dialysis a compound containing the radioactive atom was slowly dissociating from the active-site of the enzyme. The product of dialysis was analysed for enzyme activity, however it was found that the protein had remained totally inactive. In addition, scintillation counting showed that very little radioactivity (less than 1 %) had been retained in the inactive protein (Table 5.1).

One possible explanation for this observed behaviour is that the inhibitor binds to the enzyme via a slowly reversible covalent bond and that this process results in an

irreversible change to the protein, either from a change in the structure or a chemical modification of an amino acid.

In order to establish whether the remaining radiolabel was covalently linked to the enzyme, the dialysis product was subjected to anion-exchange chromatography. The major peak in UV absorbance eluted between 240-260 mM sodium chloride and was shown by SDS-PAGE analysis to have a mass of 45 kDa, consistent with methylaspartase. However, the only peak in radioactivity eluted after only 0.6 column volumes before the salt gradient was applied.

An authentic sample of ^{14}C-acetyl hydrazide was subjected to an identical analysis and the only peak in radioactivity was observed with a retention volume of 0.6 column volumes. This suggested that following dialysis, the remaining radioactivity was not bound to the enzyme.

If the inactivation of the enzyme and loss of radiolabelled inhibitor involves covalent bond formation, then removal of the protein tertiary structure during the inhibition process may result in the isolation of a reasonable concentration of the enzyme/inhibitor complex. In an attempt to achieve this an experiment was designed in which methylaspartase was treated with [^{14}C]-acetyl hydrazide until 100% inhibition was achieved. The tertiary structure was then compromised by partial digestion with trypsin.

Methylaspartase (3.5 mg, specific activity 157 units/ mg) was incubated with with 100 mM ^{14}C-acetyl hydrazide (specific activity 0.5 μCi/ mmole, 5.3 μCi) in 50 mM Tris buffer at pH 9.0. The sample was then divided into two portions and one aliquot was dialysed extensively against 50 mM potassium phosphate buffer at pH 9.0 until only background radioactivity was detected in the dialysis buffer. This was achieved with 10

changes of buffer. The second aliquot was dialysed against two changes of 50 mM potassium phosphate buffer at pH 9.0. Table 5.1 shows the radioactivity used in each experiment and retained by the protein following dialysis.

Table 5.1: *Radio-labelling of methylaspartase*

Protein (mg)	*Total Radioactivity (μCi)*	*No. of buffer changes*	*Radioactivity remaining in protein after dialysis (μCi)*
1.75	2.65	2	1.9
1.75	2.65	10	0.037

Both samples which had been subjected to partial and extensive dialysis were analysed by anion-exchange chromatography. In both cases methylaspartase eluted with a retention volume of 10.5 column volumes (12% sodium chloride) and the major peak in radioactivity with a retention volumes of 16.25 column volumes (20% sodium chloride). The aliquot which had undergone limited dialysis was then treated with trypsin. After 3 hours the reaction was quenched with acetic acid (1 drop) and the sample lyophilised.

The sample was analysed by RP-HPLC (0-60% acetonitrile applied over 15 column volumes) and an aliquot from each fraction retained for scintillation counting. Fig 5.5 shows the resulting HPLC elution profile and overlayed is the trace for ^{14}C elution. An envelope of radioactivity was observed which encompassed almost all of the peptide peaks. Within this envelope was one major peak of radioactivity which eluted with a retention volume of 5.78 column volumes.

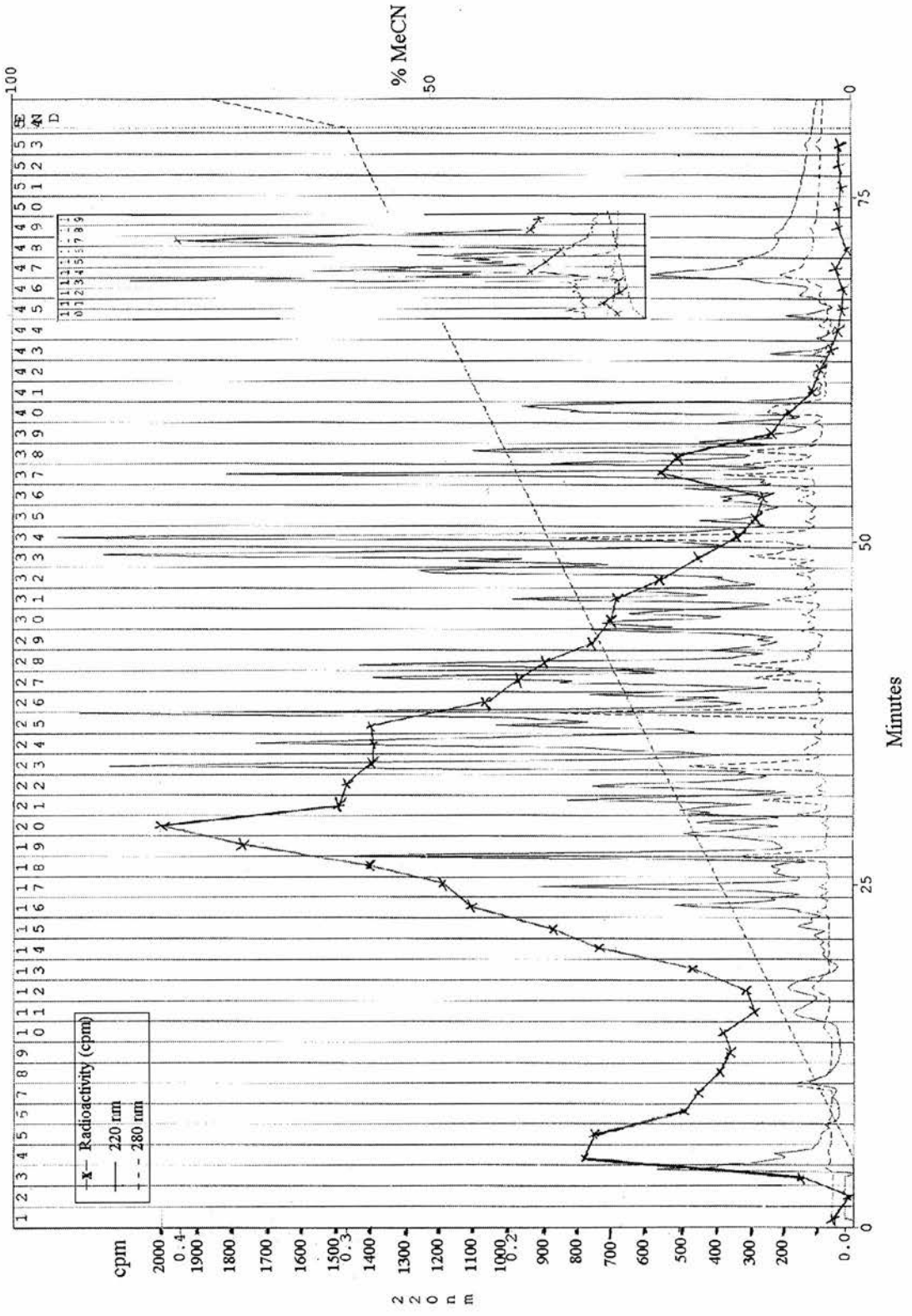

Figure 5.5: *HPLC elution profile of ^{14}C-acetylhydrazide inhibited methylaspartase following tryptic digestion*

The fractions comprising the major peak in radioactivity (F19-21) were pooled and re-chromatographed by RP-HPLC, under slightly different gradient conditions, in order to attempt to separate the components of the sample. However, the peak in radioactivity did not correspond to a peptide peak in the profile detected by UV absorbance at 220 nm.

This series of experiments shows that following inactivation of the protein by [^{14}C]-acetyl hydrazide, the inhibitor or at least a proportion of the inhibitor containing the ^{14}C label is released from the protein leaving it inactivated. These results are in accord with findings described earlier on immobilisation by the solid phase hydrazide.

5.2 Phenylhydrazine as an inhibitor of methylaspartase

Having established that acetyl hydrazide can irreversibly inactivate methylaspartase, it remained to investigate the precise mechanism of inactivation and to further probe the mechanism of release of the inhibitor from the inactive enzyme/inhibitor complex.

A range of aliphatic and aromatic hydrazines were investigated as inhibitors of methylaspartase, including phenylhydrazine. The results of enzyme inactivation at a 1 mM concentration of all the inhibitors is shown in Fig 5.6.

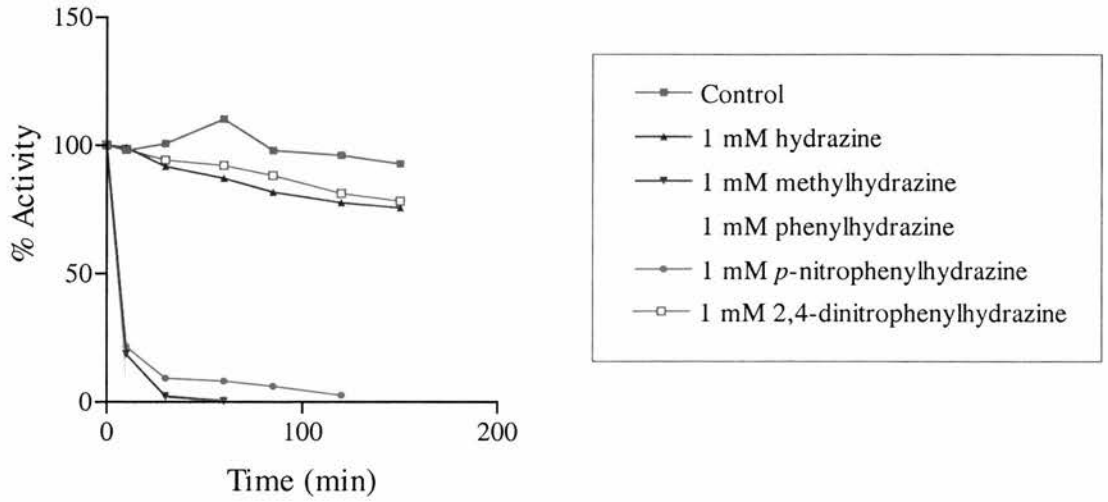

Figure 5.6: *Inhibition of methylaspartase by various hydrazines at pH 8.0*

Other studies in which phenylhydrazine acts as an irreverisble enzyme inhibitor, showed that the nucleophilicity of the terminal nitrogen of phenylhydrazine increased with the electron-withdrawing power of a *para* substituent, resulting in an increased rate of inactivation.[157, 158] However, our results with methylaspartase are not consistent and show that at 1mM concentration, phenylhydrazine was found to be the best time-dependent inhibitor of methylaspartase with 99% inhibition within 30 minutes and therefore is a slightly more potent inhibitor of methylaspartase than *p*-nitrophenylhydrazine. This prompted us to investigate further the kinetics of inhibition of methylaspartase by phenylhydrazine.

The concentration dependence of phenylhydrazine inhibition of methylaspartase at pH 9.0 was then determined and the results are shown in Figure 5.7.

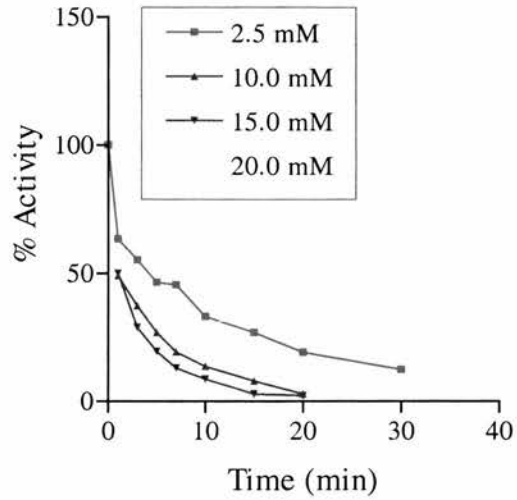

Figure 5.7: *Concentration dependence of inhibition of methylaspartase by phenylhyrazine at pH 9.0*

These results suggested that at pH 9 the inactivation reaction proceeds with biphasic saturation kinetics. The initial phase of inhibition is rapid with 51% inhibition occuring within 1 minute at 10 mM. This is followed by a second slower phase of inhibition leading to total inactivation within 30 minutes. Inactivation was irreversible, as the enzyme activity could not be restored by dilution or dialysis.

A secondary plot was obtained from the non-linear regression analysis of the rate of inactivation from the initial rapid phase (t1/2) *versus* concentration of phenylhydrazine. This plot intersected the y-axis near the origin and an approximate K_i value of 5.18 mM was determined for phenylhydrazine. This value compares with a K_m for the natural substrate (2*S*,3*S*)-3-methylaspartic acid of 2.3 mM (Fig. 5.8).

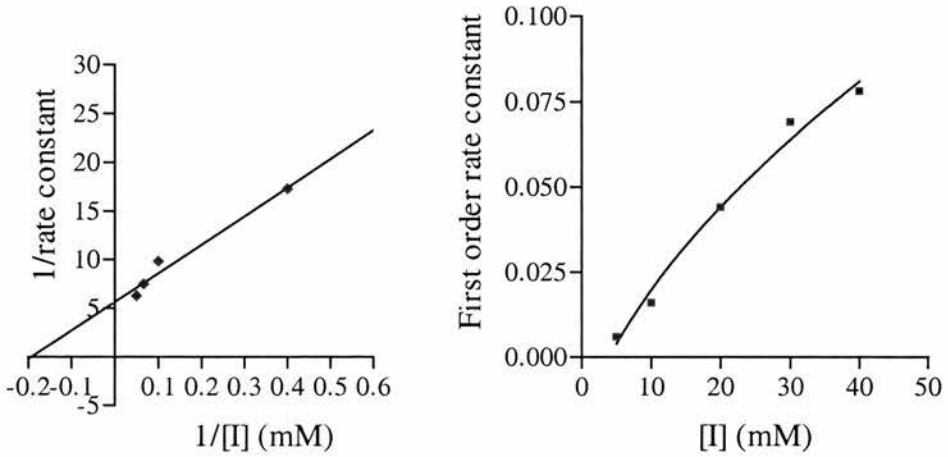

Figure 5.8: *Determination of K_s for phenylhydrazine*

In the presence of either magnesium (0.4 mM) or ammonia (up to 40 mM) the rate of inhibition of methylaspartase by phenylhydrazine remained unchanged.

Complete protection from inactivation by phenylhydrazine was afforded by pre-incubation with 0.5 M (2*S*,3*S*)-3-methylaspartic acid, suggesting that phenylhydrazine inhibition is directed at or near the active site of the enzyme.

The rate of the initial phase of inhibition was then studied over a range of pH values.

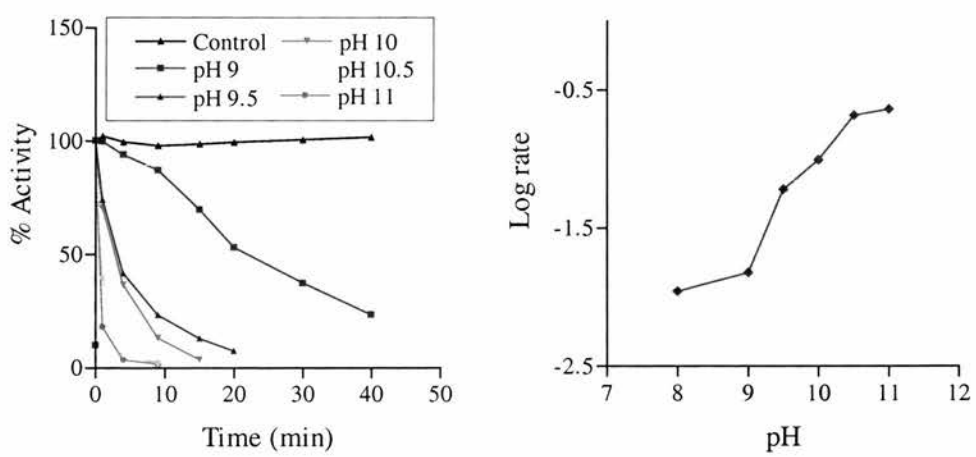

Figure 5.9: *pH dependence of inhibition of methylaspartase by phenylhydrazine*

The inactivation was found to be dependent on the pH of the incubation. The rate of inactivation was higher at basic pH. A plot of the log of the rate of inactivation *versus* pH of the buffer is shown in Fig 5.9. The slope of the graph is greater than unity, which reflects the requirement for more than one ionisable group, which controls the rate of the initial inactivation process. Phenylhydrazine has a pK_a of 5.27 therefore $C_6H_5N_2H_3$ is the dominant species present under the pH conditions studied.[159]

The solution phase properties of phenylhydrazine were studied in detail. A solution of phenylhydrazine (50 mM) in buffer (50 mM Tris, pH 9.0) was prepared and left at room temperature overnight. The resulting solution was extracted into ethyl acetate and analysed by gas chromatography and compared to that for aniline (Fig. 5.10).[160]

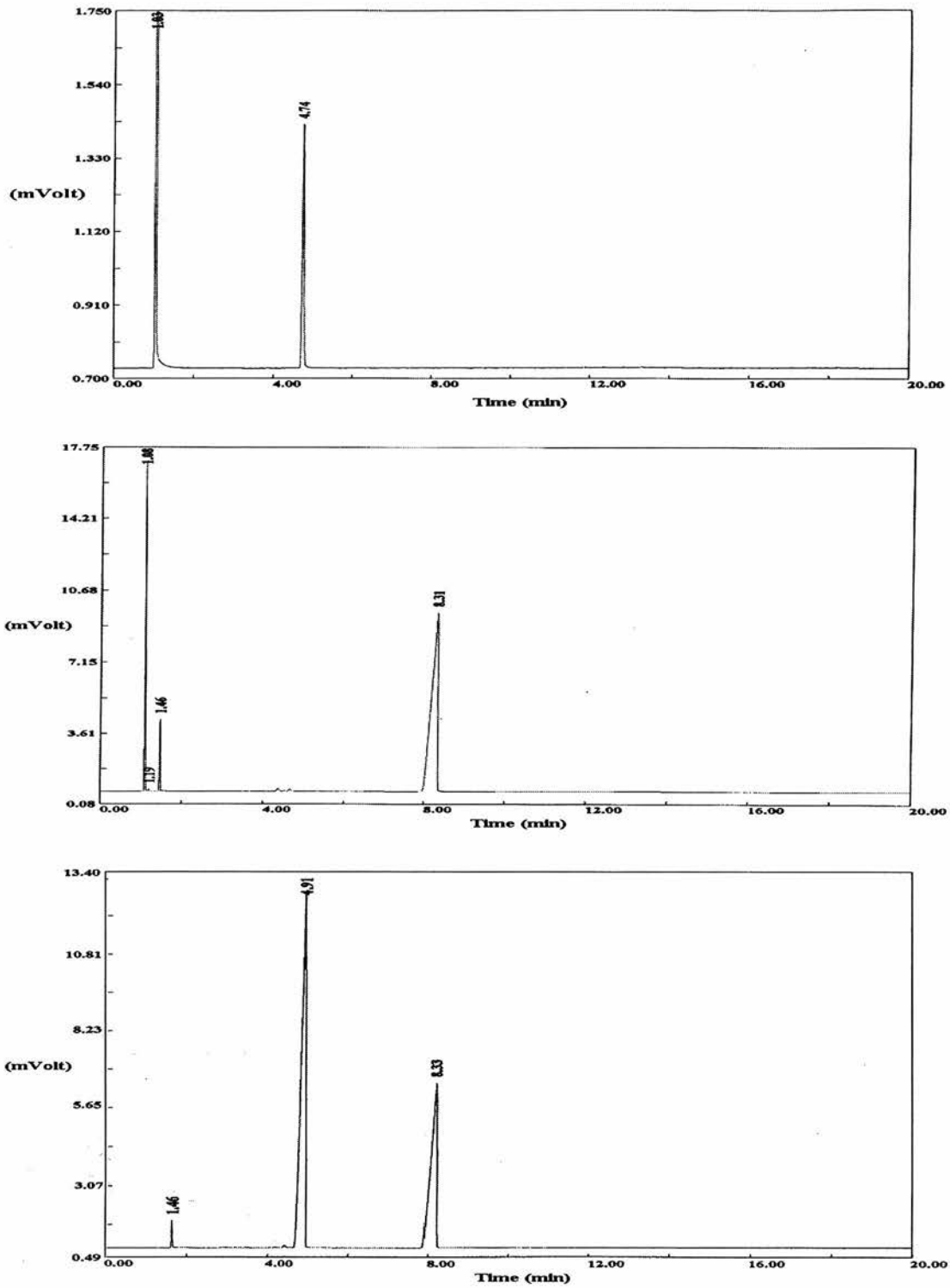

Figure 5.10: *Gas chromatogram of a) phenylhydrazine, b) aniline, c) degraded Phenylhydrazine*

Inspection of the chromatograms showed that phenylhydrazine decomposes in aqueous solution to afford aniline and presumably a second nitrogen containing compound such as ammonia or hydroxylamine. It was proposed that ammonia would be generated as a direct result of nitrogen-nitrogen bond cleavage. Hydroxylamine, may be formed *via* water acting as a nucleophile in cleaving the nitrogen-nitrogen bond.

As a result of these studies aniline was tested as an inhibitor of methylaspartase. Methylaspartase was incubated with aniline at pH 9.0 at a range of concentrations between 1-40 mM. Under these conditions aniline was found to have no inhibitory activity with methylaspartase.

A potential mechanism for inhibition of methylaspartase by phenylhydrazine was proposed which incorporates the observed experimental behaviour, biphasic kinetics and the release of at least part of the inhibitor (Scheme 5.2). An initial rapid and reversible attack of the primary amine at the β-carbon atom of dehydroalanine, leads to the formation of the covalent enzyme/inhibitor complex. There is evidence from chemical modification studies [65] that at least one cysteine residue and possibly more exist at the active site of the enzyme and it is proposed that one of these acts as a nucleophile, in an equivalent manner to water, attacking the benzylic nitrogen, leading to cleavage of the nitrogen-nitrogen bond, formation of a thiol-amine intermediate (**110**) and the diaminopropanoic acid form of the dehydroalanine residue, which has been proposed to exist as an intermediate in the natural reaction. A second thiolate can then displace aniline from the active site leading to the generation of an internal disulfide bond (**111**) and release of the aryl component to the bulk solvent. It is proposed that the formation of this disulfide bond is in fact the inactive form of the enzyme (Scheme 5.2).

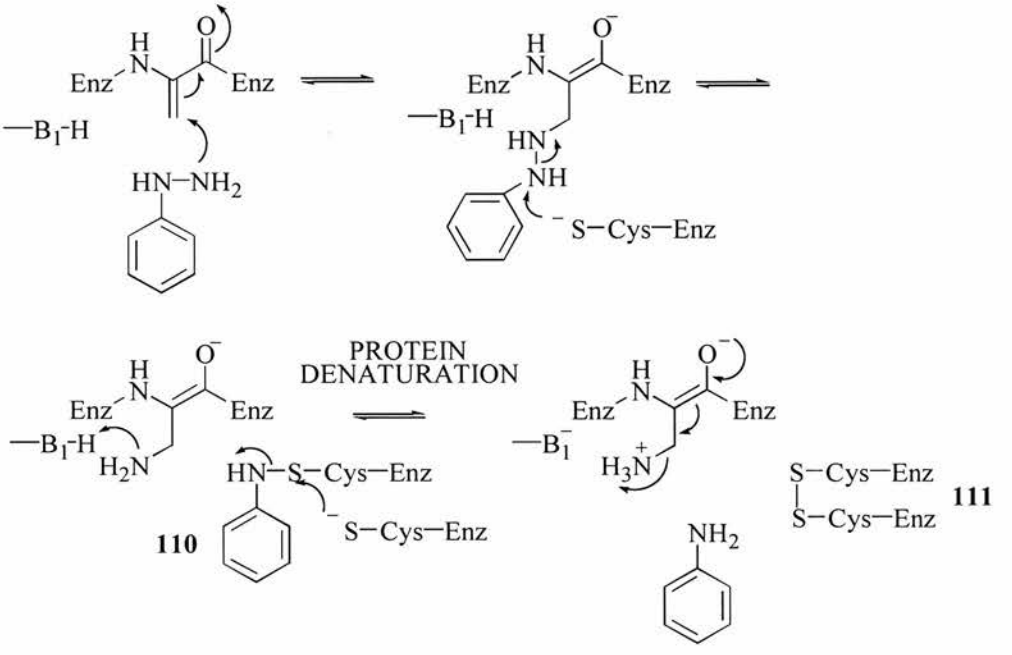

Scheme 5.2: *Proposed mechanism for inhibition of methylaspartase by phenylhydrazine*

In order to probe the formation of a disulfide link in the irreversible step of inhibition by phenylhydrazine the effects of an alternative thiol containing reagent β-mercaptoethanol on the kinetics of inhibition were characterised. It was anticipated that mercaptoethanol would be able to either reduce the disulfide linkage or compete with the active site thiol, in both cases, leading to a reduction in the rate of inhibition.[161]

Methylaspartase was incubated with 20 mM inhibitor phenylhydrazine both in the absence and the presence of 1 mM β-mercaptoethanol. The results show that in the absence of mercaptoethanol complete inactivation of the enzyme occurred within 50 minutes (Fig. 5.11). However, in the presence of 1 mM mercaptoethanol greater than 60% activity remained after 50 minutes.

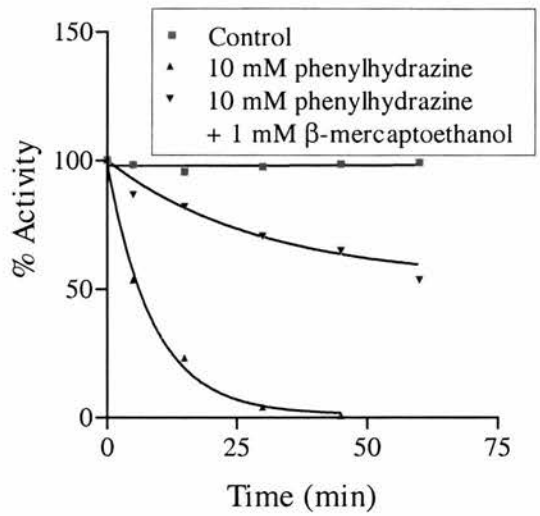

Figure 5.11: *Effect of mercaptoethanol on inhibition of methylaspartase by phenylhydrazine*

In order to rule out a reaction between mercaptoethanol and the phenylhydrazine inhibitor, which would lead to a reduction in inhibitor concentration and hence an explanation for the reduction in the rate of inhibition, methylaspartase was treated with reduced concentrations of phenylhydrazine. The results shown in Fig 5.12 show that the rate of inhibition of methylaspartase by 15 mM and 20 mM phenylhydrazine are very similar, however 20 mM phenylhydrazine in the presence of 5 mM mercaptoethanol leads to a significant reduction in the rate of inhibition.

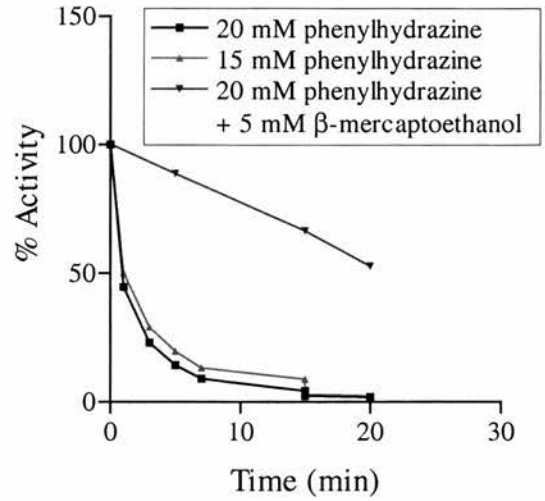

Figure 5.12: *Inhibition of methylaspartase by phenylhydrazine in the absence and presence of mercaptoethanol*

This clearly demonstrates that mercaptoethanol acts to protect the active site of the enzyme from inhibition by phenylhydrazine.

In a second experiment methylaspartase was incubated with 20 mM phenylhydrazine and the reaction was monitored until 80% inactivation of the enzyme had occurred. Mercaptoethanol (2 mM) was then added and the enzyme activity was measured at regular intervals for a further 30 minutes (Fig. 5.13).

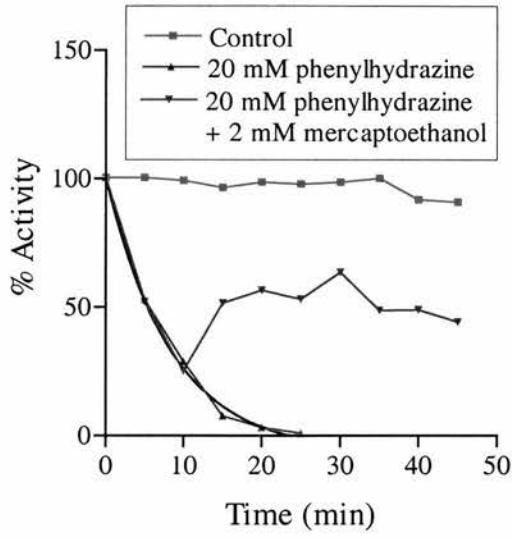

Figure 5.13: *Effect of the addition of mercaptoethanol to partially inactivated enzyme*

The results show that following initial rapid inhibition by phenylhydrazine, addition of the reducing agent resulted in an increase in enzyme activity, which remained constant for 30 minutes. This result clearly shows that mercaptoethanol is able to rescue the irreversibly inactivated enzyme and further protect it from additional inhibition.

As we had only investigated the effect of addition of mercaptoethanol at a fixed concentration of thiol, we therefore undertook to examine the effect of various concentrations of mercaptoethanol in the presence of a fixed concentration of phenylhydrazine (20 mM) (Fig. 5.14).

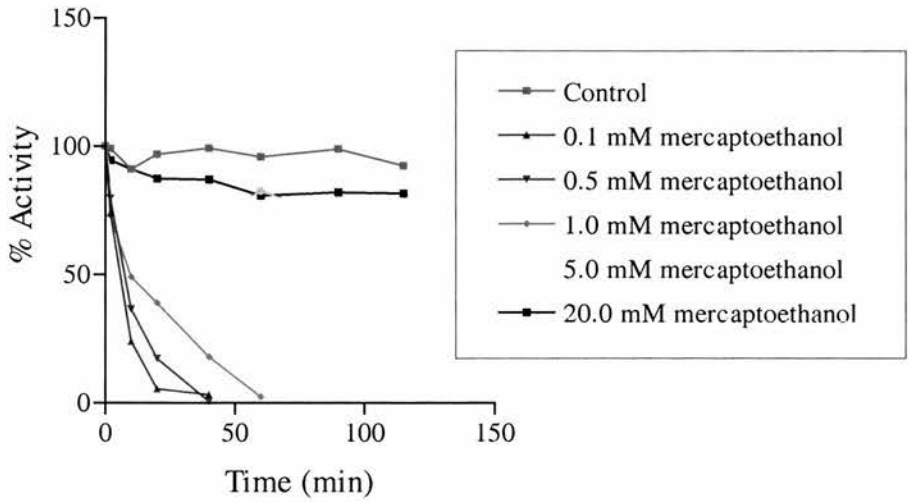

Figure 5.14: *Effect of varying concentrations of mercaptoethanol on inhibition of methylaspartase by phenylhydrazine*

The effect on the kinetic parameters for inhibition by phenylhydrazine in the presence of mercaptoethanol was probed by measuring the initial rate of inhibition in the presence of 2 mM mercaptoethanol with various concentrations of phenylhydrazine. The rate constant was determined from the initial rapid phase of inhibition for each concentration of mercaptoethanol (Fig. 5.15).

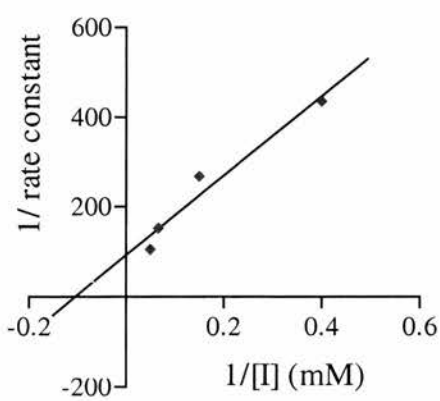

Figure 5.15: *Determination of K_s for phenylhydrazine in the presence of mercaptoethanol*

In the presence of mercaptoethanol, the value of K_i for phenylhydrazine is 9.48 mM. This increase in the value of K_i from 5.18 mM to 9.48 mM suggests that the reduced rate of phenylhydrazine inhibition in the presence of mercaptoethanol may be due to reduced binding of phenylhydrazine to the enzyme. However, with less than a two-fold difference between the two values, too much emphasis should not be placed on this result. Mercaptoethanol was tested and was found not to be an inhibitor of methylaspartase.

Whilst the role of mercaptoethanol in reducing the rate of inactivation by phenylhydrazine can be explained by simple competition for the active site, the observation that mercaptoethanol can rescue inactive enzyme requires more careful consideration. On the basis of the mechanism for inactivation by phenylhydrazine proposed in Scheme 5.3, three plausible mechanisms for the reactivation of the inactive enzyme by mercaptoethanol can be envisaged.

In the first of the reactivation mechanisms, following the formation of the phenylhydrazine-enzyme complex, it can be envisaged that the thiolate of mercaptoethanol could act in place of the active site cysteine (Scheme 5.3a), attacking the benzylic nitrogen and leading to the formation of a thioamine adduct (**112**) (Scheme 5.3b). This non-enzyme bound adduct is then free to dissociate, leaving the aminated enzyme, which can readily eliminated to produce the active form of methylaspartase.

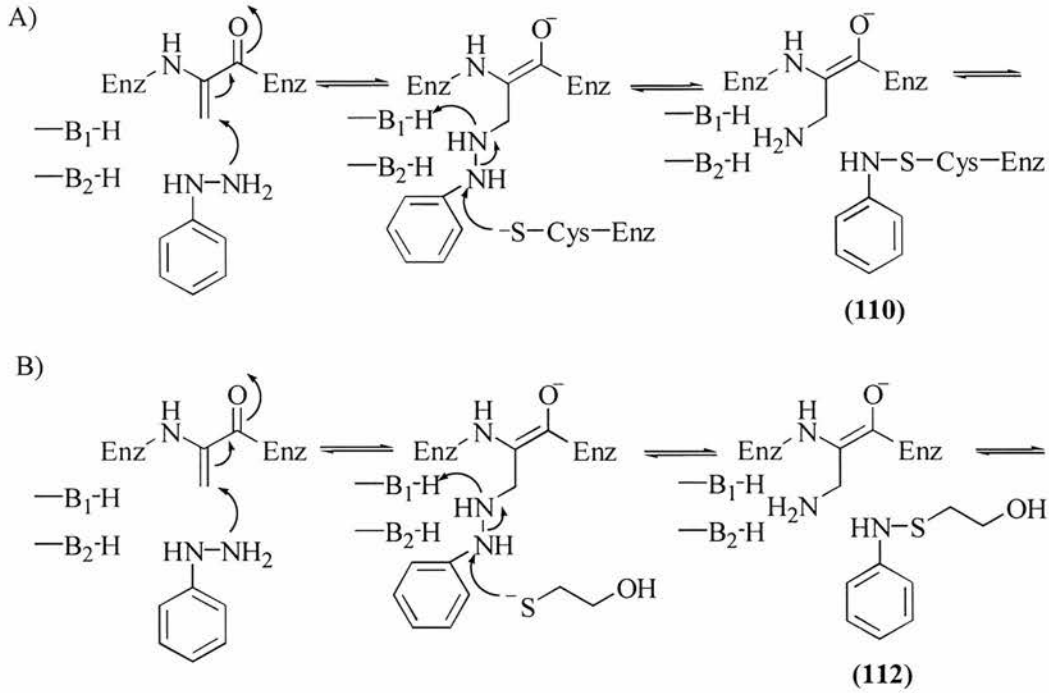

Scheme 5.3: *a) Proposed formation of thioamine adduct during inactivation of methylaspartase by phenylhydrazine b) Proposed involvement of mercaptoethanol in the inactivation of methylaspartase by phenylhydrazine*

In the second mechanism it can be envisaged that mercaptoethanol acts at a later stage in the inactivation process, replacing the second proposed active site cysteine (Scheme 5.4b). In this case the mercaptoethanol thiolate may attack the aniline-enzyme complex (**113**) at the cysteine sulfur, eliminating aniline, which would be free to dissociate, the driving force of the reaction being the formation of a stable disulfide (active-site cysteine and mercaptoethanol) (Scheme 5.4b, **114**).

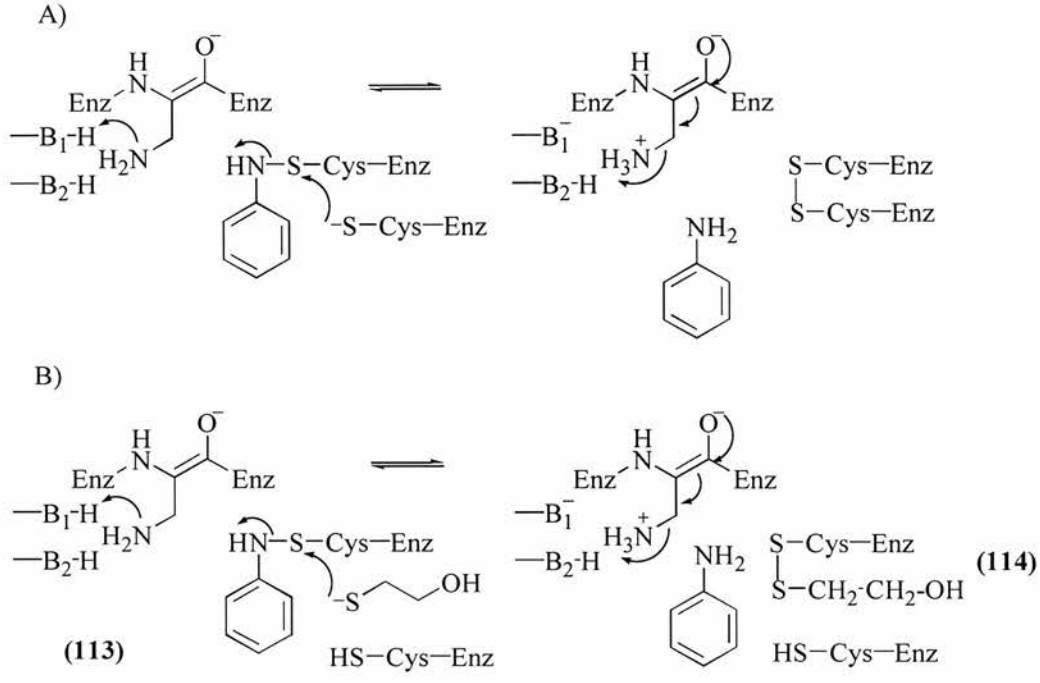

Scheme 5.4: *a) Proposed formation of disulfide bond during inactivation of methylaspartase by phenylhydrazine, b) Proposed involvement of mercaptoethanol later in inactivation of methylaspartase by phenylhydrazine*

In the third mechanism, mercaptoethanol could act at a very late stage in the inactivation mechanism, reducing the active site disulfide (**114**), which would presumably be the final inactive species (Scheme 5.4b).

In an attempt to address these three possible mechanisms, the ability of the alternative reducing agent DTT to reactivate the phenylhydrazine inhibited enzyme was investigated.[162] It was envisaged that the more bulky and sterically hindered DTT is more likely to participate in a redox process, i.e. reduction of the disulfide rather than as a nucleophile, therefore allowing the mechanism to be probed.

Methylaspartase was incubated with 20 mM phenylhydrazine in buffer (50 mM Tris, pH 9). 1.6 mM dithiothreitol was added after 88% of the enzyme activity had been

lost. This resulted in an increase in activity of 50%, which then remained constant over the following 30 minute time course of the experiment (Fig. 5.16).

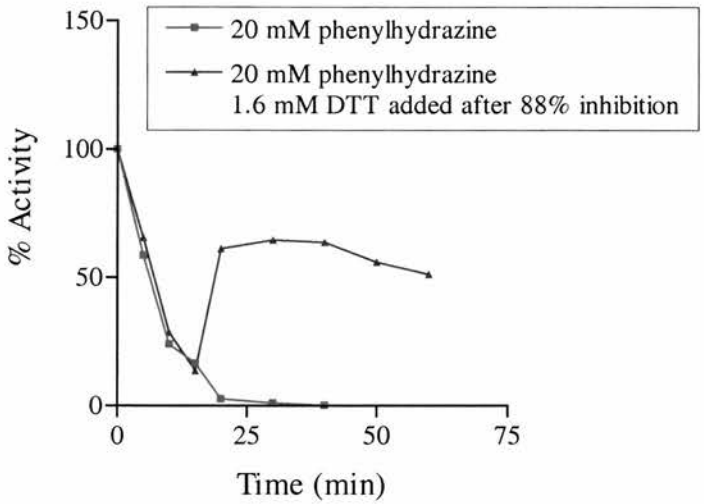

Figure 5.16: *Effect of addition of DTT on inhibition of methylaspartase by phenylhydrazine*

This result showed that along with mercaptoethanol, DTT was also able to rescue phenylhydrazine inactivated methylaspartase and protecting it from further loss of activity (Fig. 5.16). The effect of a third reducing agent, *tert*-tributylphosphine was then studied. This was selected as it does not contain any thiol groups and is known to be efficient at reducing disulfide bonds. The reducing agent (2 mM) was added after 80% inhibition of methylaspartase had occurred with phenylhydrazine (25 mins).

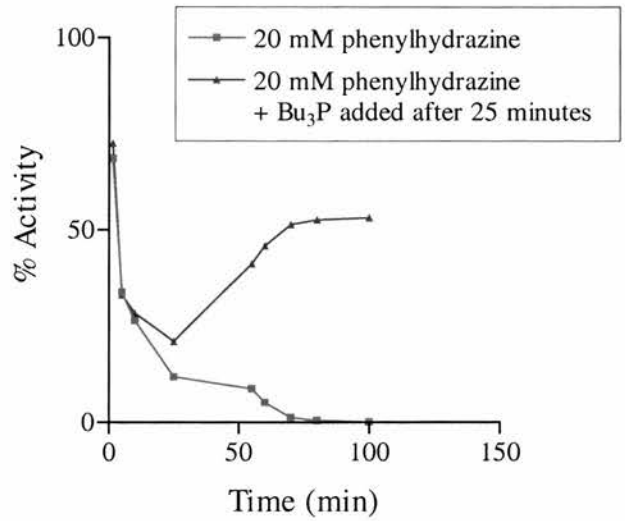

Figure 5.17: *Effect of addition of tributyl phosphine on inhibition of methylaspartase by phenylhydrazine*

This resulted in a less dramatic increase in enzyme activity (30%) (Fig. 5.17). Although the increase in activity resulting from addition of tributyl phosphine was less marked than with mercaptoethanol/ DTT, it none the less did result in an increase in enzyme activity and furthermore protected the enzyme from further inactivation (Fig. 5.17).

In the knowledge that tributyl phosphine is unstable in water and is readily oxidised to tributyl phosphine oxide, it is perhaps unsurprising that the increase in activity was only 20%.

In a second experiment, methylaspartase was incubated with both phenylhydrazine and tributyl phosphine. Due to the inherent insolubility of tributyl phosphine the reducing agent was initially dissolved in isopropanol and then added to the enzyme solution. Consequently a control was carried out to assess the effect of the solvent on enzyme activity at a 10% concentration.

Methylaspartase was incubated in buffer (50 mM Tris, pH 9.0) containing 10% propanol and the activity determined over a period of 100 minutes. The results shown in figure 5.18 clearly show, that activity is not affected by the solvent. Methylaspartase was also incubated in the absence and the presence of tributyl phosphine and the activity of the enzyme measured at regular time intervals. The results show that tributyl phosphine was able to completely protect the enzyme against inactivation by phenylhydrazine (Fig. 5.18). Since phenylhydrazine was present in 10-fold excess compared to tributyl phosphine, then this observation suggests that tributyl phosphine is able to protect against inactivation and is not simply reacting with phenylhydrazine (Fig. 5.18).

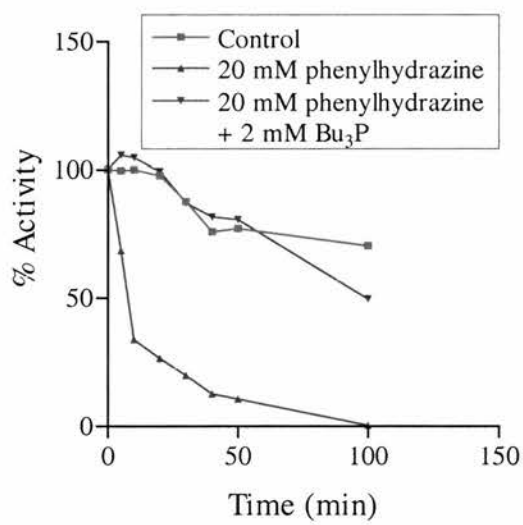

Figure 5.18: *Effect of addition of tributyl phosphine on inhibition of methylaspartase by phenylhydrazine*

This series of experiments with a range of reducing agents clearly indicates that inactivation by phenylhydrazine results in the formation of disulfide bonds at the active site of the enzyme, thus supporting the mechanism of inactivation proposed in Scheme 5.3.

Having gained strong evidence that disulfide bond formation is involved in the inactivation of methylaspartase by phenylhydrazine, it remained to establish which residues were involved. In order to probe the cysteine residues proposed at the active site, a peptide mapping experiment with the site-specific chemical modifying agent NEM was carried out. Attempts with *N*-[2-^{14}C]-NEM and phenylhydrazine involved modification of cysteines not involved in disulfide bonds followed by digestion of the labelled protein. However, labelled peptides were not observed possibly because only low levels of labelled peptide were present.

5.3 Probing the mechanism of inactivation

In an alternative approach to probing the proposed mechanism of methylaspartase inactivation by phenylhydrazine, the appearance of an intermediate in the mechanism i.e. aniline was investigated. Following inactivation by phenylhydrazine it is proposed that aniline and ammonia are released into the bulk solvent and therefore could be used as markers. As discussed above (see 5.2), phenylhydrazine degrades spontaneously in water to afford aniline and presumably hydroxylamine. Consequently, the appearance of aniline produced *via* inactivation of the enzyme by phenylhydrazine would be very difficult to measure.

Therefore, suitable methods for visualisation of ammonia was sought. Nesslers' reagent is known to produce a brown precipitate when treated with ammonia and the concentration of this can be measured by a change in absorbance at 400 nm. In a control experiment phenylhydrazine was treated with Nesslers Reagent. A reaction was observed

which gave rise to a precipitate which absorbed strongly at 400 nm. This showed that it would be difficult to determine the concentration of ammonia in a sample. In an attempt to minimise this effect attempts were made to precipitate phenylhydrazine using copper sulfate, however, this only met with partial success.

5.3.1 Degradation of phenylhydrazine

As discussed above, phenylhydrazine degrades rapidly in water to give aniline, however, the nature of the other nitrogen containing species still remained unproven, although the most likely candidates were hydroxylamine or ammonia.

In an attempt to address this dichotomy the degradation of ^{15}N-phenylhydrazine was followed by NMR spectroscopy.

^{15}N-Phenylhydrazine (**115**) was prepared from aniline by diazotisation with ^{15}N-sodium nitrite. The diazonium salt was reduced with sodium sulfite and acidified with concentrated hydrochloric acid to afford ^{15}N-phenylhydrazine (**115**) as the hydrochloride salt in 75% yield (m.p. 251 °C, lit. 250 °C).[163] A sample of ^{15}N-phenylhydrazine was prepared in 50 mM Tris buffer at pH 9.0 containing deuterium oxide (10%). The sample was left at room temperature for 24 hours to allow degradation to occur and the ^{15}N-NMR spectrum was recorded. However, no signals due to ^{15}N were observed.

In an attempt to observe N-H protons in either hydroxylamine or ammonia a ^{1}H-NMR spectrum in DMSO was obtained. Under these conditions the presence of an N-H proton would be expected to appear as a singlet between 7-8 ppm. The ^{1}H-NMR spectrum obtained for the sample of degraded phenylhydrazine is shown in Figure 5.19.

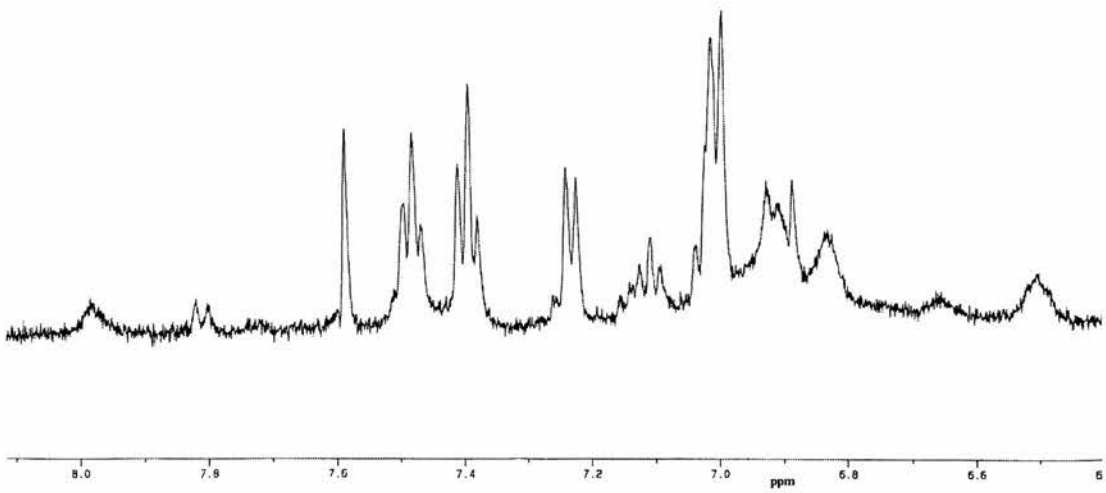

Figure 5.19: *^{1}H-NMR spectrum for degraded phenylhydrazine*

The sample was treated with hydrochloric acid and the solution filtered and reduced under pressure to afford a white solid. This was re-dissolved in d_6-DMSO and the ^{1}H-NMR spectrum obtained. The resulting ^{1}H-NMR spectrum shows the presence of a broad signal at 7.7 ppm which consistent with the presence of an N-H moiety within the molecule (Fig. 5.24).

A

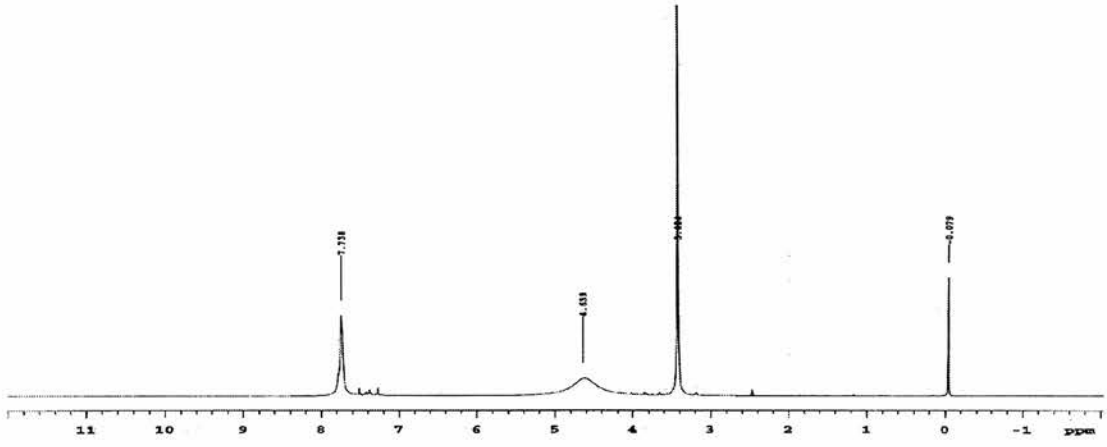

B

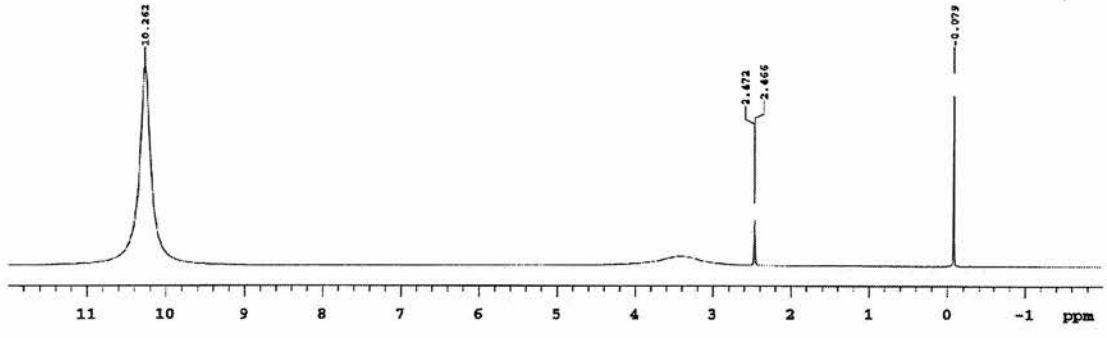

C

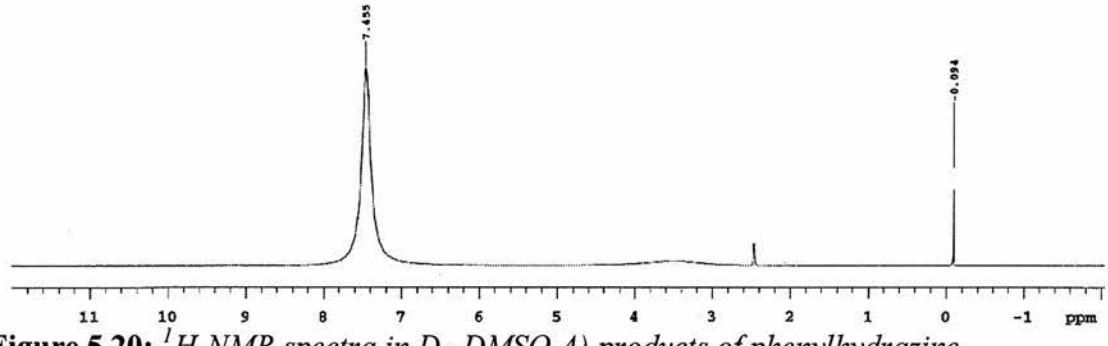

Figure 5.20: *^{1}H-NMR spectra in D_6-DMSO A) products of phenylhydrazine degradation after acidification, B) hydroxylamine hydrochloride, C) ammonium hydrochloride (internal reference = TMS)*

This spectrum was then compared with the ^{1}H-NMR spectra for authentic samples of ammonia and hydroxylamine also recorded in D_6-DMSO (Fig. 5.24). In both cases the hydrochloride salt was used as it was anticipated that following treatment of the degradation products of phenylhydrazine with hydrochloric acid the resulting ammonia or hydroxylamine would be present as the hydrochloride salt.

The spectrum for hydroxylamine showed the presence of a singlet at 10.3 ppm, thus suggesting that the nitrogen-containing species produced by degradation of phenylhydrazine was not hydroxylamine. In addition, the spectrum for ammonium hydrochloride showed the presence of a singlet at 7.5 ppm, consistent with the signal at 7.7 ppm observed in the spectrum of the degraded sample, which had been acidified. This provided strong evidence, for the formation of ammonia during the degradation of phenylhydrazine under aqueous conditions.

In order to determine more precisely that the signal at 7.7 ppm was due to ammonia, the sample of degraded phenylhydrazine was spiked with authentic ammonium chloride and a second ^{1}H-NMR spectrum recorded. The signal at 7.7 ppm was seen to increase, thus providing further evidence to suggest that ammonia is the nitrogen containing species produced as a result of phenylhydrazine degradation under basic aqueous conditions.

We have provided strong evidence to support the formation of disulfides during the mechanism of inactivation of methylaspartase by phenylhydrazine. However, all attempts to identify intermediates released into the bulk solvent have proven unsuccessful.

5.3.2 Intermediates in the pathway

In an attempt to gain further evidence for the mechanism of phenylhydrazine inactivation of methylaspartase, experiments were designed to trap-out and observe the intermediate adducts/ enzyme-inhibitor complexes.

It was envisaged that incubating the enzyme with ^{15}N-phenylhydrazine would result in the formation of a covalent bond between ^{15}N-atom and the active-site residue. In the event that the N-N bond of the inhibitor undergoes cleavage mediated by an active site cysteine as shown in Scheme 5.5, it was anticipated that a ^{15}N-labelled phenylhydrazine would result in a labelled aminated enzyme-complex which could be trapped at the active site by acetylation. This would also have the added advantage of preventing N-H exchange and thus allowing characterisation of the intermediate species by a range of NMR techniques. Scheme 5.5 shows the proposed mechanism for inhibition of methylaspartase by ^{15}N-phenylhydrazine and the trapped form of the covalent adduct by acetic anhydride.

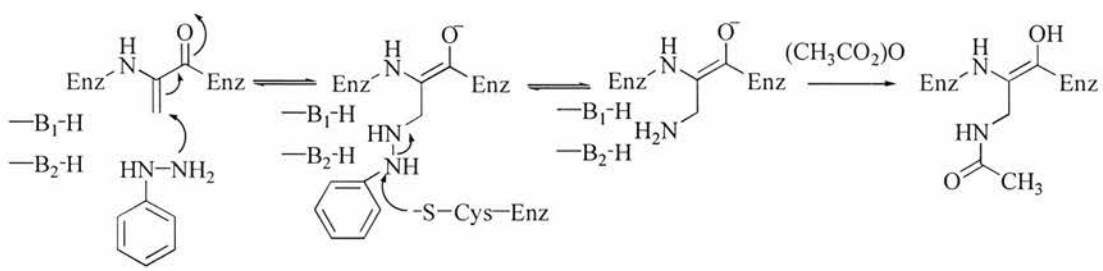

Scheme 5.5: *Trapping of methylaspartase by inhibition with ^{15}N-phenylhydrazine and acetylation*

In order for this to be successful a significant quantity of aminated enzyme must be accumulated during the inactivation process. Bearing in mind that the collapse of this complex to dehydroalanine is a step in the reaction mechanism which is likely to be slow,

it was vital that the reaction was quenched with acetic anhydride during the maximal rate of inactivation.

Methylaspartase (25 mg, 115 units/ mg) was incubated with ^{15}N-phenylhydrazine (100 mM) in potassium phosphate buffer (100 mM, pH 9.0) and the reaction left for 8 hours. After 50% inactivation had occurred, acetic anhydride was added to the sample (5 mm^3) and the mixture was left at room temperature for 2 hours. The acetylated protein was then digested with trypsin and the proteolytic reaction was quenched by addition of acetic acid (1 drop). The sample was lyophilised and dissolved in deuterium oxide/ water (1:9).

To ensure that the digest had been successful, a 1D ^{1}H-NMR spectrum was acquired for the mixture as shown in Figure 5.21.

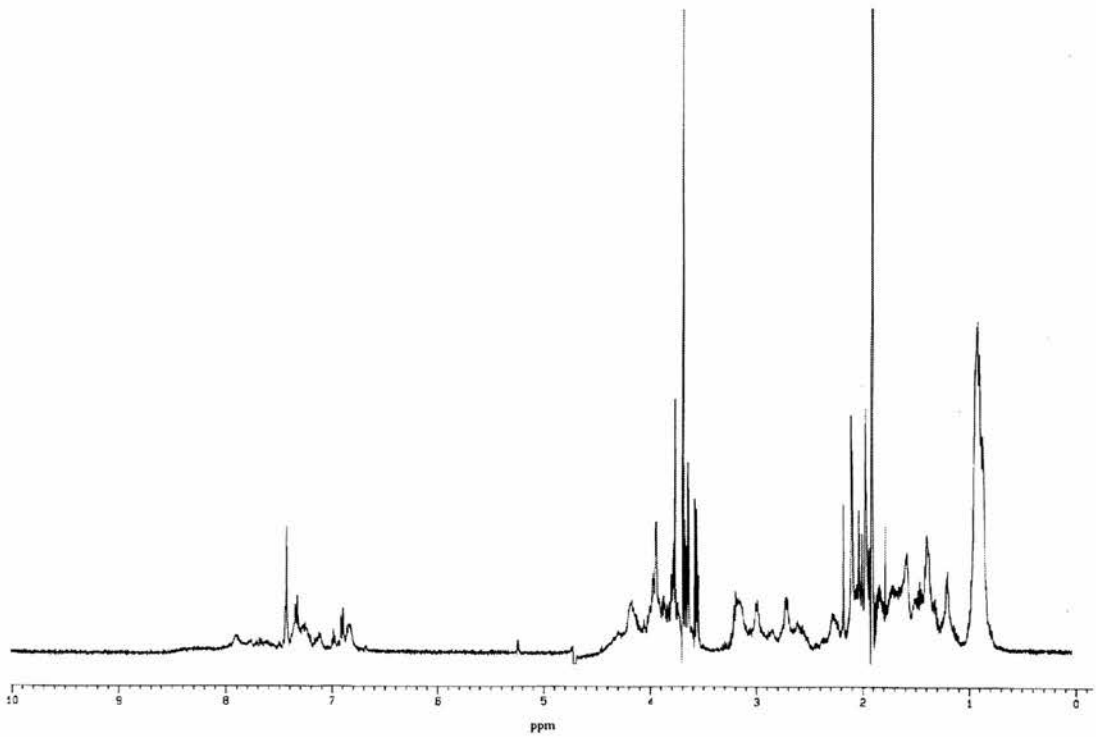

Figure 5.21: *^{1}H-NMR spectrum of ^{15}N-phenylhydrazine inhibited methylaspartase after acetylation*

The resulting spectrum, although extremely complex showed sharp, well resolved signals between 1-2.2 ppm and 3.5-4 ppm, consistent with the presence of small peptides. As with intact protein, a very broad peak range from 0.9-7.5 ppm was observed.

In order to visualise the protons attached to the ^{15}N label a ^{1}H-^{15}N HSQC (^{15}N-edited) spectrum was recorded. It was anticipated that this would show a signal for each proton attached only to a ^{15}N atom, and only one, which is covalently bound to a carbon atom. The ^{1}H-^{15}N-HSQC spectrum for digested methylaspartase after inhibition with phenylhydrazine and acetylation is shown in Figure 5.22.

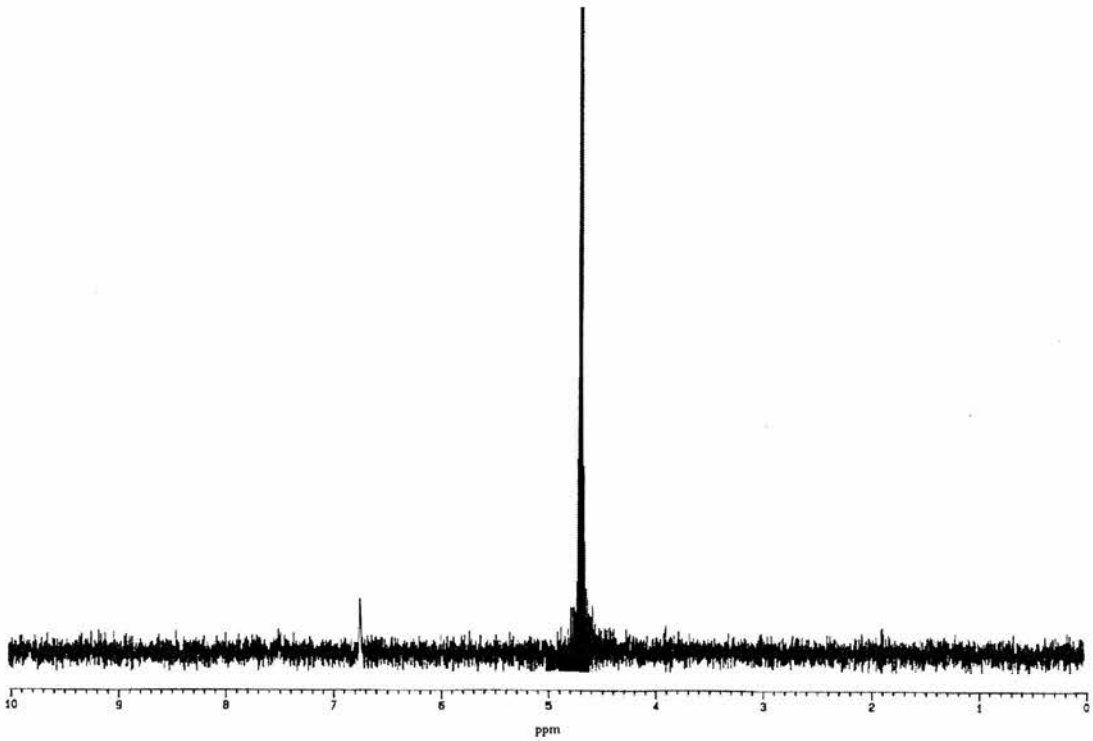

Figure 5.22: *^{1}H-^{15}N-HSQC spectrum of phenylhydrazine inhibited methylaspartase after acetylation.*

A complex multiplet with a resonance at 6.75 ppm was observed which is consistent with an N-H proton. This suggests the presence of a C-N-H functionality.

5.4 Conclusions

The inhibition characteristics of methylaspartase by various hydrazines and hydrazides have been extensively studied and in most cases this class of inhibitors have been found to irreversibly inactivate the enzyme.

Attempts to exploit this property in order to isolate a peptide derived from the active site of methylaspartase have, however, proven unsuccessful.

Phenylhydrazine showed unusual kinetic characteristics and this prompted a detailed investigation into its mode and mechanism of inactivation. It has been proposed that the formation of a disulfide bond represents a major step in the inactivation pathway, since various reducing agents have been shown to rescue enzyme activity after inactivation by phenylhydrazine and more importantly protect the enzyme from further inactivation.

NMR spectral analysis of the products/ intermediates involved in phenylhydrazine inhibition of methylaspartase has indicated that a species containing a C-N-H exists following inactivation of methylaspartase by ^{15}N-phenylhydrazine. This is not an artifact, since the signal of no other ^{15}N-labelled proton would be expected to be seen in this region of the NMR spectrum. At the active site of the enzume there is only one proposed amino acid that is electrophilic, a dehydroalanine residue. These observations lend support to the proposal that inhibition of methylaspartase by hydrazines/ hydrazides occurs *via* nucleophilic attack at the active site of the enzyme.

5.5 Future plans

Future experiments to probe the importance of the key active-site residues might involve mutating various amino acids which have been implicated in the mechanism, such as Ser-173 and testing the mutants for catalytic activity.

A substantial amount of information could also be gained from an X-ray crystal structure of methylaspartase in isolation and/ or with a range of substrates and inhibitors bound at the active site. This would provide evidence for or against the existence of an

active-site dehydroalanine residue and invaluable information about the overall shape of the active site and the residues which are involved in substrate/ inhibitor binding. Crystallographic studies are being undertaken in a collaboration outside the research group and promising 3-D crystals have now been obtained.

Chapter 6 : Experimental

6.1 General methods and materials

Elemental microanalyses were performed in the departmental microanalytical laboratory. NMR spectra were recorded on a Varian (^{1}H, 300 MHz; ^{13}C, 74.76), or a Varian Gemini 200 (^{1}H, 200 MHz; 50.31 MHz) spectrometer, unless otherwise stated. Chemical shifts are described in parts per million downfield from $SiMe_4$ and are reported consecutively as position (δ_H or δ_C), relative integral, multiplicity (s -singlet, d -doublet, t -triplet, q -quartet, d d -double of doublets, sep -septet, m -multiplet, and br -broad), coupling constant (*J*/Hz) and assignment (numbering according to the IUPAC nomenclature for the compound). ^{1}H-NMR spectra were referenced internally on ^{2}HOH (δ 4.68), $CHCl_3$ (δ 7.27) or $(CH_3)_2SO$ (δ 2.47). ^{13}C-NMR spectra were referenced on CH_3OH (δ 49.9), C^2HCl_3 (δ 77.5), or $(CH_3)_2SO$ (δ 39.70).

FT-IR spectra were recorded either on a Perkin-Elmer 1710 or on a Nicolet Inspect-IR plus FT-IR spectrometer. The samples were prepared as Nujol mulls, solutions in chloroform or as a potassium bromide disc. The frequencies (υ) as absorption maxima are given in wavenumbers (cm^{-1}). Mass spectra and accurate mass measurements were recorded on a VG 70-250 SE or a Kratos MS-50. Fast atom bombardment spectra were recorded using glycerol as a matrix. Major fragments were given as percentages of the base peak intensity (100%). UV spectra were recorded on a Shimadzu UV-VIS 2101PC scanning spectrophotometer.

Gas chromatography was performed on a BPX-5 Megabore 9μm column (15m x 0.53 i.d) using a Carlo Erba GC 8000 series with F.I.D detection, using nitrogen as the carrier gas. The injection mode was split 20:1.

Melting points were taken on an electrothermal melting point apparatus and are uncorrected. Optical rotations were measured at room temperature on an optical activity AA-1000 polarimeter using a 10 or 20 cm path length cell and are given in 10^{-1} deg cm^2 g^{-1}.

Flash chromatography was performed according to the method of Still *et al.*[164] using Fluka C60 (40-60 μm mesh) silica gel. Analytical thin layer chromatography (TLC) was carried out on 0.25 mm precoated silica gel plates (Macherey-Nagel SIL g/UV_{254}) and compounds were visualised using UV fluorescence, iodine vapour, ethanolic phosphomolybdic acid or ninhydrin.

The solvents were either distilled or of analar quality and light petroleum refers to that portion which bolis between 40 and 60 °C. Solvents were dried according to literature procedures. Ethanol and methanol were dried using magnesium turnings. Isopropanol, DMF, toluene, CH_2Cl_2, acetonitrile and triethylamine were distilled over CaH_2. THF and diethylether were dried over sodium/ benzophenone and distilled under nitrogen.

Gel exclusion chromatography was performed using Sephadex G-150-200. The gel was suspended in the appropriate buffer and allowed to settle several times to remove fine particles.

Anion exchange FPLC was performed on a TSK DEAE-5PW (75 x 8 mm) column and on a POROS 10 HQ (4.6mm x 100 mm) column. Reversed-phase HPLC was

performed on a PepMap C18 column (4.6mm X 100 mm). Affinity chromatography was performed using Qiagen Ni-NTA resin (XK 26 mm x 200 mm).

SDS-PAGE was performed following the procedure of Laemmli[165] on a discontinuous medium. A mini-Protean II Dual Slab Cell apparatus was used. Protein determinations were performed using the method of Bradford.[156]

Centrifugations were carried out on a CENTRIKON C-124 centrifuge. Pooled fractions from various steps were concentrated by ultra-filtration using an Amicon apparatus (43 or 76 mm diameter), through a YM10 or a YM30 membrane, under nitrogen.

6.2 Chemical synthesis

(2*S*, 3*S*)-3-Methylaspartic acid 2

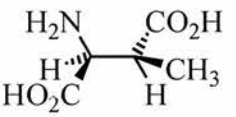

Following the procedure of Akhtar *et al.* mesaconic acid **3** (13 g, 0.1 mol) was suspended in water (50 cm^3) and adjusted to pH 9.0 by the addition of an aqueous solution of concentrated ammonia solution (40 cm^3).[56] The resulting solution was concentrated under vacuum. The diammonium mesaconate salt was redissolved in water (10 cm^3) and magnesium chloride hexahydrate (300 mg, 1.49 mmol) and potassium chloride (15 mg, 0.18 mmol) were added to the mixture. The pH was adjusted to 9.0 with an aqueous solution of concentrated ammonia.

The enzyme 3-methylaspartase (300 units) was added after removal of an aliquot of the reaction mixture. The reaction was incubated at 30 °C until no further decrease in absorbance at 240 nm was observed. The protein was denatured by heating (100 °C, 2 min) and the protein removed by filtration. The filtrate was evaporated to dryness and the residue was redissolved in water (30 cm^3) and the pH was adjusted to 3-4 by the addition of 12 mol dm^{-3} hydrochloric acid. The product crystallised on addition of the acid and was filtered, dried, and recrystallised from boiling water (15 cm^3) to afford the pure product **2** (6.66 g, 45%); mp 272-275 °C decomp.) (lit.,[56] 272-275 °C); (Found C, 40.7; H, 6.2; N, 9.2. Calc. For $C_5H_9NO_4$; C, 40.8; H, 6.15; N, 9.5%); $[\alpha]_D^{20}$ +13.3 (*c* 0.6 in 5 mol dm^{-3} HCl) (lit.,[56] +13.4°); υ_{max} (Nujol)/cm^{-1} 2925 (OH str.), 1704 (CO str.) and 1600 (NH); δ_H (200 MHz, ^2H_2O, pH 1) 0.81 (3H, d, *J* 7.2, 3-CH_3), 2.68 (1H, m, *J* 7.1, 3-CH)

and 3.51 (1H, d, *J* 3.7, 2-CH); δ_C (74.5 MHz, ^2H_2O) 7.34 (CH_3), 42.1 (3-C), 54.7 (2-C), 178.3 and 180.352 (2 x CO_2H); *m/z* (CI) 148 (100%, $[M + H]^+$), 130 (82, $[M + H - H_2O]^+$), 102 (48, $[M - CO_2H]^+$) and 74 (7, $[M + H - C_2H_4NO_2]^+$).

3,6-Dioxaoctanedioic acid dimethyl ester 95

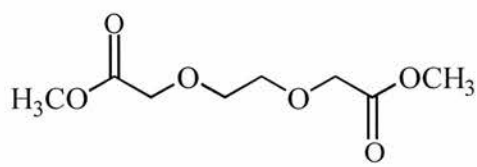

To an ice cooled solution of 3,6-dioxaoctanedioic acid **94** (1.0 g, 5.6 mmol) in THF was slowly added an ethereal solution of diazomethane until a yellow colour persisted. The solution was then stirred for 1h at room temperature and then flushed with nitrogen and the solvent removed under reduced pressure to afford the dimethyl ester **95** as a pale yellow oil (0.74 g, 70.0%), ν_{max} (neat)/ cm^{-1} 3000 (CH_3), 2955 (CH_3 str.), 1761 (carbonyl CO), 1444 (CH_2 bend), and 1229 (C-O ether); δ_H (200 MHz; C^2HCl_3) 3.70 (2H, t, *J* 6.9, OCH_2), 3.72 (3H, s, OCH_3) and 4.12 (2H, s, $COCH_2O$); δ_C (50 MHz; C^2HCl_3) 51.76 (OCH_3), 68.57 (CH_2O), 70.95 ($COCH_2$) and 170.93 (ester carbonyl).

3,6-Dioxaoctanedioic acid hydrazide 96

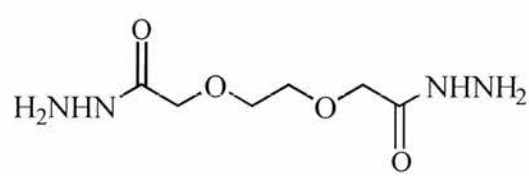

To a solution of dimethyl-3,6-dioxaoctanedioate **95** (0.62 g, 2.9 mmol) in freshly distilled methanol (25 cm^3) was added hydrazine monohydrate (0.25 cm^3, 3.3 mmol). The

mixture was heated under reflux for 2 h and the solvent removed under reduced pressure to afford the hydrazide **96** as a white crystalline solid (0.59 g, 40%), mp 134-137 °C (lit.,[166] 128-130 °C); (Found: C, 34.82; H, 6.88; N, 27.27. Calc. for $C_6H_{14}N_4O_4$: C, 34.95; H, 6.85; N, 27.15%.); (HRMS found: M + H^+, 207.110. Calc. for $C_6H_{14}N_4O_4$: 207.111); ν_{max} (Nujol)/ cm^{-1} 3304 (NH_2), 3195 (NH), 1675 (hydrazide CO) and 1137 (OCH_2); δ_H (300 MHz; ^2H_2O) 3.59 (2H, s, CH_2O), 3.96 (2H, s, CH_2CO); δ_C (75.4 MHz; ^2H_2O) 68.76 (CH_2O), 70.24 ($COCH_2$) and 171.02 (hydrazide CO); *m/z* (FAB) 207 (45, $[M + H]^+$), 135 (28, $[M + H - NH_2NHCOCH]^+$), 117 (22, $[CH_2CH_2OCH_2CONHNH_2]^+$), 102 (27, $[M + H - NH_2NHCOCH_2OCH]^+$), 60 (100%, $[CONHNH_3]^+$) and 44 (95, $[CH_2OCH_2]^+$).

Tenta-gel methyl ester 98

The tenta-gel resin was first washed with a solution of trifluoroacetic acid (0.5% in dry THF). To an ice cooled suspension of TG carboxy resin **97** (0.505 g, 0.26 mmol/ g loading as supplied) suspended in dry THF (15 cm^3) was slowly added an ethereal solution of diazomethane (10 cm^3, 11.36 mmol) until a pale yellow colour persisted and gas evolution stopped. The suspension was then stirred at room temperature for 30 min before the excess diazomethane was removed by flushing the mixture with nitrogen. The resin was washed with methanol (3 x 20 cm^3) and then filtered to afford the methyl ester **98** as a pale yellow resin (0.502 g, 0.13 mmol loading); (Found: C, 61.5; H, 8.85. Resin requires: C, 64.3; H, 9.1%); ν_{max} (KBr disc)/cm^{-1} 1751 (ester CO) and 1127 (OCH_2).

Tenta-gel hydrazide 99

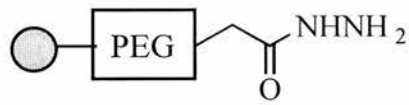

To a suspension of Tenta-gel methyl ester **98** (0.50 g, 0.12 mmol estimated loading) in methanol was added hydrazine hydrate (18.0 mm^3, 0.36 mmol). The suspension was heated at reflux for 2 h and the solvent was then removed by filtration and the resin was washed with methanol (4 x 20 cm^3) to afford the hydrazide **99** as an off-white resin (0.49 g, 0.13 mmol estimated loading), (Found: C, 64.1; H, 8.8; N, 0.85. resin requires: C, 64.15; H, 8.8; N, 0.8%); ν_{max} (KBr disc)/cm^{-1} 3503 (amide NH), 3026 (NH_2), 1654 (amide CO), and 1109 (OCH_2).

Cleavage of resin-bound peptide

(i) *Catalytic hydrogenation (see section 4.3.1, Fig. 4.9)*: To a suspension of resin-bound peptide (**100**) 25-200 mg) in dry methanol (10-25 cm^3) was added palladium on charcoal (10 μg) pre-suspended in ethanol (500 mm^3) and glacial acetic acid (10 mm^3). The mixture was flushed with nitrogen and then with hydrogen and then finally left stirring overnight under a hydrogen atmosphere. The hydrogen gas was evacuated by flushing with nitrogen and the solution was filtered over a celite pad. The filtrate was concentrated under reduced pressure and the residue re-suspended in distilled water (20-50 mm^3) and lyopholised. The resulting product was then subjected to analysis by Reversed-Phase HPLC.

(ii) *Dissolving metal reduction (see section 4.3.1)*: To a solution of liquid ammonia (5 cm^3) in dry THF (10 cm^3) at –78 °C under nitrogen was added the resin (**100**) (25-200 mg). The suspension was stirred vigorously whilst sodium metal (0.2 g, 8.7 mmol) was added in small pieces until a dark blue colour persisted. The mixture was allowed to stir for 1 h, after which methanol was added (10 cm^3), followed by water (10 cm^3). The mixture was allowed to warm to ambient temperature whilst nitrogen was bubbled through to remove excess ammonia. The solution was neutralised by the addition of a solution of hydrochloric acid (6 mol dm^{-3}), filtered and lyopholised. The resulting residue was re-dissolved in water (100 mm^3) for analysis by Reversed-Phase HPLC.

(iii) *Wilkinsons catalyst (see section 4.3.2)*: Resin (**100**) (25-200 mg) was suspended in a mixture of ethanol/ water (1:1, 1 cm^3) and tris (triphenyl phosphine)-rhodium(I)-chloride (11 mg, 0.024 mmol) was added. The flask was flushed with nitrogen (10 min) and then with hydrogen (10 min). The mixture was left stirring at reflux over night. The catalyst was then removed by filtration through a celite pad and the filtrate concentrated to dryness under reduced pressure.

(iv) *Sodium hydroxide (see section 4.3.1, Fig. 4.7)*: Resin (**100**) (25-220 mg) was suspended in a solution of sodium hydroxide (5 mol dm^{-3}) and left to stir overnight at room temperature. The resin was filtered and the supernatant was neutralised by the addition of a solution of hydrochloric acid (5 mol dm^{-3}) and then lyophilised. The cleavage mixture was then analysed by Reversed-Phase HPLC.

(v) *V8 protease (see 4.3.3):* Resin (**100**) (25-200 mg) was suspended in a solution of ammonium acetate (100 m in 50 mM Tris, pH 4.0). V8 protease (*Staphylococcus aureus*) was then added [in equal amounts to 2.0 % by weight of peptide and a further aliquot after 1 hour (total digest time was 2 h, 30 °C)]. The pH of the solution was maintained at pH 4.0 by the addition of a solution of hydrochloric acid (1 mol dm^{-3}). After digestion, the resin was washed thoroughly with water (10 x 50 cm^3) and the washings lyophilised in preparation for analysis by Reversed-Phase HPLC.

Acetylhydrazine acetate 108

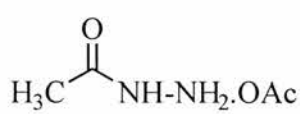

To an ice cold solution of acetic anhydride (1.68 cm^3, 15.3 mmol) in dry ether (20 cm^3) was added hydrazine hydrate (1.36 cm^3, 18.36 mmol) dropwise. The mixture was allowed to stir for a further 30 min during which time a white crystalline solid formed. The solid was filtered to afford the acetate salt **108** of the product as a white amorphous solid (3.26 g, 91%), mp 65-68 °C (lit.,[167] 67 °C); (Found: C, 41.7; H, 7.1; N, 24.4. Calc for $C_4H_{10}N_2O_3$: C, 35.8; H, 7.5; N, 20.9%); ν_{max} (Nujol)/ cm^{-1} 3242 (NH_2), 1710, (hydrazide CO) and 1560 (NH bend); δ_H (300 MHz; ^2H_2O) 1.7 (3H, s, CH_3CO_2) and 1.8 (3H, s, CH_3CON); δ_C (75.4 MHz; ^2H_2O) 19.6 (CH_3CON), 23.1 (CH_3CO_2), 173.4 (CONH), 181.6 (CH_3CO_2), *m/z* (EI) 133 (44%, $[M - H]^+$)], 85 (73, $[M - H - H_4CO_2]^+$), 57 (100, $[CH_3CON]^+$) and 55 (15, ($[CCONH]^+$).

[^{14}C]-Acetylhydrazine acetate 109

To an ice cold solution of ^{14}C-acetic anhydride (72.9 mm^3, 0.66 μmol, specific activity 2.3 mCi/ mmol) in dry THF (20 cm^3) was slowly added hydrazine hydrate (37.0 mm^3, 0.79 μmol) dropwise. The mixture was allowed to stir for a further 30 min during which time a white crystalline precipitate formed. The solid was filtered to afford the acetate salt **109** as a white amorphous solid (70.0 mg, 79.5%, specific activity 0.5 mCi/ mmol), mp 65-68 °C; δ_H (300 MHz, ^2H_2O) 1.7 (3H, s, CH_3CO_2) and 1.8 (3H, s, CH_3CON); δ_C (75.4 MHz; ^2H_2O) 19.6 (CH_3CON), 23.1 (CH_3CO_2), 173.4 (CONH) and 181.6 (CH_3CO_2).

^{15}N-Phenylhydrazine hydrochloride 115

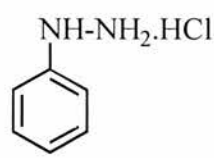

A fresh solution of sodium sulfite was prepared by bubbling sulfur dioxide through a solution of sodium hydroxide (0.44 g, 11.1 mmol) in water (2 cm^3) in the presence of phenolphthaleine indicator until the solution became colourless (pH 8-10). To an ice-cooled solution of aniline (1.0 g, 10.8 mmol) in mixture of water/ concentrated hydrochloric acid solution (1:1, 1.0 cm^3) was slowly added ^{15}N-sodium nitrite (0.75 g, 10.9 mmol) in water (2.0 cm^3) dropwise until a slight excess of nitrous acid was present. The temperature of the solution was maintained at 0 °C by the occasional addition of ice to the reaction mixture. The freshly prepared sodium sulfite was added slowly dropwise whilst the reaction mixture was maintained at 0 °C. The resulting solution was heated at

60 °C for 1h and was then acidified by the addition of concentrated hydrochloric acid solution (5 cm^3). The solution was refluxed for a further 4 h and then the solvent was removed under reduced pressure until precipitation of phenylhydrazine hydrochloride occurred. The resulting pale pink solid was filtered and recrystallised from ethanol to afford the labelled phenylhydrazine hydrochloride **115** as a white solid (1.16 g, 75%); mp 251 °C (Lit.,[163] 250-254 °C); ν_{max} (KBr disc)/cm^{-1} 3203 (NH), 3002 (NH_2) and 1580 (Ar-H); δ_H (300 MHz; ^2H_2O) 6.89 (2H, d, *J* 6.6, *o*Ar-H), 7.01 (1H, t, *J* 7.4, *p*Ar-H), 7.24 (2H, t, *J* 5.5, *m*Ar-H); δ_C (75.4 MHz; $^2H_20$) 115.6 (*p*Ar-C), 123.9 (*m*Ar-C), 129.8 (*o*Ar-C) and 143.5 (C-$NHNH_2$); *m/z* (CI) 110 (100% $[M + H - Cl]^+$), 94 (41, $[M + H - NH_2Cl]^+$) and 52 (45, $[C_4H_3 + H]^+$).

Analysis of products of phenylhydrazine degradation (see section 5.3.1, Fig. 5.20)

A solution of phenylhydrazine hydrochloride (50 mM) in Tris buffer (50 mM Tris, pH 9.0) was prepared and left at room temperature for 48 h. An aliquot of the sample (20 cm^3) was acidified by the addition of hydrochloric acid (6 mol dm^{-3}), lyophilised and then analysed by ^{1}H-NMR spectroscopy.

6.3 Biochemical methods

Methylaspartase activity assay

An aliquot (5-20 mm^3) of a suitably diluted enzyme solution was added to the assay buffer (3 cm^3, 4mM (2*S*,3*S*)-3-methylaspartic acid, 50 mM Tris, 10 mM KCl, 1 mM $MgCl_2.6H_2O$, pH 9.0) in a quartz cuvette at 30 °C. The contents of the cell were mixed thoroughly and the increase in absorbance at 240 nm was measured. One unit of enzyme is defined as that amount which catalyses the formation of 1 μmol/min of mesaconic acid or the consumption of 1 μmol/ min of (2*S*,3*S*)-3-methylaspartic acid under the assay conditions.[28, 46, 42]

Determination of kinetic parameters (see section 2.6, Table 2.6)

Incubations were conducted at pH 9 and contained 500 mM Tris-HCl, 20 mM $MgCl_2$, 1 mM KCl and (2*S*,3*S*)-3-methylaspartic acid concentrations over the range 0.5-20 mM. Reactions were initiated by the addition of enzyme (20 mm^3) and were followed spectrophotometrically at 240nm in a 10 mm path length quartz cuvette. Over the time course measured, the reactions were linear. Each rate determination was carried out in duplicate. Regression analyses gave the best straight lines. Non- linear regression analysis was used for K_m determinations.

Radioactivity assay

The sample (500 mm^3-750 mm^3) was mixed with scintillation fluid (4 cm^3) and the radioactivity measured in a scintillation counter.

Reversed Phase-HPLC analysis

All analyses were conducted on a Poros C18 reversed phase column (4.6 x 100 mm) using a gradient of 0-60 % acetonitrile applied over 20 column volumes unless otherwise stated. Buffers were prepared as follows:

Buffer A: Water + 0.05 % TFA

Buffer B: Acetonitrile + 0.1 % TFA + 0.5 % Water

Isolation of recombinant methylaspartase (pSG4) (see section 2.1, Table 2.1)

pSG4 was cultivated in 3 dm^3 of LB at 37 °C to an optical density of 10 at 660 nm. The cells were harvested by centrifugation (0 °C, 10,000 rpm, 30 min) to give 35-40 g of wet cell paste. The cells were resuspended in buffer [(20 cm^3; 50 mM potassium phosphate, pH 7.6) containing β-mercaptoethanol (1 mM) and PMSF (100 mm^3, 34 mg cm^{-3} in isopropanol)] and the suspension sonicated (0 °C, 6 x 20 sec, 120 W, 20 kHz). Acetone (20 cm^3, -20 °C), was added with stirring over 5 min, and then stirring continued for a further 10 min at 4 °C. The cell debris and precipitated protein were removed by centrifugation (0 °C, 37000 rpm, 30 min) to give the crude extract. A further portion of acetone (30 cm^3, -20 °C) was added. After stirring at 4 °C for a further 10 min the precipitated protein was collected by centrifugation (0 °C, 37000 rpm, 20 min). The

protein pellet was resuspended in buffer (2.5 cm^3, 50 mM potassium phosphate, pH 7.6) with stirring at 4 °C and the insoluble material was removed by centrifugation (10 °C, 37000 rpm, 10 min).

Purification of recombinant methylaspartase by gel filtration chromatography (see section 2.1, Table 2.1)

The protein solution from the previous step was applied to a column of Sephadex G-150 (1.3 x 170 cm) pre-equilibrated with buffer (4 °C, 50 mM potassium phosphate, pH 7.6) containing 10 mM β-mercaptoethanol. The protein was eluted with the same buffer at a flow rate of 6 cm^3 h^{-1} (collecting 6 cm^3 fractions). The active fractions were pooled and concentrated by ultrafiltration (4 °C). The protein was dialysed overnight against Tris buffer at 4 °C (3 x 1 dm^3, 50 mM Tris, pH 9).

Further purification of recombinant methylaspartase by anion-exchange chromatography (see section 2.1, Table 2.1)

The protein solution (100 mm^3) from the previous step was applied to a column of quarternised polyethyleneimine, which had been pre-equilibrated with phosphate buffer (10 mM potassium phosphate, pH 7.6) at a flow rate of 4 cm^3 min^{-1}. The column was washed with the same buffer at a flow rate of 4 cm^3 min^{-1}, collecting 4 cm^3 fractions. The application of a salt gradient (potassium chloride over the range of 0-500 mM) afforded methylaspartase, which eluted at 80 mM potassium chloride concentration. The eluted enzyme was assayed for activity using the standard procedure.[46] A Bradford assay and SDS-PAGE analysis was used to determine protein yield and purity.

Plasmid stability test (see section 2.3.2, Table 2.4)

Starter cultures of transformed *E. coli* cells were grown in 5 cm^3 portions of LB medium containing 100 mg/cm^3 ampicillin overnight at 37 °C with vigorous shaking at 150 rpm. Each starter culture was transferred into 500 cm^3 of fresh LB medium containing 100 mg/cm^3 ampicillin and allowed to grow at 37 °C to an OD_{600} reading of 0.6. Three aliquots of 1000 mm^3, 147 mm^3 and 135 mm^3 of LB were transferred into three sterile eppendorfs. A primary dilution of bacteria was prepared by transferring 1 mm^3 of log phase culture into 1000 mm^3 of LB. Two secondary dilutions were prepared by transferring 3 mm^3 and 15 mm^3 of the primary dilution into tubes containing 147 mm^3 (dilution A) and 135 mm^3 (dilution B) of LB, respectively. Bacteria were plated onto agar as indicated in Table 6.1. Plates were incubated overnight at 37 °C.

Table 6.1: *Plasmid stability test*

Volume of bacteria	LB additives
50 mm^3 of dilution A	No additives
50 mm^3 of dilution A	Ampicillin (100 $\mu g/cm^3$)
50 mm^3 of dilution B	IPTG (0.4 mM)
50 mm^3 of dilution B	Ampicillin (100 mg/cm^3) + IPTG (0.4 mM)

Optimisation of IPTG induction (10 x his-tagged methylaspartase) (see section 2.3.1, Table 2.3)

A starter culture was prepared for each of the recombinant plasmids pMASM 2 + 3. *E. coli* BL21 (DE3) cells were used for expression. For overexpression, cells from clones 2 and 3 were induced by the addition of IPTG to a final concentration of 1 mM and incubated for a further 3, 6 and 16 h respectively and harvested by centrifugation at (4 °C, 8000 rpm, 10 mins). The cell pellet from each of the three cultures (5 g wet weight) was suspended in 5 cm^3 sonication buffer (50 mM potassium phosphate, 350 mM sodium chloride, 50 mM imidazole, pH 8) and PMSF and mercaptoethanol added to final concentrations of 1 mM to each. The cells were disrupted by sonication (0 °C, 3 x 30 sec, 120 W, 20 kHz) and the cell debris was spun down by centrifugation (4 °C, 8000 rpm, 10 min). Resulting enzyme preparations from clones 2 and 3 were assayed for activity.

Isolation of recombinant 10 x His-tagged methylaspartase (from pET-5 vector) (see section 2.3, Table 2.2)

E. coli BL21 (DE3) cells were the host used for expression. Starter cultures (5 cm^3) were grown for 16 h in LB media supplemented with ampicillin (2.5 x 10^{-5} g/ cm^3) at 37^{o}C and at 150 rpm without induction. A starter culture was added to each large culture (500 cm^3) and the cells grown to an OD_{600} of 0.6-0.9. Overexpression was induced by the addition of 1-2 mM IPTG and the cultures were incubated at 37 °C for 4 h, after which time the cells were harvested by centrifugation (4 °C, 8000 rpm, 20 mins) to give a cell pellet (6 g/ L wet weight). The cell pellet was re-suspended in sonication buffer (1 cm^3/ g) (50 mM potassium phosphate, 350 mM sodium chloride, 50 mM imidazole, pH 8) and PMSF and mercaptoethanol was added to final concentrations of 1 mM each.

The cells were disrupted by sonication for (0 °C, 5 x 30 sec, 120 W, 20 kHz), and the cell debris spun down by centrifugation (4 °C, 20000 rpm, 30 min). The resulting preparation was assayed for activity before further purification.

Purification of 10 x His-tag recombinant methylaspartase by metal affinity chromatography (beads) (see section 2.5.1)

Nickel resin (5 cm^3) was suspended in wash buffer (2cm^3, 50 mM potassium phosphate, 350 mM sodium chloride, 20 mM imidazole and azide). The wash buffer was removed and the resin (5 cm^3) and crude enzyme extract (25 cm^3, 10,765 units) were stirred together for 1 h at 4 °C to allow binding of protein to the resin. The resin was removed by centrifugation (1000 rpm, 5 min) and the supernatant solution was tested for methylaspartase activity using the standard assay procedure. When no methylaspartase activity remained the beads were resuspended in the wash buffer (45 cm^3, 50 mM potassium phosphate, 500 mM sodium chloride, 30 mM imidazole, pH 8) and shaken (2 min), centrifuged (1000 rpm, 2 min) and the supernatant removed and tested for activity. This wash was repeated until the A_{280} reading was identical to a blank reading for the buffer indicating that all unbound contaminating material had been removed from the beads. Before elution of the enzyme the beads were washed with wash buffer (6 x 45cm^3, 50 mM potassium phosphate, 500 mM sodium chloride, pH 8).

The enzyme was eluted from the nickel beads by addition of 1 x bed volume (1 cm^3) of eluting buffer (50 mM potassium, 450 mM imidazole, 100 mM sodium chloride, pH 8) and the beads removed by centrifugation (1000 rpm, 2 min). The eluting wash was repeated until no more activity was detected in the supernatant solution as determined by

the standard assay. All fractions were assayed for activity, pooled and concentrated by ultrafiltration.

Purification of His-tagged methylaspartase by metal affinity chromatography (HPLC) (see section 2.5.2)

E. coli cell pellet was suspended in sonication buffer (1 cm^3/ g) (50 mM potassium phosphate, 350 mM sodium chloride, 50 mM imidazole, pH 8) and PMSF and mercaptoethanol were added to final concentrations of 1 mM each.

The cells were disrupted by sonication for 5 x 30 second bursts (40 Hz), and the cell debris was removed by centrifugation (20000 rpm, 30 min). The resulting crude enzyme solution was filtered and then applied to column containing nickel resin (25 cm^3) which had been pre-equilibrated with sonication buffer (50 mM potassium phosphate, 350 mM sodium chloride, 50 mM imidazole, pH 8) at a flow rate of 3 cm^3 min^{-1}. The column was washed (50 mM imidazole, 50 mM sodium phosphate, 350 mM sodium chloride, pH 8) and the protein eluted using an imidazole gradient (50-1000 mM imidazole, 50 mM sodium phosphate, 100 mM sodium chloride, pH 8) and collected in 4 cm^3 fractions. All the fractions were assayed for activity and the active fractions pooled and concentrated by ultrafiltration.

Purification of His-tagged methylaspartase by anion-exchange chromatography (see section 2.5.2, Fig. 2.1)

The concentrated protein solution from above (100 mm^3) was applied to a column of quarternised polyethyleneimine (Bio-Cad HQ POROS 20, 4 mm x 100 mm) which had been pre-equilibrated with Tris buffer (20 mM, pH 9) at ambient temperature and at a flow rate of 8 cm^3/ min. Prior to protein elution at the same flow rate the column was washed using 100 mM sodium chloride. The application of a salt gradient of sodium chloride over the range 100-500 mM (25 column volumes) afforded methylaspartase. The enzyme which eluted at 200 mM sodium chloride concentration was assayed for activity. The active fractions were pooled and concentrated by ultrafiltration. A Bradford assay and SDS-PAGE analysis were used to determined protein yield and purity.

Isolation of His-tagged methylaspartase using serine supplemented growth media (see section 3.2, Table 3.1)

BL21 (DE3) host cells were used for over-expression of methylaspartase. Starter cultures (5 x 5 cm^3) were grown for 16 h in LB media containing ampicillin (2.5 x 10^{-5} g/cm^3), at 37 °C and at 150 rpm. Each of the cultures was transferred into fresh LB media (500 cm^3) and ampicillin was added (2.5 x 10^{-5} g/cm^3). (2*S*)-Serine was added to one of the cultures at pre-determined times (Table 6.2). The cells were then grown to an OD_{600} of 0.6-0.9. Overexpression was induced by the addition of IPTG to a final concentration of 1-2 mM and the cells were incubated at 37 °C for a further 4 h. The cells were harvested as described previously.

Table 6.2: *Supplementation of culture medium with (2S)-serine*

Culture	*Time of serine addition to main culture*
1	Control
2	Start of log phase growth
3	During log phase growth
4	Before IPTG addition
5	After IPTG addition

Incorporation of ^{14}C-serine into methylaspartase using LB media supplemented with ^{14}C-serine (see section 3.3)

Starter cultures (5 cm^3) were grown for 16 h in LB media containing [U-^{14}C]-(2*S*)-serine (Specific Activity 141 mCi/mmol, 0.05 μCi) and ampicillin (2.5 x 10^{-5} g/ cm^3) at 37 °C and at 150 rpm and. The starter cultures were transferred into fresh media (500 cm^3) containing ampicillin (2.5 x 10^{-5} g/ cm^3) and [U-^{14}C]-L-serine (10.0 μC_i) and grown to an OD_{600} of 0.6-0.9. To each culture, IPTG was added to a final concentration of 1-2 mM, and incubated at 37 °C for a further 4 h. Cells were harvested by centrifugation (4 °C, 8000 rpm, 20 min) and the resultant pellet was resuspended in phosphate buffered saline (50m M sodium phosphate, 350 mM sodium chloride, pH 8) with the addition of PMSF (34 mg/ cm^3) and mercaptoethanol to a final concentration of 1 mM. The cells were disrupted by sonication (0 °C, 5 x 20 sec, 120 W, 20 kHz) and the cell debris removed by centrifugation (20000 rpm, 30 min).

Isolation of His-tagged methylaspartase using Davis/ LB broth supplemented with ^{14}C-serine (see section 3.3, Tables 3.2 and 3.3)

Starter cultures (5 cm^3) were prepared for each trial experiment and grown for 16 h in media of varying composition (Table 6.3) containing ampicillin (2.5 x 10^{-5} g/ cm^3) at 37 °C and at 150 rpm. The starter cultures were transferred into fresh media (500 cm^3) of varying composition (Table 6.3) containing ampicillin (2.5 x 10^{-5} g/ cm^3) and grown to an OD_{600} of 0.6-0.9. To each culture, [U-^{14}C]-L-serine (0.5-5.0 μCi) was added along with IPTG to a final concentration of 1-2 mM, and incubated at 37 °C for a further 4 h. The cells were harvested as described above.

Table 6.3: *Composition of media*

o/n culture	*main culture*
%LB / %DMB	*%LB/ %DMB*
12.5 / 87.5	12.5 / 87.5
25.0 / 75.0	25.0 / 75.0
100 / 0	25.0 / 75.0
100 / 0	100 / 0

Isolation of His-tagged methylaspartase using a media of defined amino acid composition (see section 7.1 and section 3.3, Table 3.4)

All the amino acid components of the media were dissolved in distilled water (250 cm^3) and the mixture sonicated (20 Hz, 2 x 5 min). The mixture was centrifuged (20 min, 8000 rpm) to remove the insoluble fraction. The inorganic salts and glycerol were then added and the solution sterile filtered. The cells were grown under identical conditions to those described for LB media.

Effect of varying the time of [U-^{14}C]-L-serine addition using media of defined amino acid composition (see section 3.3.1, Table 3.5)

Cells were grown as described above except that [U-^{14}C]-L-serine (5.0 μCi) was added 1, 2 or 3 h after induction with IPTG.

Optimisation of [U-^{14}C]-L-serine incorporation using media of defined amino acid composition (see section 3.3.2)

Six starter cultures (5 cm^3) of LB media were prepared, innoculated and incubated for 16 h at 37 °C (150 rpm). Each culture was transferred into fresh media (500 cm^3) containing all the amino acids. The cells were grown to an OD_{600} of 0.6-0.9 and harvested centrifugation (20 min, 8000 rpm). The cell pellet was washed with phosphate buffer (59 mM sodium phosphate, pH 7.6) containing 0.8% v/v saline. The cells were resuspended in the growth media (3 dm^{-3}) and shaken at 37 °C (110 rpm). After 20 min, UL-(2*S*)-^{14}C-

serine (0.5 μCi) was added with IPTG (1 mM) and the cells shaken for 3 h, before being harvested by centrifugation.

Incorporation of [1-^{13}C]-(2*S*)-serine into Methylaspartase (see section 3.4)

Precise details of enzyme expression and isolation are as described above except that [1-^{13}C]-(2*S*)-serine (0.472 g) was used instead of UL-(2*S*)-^{14}C-serine.

Testing the reversibility of β-methylaspartase binding to the resin bound hydrazide inhibitor (see section 4.1.3)

To a suspension of the resin bound hydrazide inhibitor (500 mg) in Tris buffer (5 cm^3, 50 mM Tris, pH 9.0) was added β-methylaspartase (5 cm^3, 460 units, 5 mg, 90 U / mg) and the suspension stirred at ambient temperature until the remaining activity was ~ 50 % (48 h). The resin was washed to remove excess unbound protein. Resin (200 mg) with bound protein was suspended in a solution of ammonium chloride (20 cm^3, 100 mM) in Tris buffer (50 mM Tris, pH 9.0) and left at ambient temperature overnight. The supernatant (50 mm^3) was analysed periodically by Bradford assay to assess the extent of protein debinding.

Tryptic digestion of methylaspartase (see section 4.2)

A solution of β-methylaspartase (1 cm^3, 5 mg) in Tris buffer (50 mM Tris, pH 7.8) was denatured by heating (100 °C, 15 min). Trypsin (4 mg/cm^3 in 1 mM $CaCl_2$) was added in amounts equal to 2.5% by weight of enzyme. A second aliquot of trypsin was added after 3 h. After complete digestion the solution was lyophilised and analysed by RP-HPLC.

Tryptic digestion of immobilised methylaspartase (see section 4.2, Fig. 4.5)

The resin bound hydrazide inhibitor (**99**) (50 mg) was suspended in Tris buffer (2 cm^3, 100 mM Tris, pH 9.0) and β-methylaspartase (1268 units, 5.5 mg, 230.6 U/mg) was added to the resin suspension and left stirring at ambient temperature until the remaining activity of the supernatant was ~50% of the starting activity. The resin was washed with Tris buffer (6 x 1 cm^3, 50 mM Tris, pH 7.8) to remove excess unbound protein. The washings were analysed by Bradford assay to determine the amount of protein bound to the resin. The resin bound enzyme was denatured at 100 °C for 15 min. Digestion was carried out with a freshly prepared trypsin solution (4 mg/cm^3 in 1 mM $CaCl_2$). Addition of trypsin in two portions to 2.5% by weight of β-methylaspartase was made initially and also 3 h after digestion. The solution was maintained at pH 7.8 by 50mM Tris buffer. The resin was washed thoroughly with Tris buffer (10 x 1 cm^3, 50 mM Tris, pH 7.8) to remove the tryptic digest. The digest solution was lypholised and the resulting residue was re-suspended in water and then filtered and analysed by RP-HPLC.

Digestion of methylaspartase with V8 protease (see section 4.2.1, Fig. 4.6)

Resin immobilised protein (200 mg) was suspended in a solution of ammonium acetate [(100 mM in Tris buffer (50 mM Tris, pH 4.0)] and the resin bound protein was denatured (30 min, 100 °C).

V8 protease (*Staphylococcus aureus*) was then added in two portions (at 0h and 10 h to 2.0% by weight of β-methylaspartase) and the digestion was incubated at 30 °C for 18 hours. The solution was maintained at pH 4.0 by the addition of hydrochloric acid (1 mole dm^{-3}). After digestion, the resin was washed thoroughly with water (10 x 50 cm^3) and the resulting supernatant was lyophilised, resuspended in water and filtered prior to analysis by RP-HPLC.

Labeling of the active site of MAL with ^{14}C-acetylhydrazide (see section 5.1, Fig. 5.4)

To a solution of β-methylaspartase (5 mg, 950 units, specific activity 180 U/mg) in Tris buffer (1 cm^3, 50 mM Tris, pH 9.0) was added ^{14}C-acetylhydrazide acetate (20.8 mg, 200 μmoles, specific activity 0.5 mCi/ mmole) to a final concentration of 200 mM. The solution was incubated at 30°C until a complete loss of enzyme activity was observed (10 h). The solution was then dialysed against Tris buffer (50 mM Tris, pH 9.0) until the radioactivity in the dialysis buffer was equal to background levels as judged by scintillation counting.

Analysis of ^{14}C-acetylhydrazide inhibited MAL by anion-exchange chromatography (see section 5.1)

A solution of ^{14}C-acetylhydrazide labelled methylaspartase (100 mm^3) was applied to a column of quarternised polyethyleneimine which had been pre-equilibrated with Tris buffer (20 mM Tris, pH 9.0) at ambient temperature and at a flow rate of 8 cm^3/min.

Prior to protein elution (monitored at 220/280 nm) the column was washed with Tris buffer (20 mM Tris, pH 9.0) containing sodium chloride (50 mM) at a flow rate of 8 $cm^3\ min^{-1}$.

A gradient of sodium chloride (50-600 mM) was then applied and fractions were collected (750 mm^3). From each a 500 mm^3 sample was removed and total radioactivity content determined. The trace for radioactivity was overlayed onto that for the trace of the absorbance recorded at 220 nm.

Tryptic digestion of ^{14}C-acetylhydrazide inhibited MAL (see section 5.1, Fig. 5.5)

To a solution of ^{14}C-acetylhydrazide inhibited β-methylaspartase (3.5 mg) in Tris buffer (50 mM Tris, pH 7.8) was added trypsin (4 mg/ cm^3 in 1 mM $CaCl_2$) to a level equal to 2.5% by weight of β-methylaspartase. A second aliquot of trypsin was added after 3 h. After complete digestion the solution was lyopholised and analysed by RP-HPLC. Fractions were collected (53 x 750 mm^3) and from each a 500 mm^3 sample was removed and the radioactivity content determined by scintillation counting.

Modification of thiol groups of methylaspartase with *N*-[2-^{14}C]-ethylmaleimide after inactivation with phenylhydrazine (see section 5.2)

A solution of methylaspartase (1 cm^3, 1400 units, 7 mg) was split into two equal pools. To pool A was added a solution of phenylhydrazine (0.5 cm^3, 50 mM) in Tris buffer (Tris, 100 mM, pH 9) to a final concentration of 25 mM. When no enzyme activity remained, both pool A and pool B were dialysed against phosphate buffer (2 x 2 dm^3, potassium phosphate, 50 mM, pH 7.8) at 4 °C for 4 h.

To the product of dialysis was then added an aliquot of a 1.5 M solution of (2*S*,3*S*)-3-methylaspartic acid (sodium salt) in water (1 cm^3) to a final concentration of 0.75 M and the reaction was incubated at 30 °C for 1 h. *N*-Ethylmaleimide was then added to both pool A and B to a final concentration of 2 mM (200 mm^3 of a 20 mM stock solution) and the solutions were left at 30 °C for 1 h, after which time both pool A and B were then dialysed against phosphate buffer (2 x 2 dm^3, potassium phosphate, 50 mM, 5 mM (2*S*,3*S*)-3-methylaspartic acid, pH 7.8) for 4 h and finally against phosphate buffer (potassium phosphate, 50 mM, 1 mM magnesium chloride hexahydrate, pH 7.8).

Pool A and Pool B were then further sub-divided into two pools (A1, A2, B1, B2). To pool A1 and B1 was added a solution of mercaptoethanol (0.1 cm^3, 20 mM) in water to a final concentration of 2 mM and left at 30 °C for 1 h. Each sample was reduced in volume by centrifuge filtration to a final volume of 250 mm^3, prior to addition of *N*-[2-^{14}C]-ethylmaleimide (SA 30 mCi/ mmol) to a final concentration of 0.25 mM. All the solutions were incubated at 30 °C for 3 h. The radio-labeled samples were then dialysed against water (3 x 1 dm^3) for 3 h at 4 °C.

The dialysed protein products (A1, A2, B1, B2) were denatured (100 °C, 15 min) and then treated with the trypsin (4 mg, cm^3, 2,5% w/w, 1 mM calcium chloride) and left at room temperature for 2 hours. The samples were lyopholised and analysed by RP-HPLC.

Inhibition of methylaspartase by a range of hydrazines (see section 5.2, Fig. 5.6)

Solutions of hydrazine, methylhydrazine, phenylhydrazine, *p*-nitrophenylhydrazine and 2,4-dinitrophenylhydrazine (1 cm^3, 1 mM) were each prepared in Tris buffer (Tris, 50 mM, pH 8) and incubated at 30 °C. To each solution was added methylaspartase (50 mm^3, 0.75 mg, 125 units, SA 166 U/ mg) and at various time intervals an aliquot of each incubation (20 mm^3) was removed. The enzyme activity was measured under standard conditions and was compared to a control (Tris, 50 mM, pH 9) containing no inhibitor.

Inhibition of methylaspartase by a range of hydrazide analogues (see section 4.1.3, Fig. 4.4)

Solutions of 3,6-hydrazinodioxaoctanedioate (500 mm^3, 50 mM) and tentagel hydrazide (loading 0.208 mmole g^{-1}) (50 mM) were prepared in Tris buffer (Tris, 50 mM, pH 9). A control was also prepared containing Tris buffer (Tris, 50 mM, pH 9). To each solution was added methylaspartase (50 mm^3, 6.3 units, 0.135 mg, SA 46.6 U/ mg) and the solutions were incubated at 30 °C. At various time intervals an aliquot (20 mm^3) was removed from each sample and assayed under standard conditions.

Nature of inhibition of methylaspartase by 3,6-hydrazinodioxaoctanedioate (see section 4.1.1, Fig. 4.2)

Three solutions in Tris buffer (1 cm^3, Tris, 50 mM, pH 9) were prepared as follows:

1) Buffer only
2) 3,6-hydrazinodioxaoctanedioate (1 mM).
3) (2*S*,3*S*)-3-methylaspartic acid (0.5 M). After 2 h inhibitor was added to a final concentration of 1 mM.

To each solution methylaspartase was added (50 mm^3, 14.9 units, 0.068 mg, SA 219 U/ mg). The solutions were incubated at 30 °C and at various time intervals an aliquot (10 mm^3) was removed from each sample and was assayed under standard conditions.

Reversibility of inhibition of β-methylaspartase by 3,6-hydrazino-dioaxaoctanedioate (see section 4.1.1)

To a solution of the inhibitor (5 cm^3, 50 mM) in Tris buffer (50 mM Tris, pH 9.0) was added an aliquot of β-methylaspartase (250 mm^3, 400 units, 2.2 mg, SA 180 U / mg).

The mixture was incubated at 30 °C. At various times an aliquot (10 mm^3) was removed and assayed under standard conditions. When the enzyme was totally inactivated the enzyme solution (5.25 cm^3) was dialysed against buffer (6 x 1 dm^3, 50 mM Tris, pH 9.0) for 6 h and the enzyme was assayed under standard conditions.

Inhibition of methylaspartase by acetylhydrazine (see section 5.1)

pH dependence (Fig. 5.3): A series of solutions of acetyllhydrazide (1 cm^3, 50 mM) in Tris buffer (Tris, 50 mM, pH 6-9) were prepared. An aliquot of methylaspartase (50 mm^3, 40 units, 0.2 mg, SA 200 U/ mg) was added to each solution. The enzyme activity of each solution was measured at various time intervals.

***Concentration dependence (see Fig. 5.1a and 5.1b)*:** A series of five solutions of acetylhydrazide (1 cm^3, 50-1000 mM) in buffer (Tris, 50 mM, pH 9) were prepared. To each solution was added an aliquot of methylaspartase (50 mm^3, 40 units, 0.2 mg, SA 200 U/ mg). The enzyme activity of each solution was measured at various time intervals.

***Reversibility*:** To a solution of acetylhydrazide (4.5 cm^3, 0.5 M) in Tris buffer (Tris, 50 mM, pH 9) was added methylaspartase (0.5 cm^3, 300 units, 1.63 mg, SA 184 U/ mg). After complete inactivation was observed (24 hrs), the solution was dialysed against Tris buffer (Tris, 50 mM, pH 9, 4 x 1 dm^3) and the enzyme activity was determined under standard conditions.

***Substrate protection (see Fig. 5.2)*:** Three solutions (1 cm^3) of acetylhydrazide were prepared in Tris buffer (50 mM Tris, pH 9):

1) Buffer only.
2) 200 mM Inhibitor.
3) 0.5 M (2*S*,3*S*)-3-methylaspartic acid (200 mM Inhibitor added after 30 mins).

To each sample was added methylaspartase (100 mm^3, 12 units, 0.15 mg, SA 80 U/ mg). At various time intervals an aliquot (10 mm^3) from each sample was removed and was assayed.

Inhibition of methylaspartase by phenylhydrazine (see section 5.2, Fig. 5.7)

A series of solutions (1 cm^3) of phenylhydrazine hydrochloride over the concentration range 0-20 mM in Tris buffer (Tris, 50 mM, pH 9) were prepared. An aliquot of methylaspartase (25 mm^3, 16.1 units, 0.076 mg, SA 208 U/ mg) was added to each solution which was then incubated at 30 °C. At various times intervals an aliquot (20 mm^3) was removed from each incubation and the enzyme activity assayed under standard conditions. A sample containing only buffer and enzyme was also assayed under identical conditions.

Inhibition of methylaspartase by phenylhydrazine (substrate protection) (see section 5.2)

Methylaspartase (30 mm^3, 20 units) was added to a solution of phenylhydrazine hydrochloride (1 cm^3, 20 mM) in Tris buffer (Tris, 50 mM, pH 9). To an aliquot of enzyme (30 mm^3, 20 units, 0.08 mg, SA 208 U/ mg) incubated in a solution of (2*S*,3*S*)-3-methylaspartic acid) (0.5M) for 1 h was also added phenylhydrazine hydrochloride to a final concentration of 20 mM. At various times intervals an aliquot (20 mm^3) was removed and the enzyme was assayed and compared to a control, containing buffer only.

Inhibition of methylaspartase by phenylhydrazine (followed by reaction with acetic anhydride) (see section 5.3.2)

Methylaspartase (25 mg, 2875 units, SA 115 units/ mg) was incubated with ^{15}N-phenylhydrazine (100 mM) in potassium phosphate buffer (5 cm^3, 100 mM, pH 9.0).

When inactivation was 50% complete (~8 hours), acetic anhydride was added (5 mm^3) and the mixture was stored at room temperature for 2 h. The resulting protein was digested with trypsin (10 mg/ cm^3, 1 mM calcium chloride, pH 7.8, 1% w/w). A second aliquot of trypsin was added after 2 h (1% w/w). The reaction was quenched by addition of acetic acid (1 drop) and the sample lyophilised and dissolved in deuterium oxide/ water (1:9, 600 mm^3).

Effect of magnesium ion on inhibition of methylaspartase by phenylhydrazine (see section 5.2)

A series of solutions of phenylhydrazine hydrochloride (1 cm^3, 0-20 mM) containing magnesium chloride hexahydrate were prepared in Tris buffer (Tris, 50 mM, pH 9). Methylaspartase was added to each solution (20 mm^3, 7.3 units, 0.035 mg, SA 217 U/ mg). At various time intervals an aliquot (20 mm^3) was removed and assayed under the standard conditions.

Effect of ammonium ion on inhibition of methylaspartase by phenylhydrazine (see section 5.2)

A series of solutions of phenylhydrazine hydrochloride (1 cm^3, 5, 10 and 20 mM) were prepared in Tris buffer (Tris, 50 mM, pH 9) in triplicate. To each was added ammonium chloride to a final concentration of 5, 20 or 40 mM. Each solution was incubated at 30 °C and methylaspartase was added (20 mm^3, 10 units, 0.045 mg, SA 217

U/ mg). At various times intervals an aliquot (20 mm^3) was removed from each incubation, and the activity was assayed under standard conditions.

pH rate profile for inhibition of methylaspartase by phenylhydrazine (see section 5.2, Fig. 5.9)

A series of solutions of phenylhydrazine hydrochloride (20 mM) were prepared in Tris buffer (Tris, 50 mM) over the pH range 9-11. Each solution was incubated at 30 °C and methylaspartase (10 mm^3, 22 units, 0.1 mg, SA 217 U/ mg) was added. At various time intervals an aliquot (20 mm^3) from each incubation was removed and assayed for activity under standard conditions.

Effect of mercaptoethanol on inhibition of methylaspartase by phenylhydrazine (+/- 1 mM) (see section 5.2, Fig. 5.11)

Two solutions of phenylhydrazine hydrochloride (1 cm^3, 20 mM) in Tris buffer (Tris, 50 mM, pH 9) were prepared. To one of these was added β-mercaptoethanol to a final concentration of 1 mM. An aliquot of methylaspartase (50 mm^3, 8.0 units, 0.037 mg, SA 215 U/ mg) was added to each solution, and the solution incubated at 30 °C. At various times intervals an aliquot (20 mm^3) was removed from each incubation and the enzyme activity was determined. A sample containing only buffer and enzyme was also assayed under identical conditions.

Effect of mercaptoethanol on inhibition of methylaspartase by phenylhydrazine (varied β-mercaptoethanol concentration) (see section 5.2, Fig. 5.14)

A series of solutions of phenylhydrazine hydrochloride (1 cm^3; 20 mM) were prepared in Tris buffer (Tris, 500 mM, pH 9), along with a control containing only Tris buffer (Tris, 500 mM, pH 9). To each solution was added β-mercaptoethanol in buffer to a final concentration of 0.1-20 mM. Each solution was incubated at 30 °C and methylaspartase (50 mm^3, 3.8 units, 8.8 μg, SA 215 U/ mg) was added to each incubation. At various time intervals, an aliquot (50 mm^3) from each incubation was removed, and was assayed for activity under standard conditions.

Determination of the K_i for phenylhydrazine in the presence of β-mercaptoethanol (see section 5.2, Fig. 5.15)

A series of solutions of phenylhydrazine hydrochloride (1 cm^3; 5-40 mM) were prepared in Tris buffer (Tris, 500 mM, pH 9). To each was added β-mercaptoethanol to a final concentration of 2 mM. Each solution was incubated at 30 °C and methylaspartase was added (50 mm^3, 90 units, 0.4 mg, SA 225 U/ mg). At various time intervals an aliquot (5 mm^3) from each solution was removed and was assayed under standard conditions.

Effect of mercaptoethanol on enzyme activity after partial inhibition of methylaspartase by phenylhydrazine (see section 5.2, Fig. 5.13)

Two solutions of phenylhydrazine hydrochloride (1 cm^3, 20 mM) were prepared in Tris buffer (Tris, 500 mM, pH 9). To each solution was added methylaspartase (50 mm^3, 9.9 units, 0.046 mg, SA 215 U/ mg). At various time intervals an aliquot (50 mm^3) was removed from each incubation and assayed under standard conditions. When the activity had fallen to ~ 25 % of the initial, an aliquot of β-mercaptoethanol (1 mm^3, final conc. 2 mM) was added to one of the incubations. The enzyme activity was measured for each incubation. A second aliquot of mercaptoethanol (1 mm^3) was added after 30 min.

Effect of tribuytlphosphine on enzyme activity after partial inhibition of methylaspartase by phenylhydrazine (see section 5.2, Fig. 5.17)

Two solutions of phenylhydrazine hydrochloride (5 cm^3; 20 mM) in Tris buffer (Tris, 50 mM, pH 9) were prepared and degassed under argon (5 mins). Methylaspartase (100 mm^3, 4.0 units, 0.018 mg, SA 222 U/ mg) was added to each solution and each solution was then incubated at 30 °C. At various times intervals an aliquot (20 mm^3) was removed from each incubation and the enzyme activity was determined. A sample containing only buffer and enzyme was also assayed under identical conditions. After 80% of the enzyme activity had been lost isopropanol was added to each of the solutions, including the control. An aliquot of tributylphosphine (5 mm^3, 4.5 mM) was added to one of the solutions containing inhibitor and enzyme. At various time intervals an aliquot (20 mm^3) was removed from each incubation and the enzyme activity was measured.

Effect of dithiothreitol on enzyme activity after partial inhibition of methylaspartase by phenylhydrazine (see section 5.2, Fig. 5.16)

Two solutions of phenylhydrazine hydrochloride (5 cm^3; 20 mM) in buffer (Tris, 50 mM, pH 9) were prepared. Methylaspartase (100 mm^3, 4.0 units, 0.018 mg, SA 222 U/ mg) was added to each solution and each solution was then incubated at 30 °C. At various times intervals an aliquot (20 mm^3) was removed from each incubation and the enzyme activity measured under standard conditions. A sample containing only buffer and enzyme was also tested for activity. After 80% of the enzyme activity had been lost dithiothreitol (final concentration, 1.6 mM) was added to one of the solutions containing inhibitor and enzyme. At various time intervals an aliquot (20 mm^3) was removed from each incubation and the enzyme activity was measured.

Testing aniline as an inhibitor of methylaspartase (see section 5.2)

A series of solutions of aniline hydrochloride (1 cm^3; 1-40 mM) were prepared in Tris buffer (Tris, 500 mM, pH 9). To each incubation at 30 °C was added methylaspartase (100 mm^3, 40 units, 0.2 mg, 200 U/ mg). At various time intervals, an aliquot (20 mm^3) from each incubation was removed and the enzyme activity was determined.

Testing for enzyme-mediated generation of aniline during inhibition of methylaspartase by phenylhydrazine (see section 5.3)

Two incubations were prepared as follows:

1) Phenylhydrazine hydrochloride (3 cm^3, 2 mM) in Tris buffer (Tris, 50 mM, pH9)
2) Phenylhydrazine hydrochloride (2 cm^3, 2 mM) in Tris buffer (Tris, 50 mM, pH 9) and methylaspartase (1 cm^3, 2400 units, 20 mg, SA 120 U/ mg)

Both solutions were incubated in the dark until there was no activity remaining in solution 2. Both solutions were extracted into ethylacetate (2 x 10 cm^3), dried ($MgSO_4$) and the solvent removed under reduced pressure. The samples were then re-dissolved in ethylacetate (0.5 cm^3) and analysed by gas chromatography.

Chapter 7 : Appendices

7.1 Composition of synthetic culture medium

Amino Acid	Weight (g/ L))
Alanine	0.90
Arginine	0.59
Aspartic acid	1.56
Glutamine	2.11
Glycine	0.45
Histidine	0.25
Isoleucine	0.53
Leucine	0.87
Lysine	0.74
Methionine	0.13
Phenylalanine	0.45
Proline	0.47
Serine	0.94
Threonine	0.58
Tyrosine	1.17
Valine	0.98

Inorganic *Component*	Weight (g/ L)
K_2HPO_4	1.8
KH_2PO_4	1.4
$MgSO_4.7H_2O$	1.0
$CaCl_2$	0.011
NH_4Cl	0.78
Glycerol	10.0

REFERENCES

1. A. L. Mackay *A dictionary of scientific quotations*; Instutute of physics publishing: Bristol, 1992.
2. H. R. Horton, L. A. Moran, R. S. Ochs, J. D. Rawn and K. G. Scrimgeour *Principles of Biochemistry*; Neil Patterson: Prentice Hall:, 1993.
3. S. M. Roberts and C. R. Ganellin *Medicinal Chemistry*; 2nd ed.; Academic Press:, 1993.
4. G. Gottschalk *Bacterial metabolism* New York, 1986.
5. H. A. Barker, *Ann. Rev. Biochem.*, 1981, **50**, 23-40.
6. H. A. Barker *Fermentation of nitrogenous organic compounds.*; 1 ed.; New York: Academic.: Fermentation of nitrogenous organic compounds., 1961; Vol. 2.
7. W. Buckel and H. A. Barker, *J. Bacteriol.*, 1974, **117**, 1248-1260.
8. B. M. Rosner, F. A. Rainey, R. M. Kroppenstedt and B. Schink, *FEMS Microbiology Letters*, 1997, **148**, 175-180.
9. D. DeBiase, A. Tramonti, F. Bossa and P. Visca, *Molecular Microbiology*, 1999, **32**, 1198-1211.
10. S. Gharbia and H. N. Shah, *J. Gen. Microbiol*, 1991, **137**, 1201-1206.
11. D. Gani, *Grant proposal*, 1994,
12. J. M. Merrick and S. Roseman, *J. Biol. Chem.*, 1960, **235**, 1274-1280.
13. T. J. Carty, B. M. Babior and R. H. Abeles, *J. Biol. Chem.*, 1971, **246**, 6313-6317.
14. R. N. Costilow and L. Laycock, *J. Biol. Chem.*, 1971, **246**, 6655-6660.
15. J. C. Rabinowitz and W. E. Pricer, *J. Am. Chem. Soc.*, 1956, **78**, 5702-5704.

16. P. R. Vagelos, J. M. Earl and E. R. Stadtman, *J. Biol. Chem.*, 1959, **234**, 490-497.

17. K. Mizuta and M. Tokushige, *Biochmimica et Biophysica Acta*, 1975, **403**, 221-231.

18. T. B. Dougherty, V. R. Williams and E. Younathan, *Biochemistry*, 1972, **11**, 2493-2498.

19. V. R. Williams and D. J. Lartigue, *J. Biol. Chem.*, 1967, **242**, 2973-2978.

20. R. H. Depue and A. G. Moat, *J. Bacteriol*, 1961, **82**, 383-386.

21. R. R. Fritz, D. S. Hodgkins and C. W. Abell, *J. Biol. Chem.*, 1976, **251**, 4646-4650.

22. K. R. Hanson and E. A. Havir, *Arch. Biochem. Biophys.*, 1970, 1-17.

23. M. R. Young, *Phytochemistry*, 1966, **5**, 1121-1132.

24. A. Peterkofsky, *J. Biol. Chem.*, 1962, **237**, 787-795.

25. J. L. Givot, T. A. Smith and R. H. Abeles, *J. Biol. Chem.*, 1969, **244**, 6341-6353.

26. M. M. Rechler, *J. Biol. Chem.*, 1969, **244**, 551-559.

27. H. Bright, *J. Biol. Chem.*, 1964, **239**, 2307-2315.

28. H. A. Barker, R. D. Smyth, R. M. Wilson and H. Weissbach, *J. Biol. Chem.*, 1958, **234**, 320-328.

29. H. A. Barker, R. D. Smyth, E. J. Wawszkiewicz, M. N. Lee and R. M. Wilson, *Arch. Biochem. Biophys.*, 1958, **78**, 468-476.

30. P. Sykes *A guide book to mechanisms in organic chemistry*; Longman: London, 1985.

31. T. Bugg *An Introduction to Enzyeme and Coenzyme Chemistry.* Cambridge, MA, 1997.

32. J. March *Advanced organic chemistry: Reactions, mechanisms and structure.*; 4th ed.; Wiley Interscience Publication: Toronto, 1992.

33. J. A. Gerlt and P. G. Gassman, *J. Am. Chem. Soc.,*1992, **114**, 5928-5934.

34. D. R. Palmer, S. J. Wieczorek, B. K. Hubbard, G. T. Mrachko and J. A. Gerlt, *J. Am. Chem. Soc.,*1997, **119**, 9580-9581.

35. B. J. Bahnson and V. E. Anderson, *Biochemistry,*1991, **30**, 5894-5906.

36. R. V. J. Chari, C. P. Whitman, J. W. Kozarich, K.-L. Ngai and L. N. Ornston, *J. Am. Chem. Soc.,*1987, **109**, 5514-5519.

37. R. V. J. Chari, C. P. Whitman and J. W. Kozarich, *J. Am. Chem. Soc.,*1987, **109**, 5520-5521.

38. A. D. N. Vaz, J. R. Butler and M. J. Nugent, *Journal of the American Chemical Society.,*1975, **97**, 5914-5915.

39. R. M. Waterson and R. L. Hill, *J. Biol. Chem.,*1972, **247**, 5258-5265.

40. H. J. Bright, L. L. Ingraham and R. E. Lundin, *Biochem. Biophys. Acta,*1964, **81**, 576-584.

41. K. R. Hanson and E. A. Havir *3-methylaspartate ammonia-lyase*; Academic Press:, 1969; Vol. 3.

42. M. W. Hsiang and H. J. Bright, *J. Biol. Chem.,*1967, **242**, 3079-3088.

43. W. T. Wu and V. R. Williams, *J. Biol. Chem.,*1968, **243**, 5644-5650.

44. M. W. Hsiang and H. J. Bright, *Methods in Enzymology,*1969, 347-354.

45. N. P. Botting, M. Akhtar, C. H. Archer, M. A. Cohen, N. R. Thomas, S. Goda, N. P. Minton and D. Gani, *Catalytic Mechanism and Active-Site Structure of Methylaspartate Ammonia-lyase: Possible Involvement of an Electrophilic*

Dehydroalanine Reaction Centre; Royal Society of Chemistry: Cambridge, 1992, 95-109.

46. S. K. Goda, N. P. Minton, N. P. Botting and D. Gani, *Biochemistry,* 1992, **31**, 10747-10756.

47. P. C. Babbit, M. S. Hasson, J. E. Wedekind, D. R. J. Palmer, W. C. Barrett, G. H. Reed, I. Rayment, D. Ringe, G. L. Kenyon and J. A. Gerlt, *Biochemistry,* 1996, **35**, 16489-16501.

48. V. R. Williams and W. Y. Libano, *Biochem. Biophys. Acta,* 1966, **118**, 144-156.

49. H. J. Bright and R. Silverman, *Biochem. Biophys. Acta,* 1964, **81**, 175-177.

50. V. R. Williams and J. Selbin, *J. Biol. Chem.,* 1964, **239**, 1635-1639.

51. H. J. Bright, *Biochemistry,* 1967, **6**, 1191-1203.

52. H. J. Bright, *J. Biol. Chem.,* 1965, **240**, 1198-1210.

53. N. P. Botting, M. Akhtar, M. A. Cohen and D. Gani, *J. Chem. Soc. Chem. Com.,* 1987, 1371-1373.

54. N. P. Botting, M. A. Cohen, M. Akhtar and D. Gani, *Biochemistry,* 1988, **27**, 2956-2959.

55. N. P. Botting, M. Akhtar, M. A. Cohen and D. Gani, *Biochemistry,* 1988, **27**, 2953-2955.

56. M. Akhtar, N. P. Botting, M. A. Cohen and D. Gani, *Tetrahedron,* 1987, **43**, 5899-5908.

57. M. Akhtar, M. A. Cohen and D. Gani, *J. Chem. Soc. Chem. Com.,* 1986, 1290-1291.

58. H. J. Bright, R. E. Lundin and L. L. Ingraham, *Biochemistry,* 1964, **3**, 1224-1230.

59. C. H. Archer, N. R. Thomas and D. Gani, *Tetrahedron Asymmetry,* 1993, **4**, 1141-1152.

60. C. H. Archer and D. Gani, *J. Chem. Soc. Chem. Com.,* 1993, 140-142.

61. M. S. Gulzar, M. Akhtar and D. Gani, *J. Chem. Soc., Perkin I,* 1997, 649-655.

62. D. B. Northrop, *Biochemistry,* 1975, **14**, 2644-2651.

63. W. W. Cleland, *CRC critical reviews in biochemistry,* 1982, **13**, 385-428.

64. V. E. Anderson, *Current Opinion in Structural Biology,* 1992, **2**, 757-764.

65. J. R. Pollard, S. H. Richardson, M. Akhtar, P. Lasry, T. Neal, N. P. Botting and D. Gani, *Bioorg. Med. Chem.,* 1999, **7**, 949-975.

66. R. B. Wickner, *J. Biol. Chem.,* 1969, **244**, 6550-6552.

67. M. Langer, G. Reck, J. Reed and J. Retey, *Biochemistry,* 1994, **33**, 6462-6467.

68. M. S. Gulzar, K. B. Morris and D. Gani, *J. Chem. Soc. Chem. Com.,* 1995, 1061-1062.

69. N. P. Botting and D. Gani, *Biochemistry,* 1992, **31**, 1509-1520.

70. N. P. Botting, A. A. Jackson and D. Gani, *J. Chem. Soc. Chem. Com.,* 1989, 1583-1585.

71. K. Badiani, P. Lightfoot and D. Gani, *J. Chem. Soc. Chem. Com.,* 1997, 675-677.

72. Y. Kato and Y. Asano, *Biosciences , Biotechnology and Biochemistry,* 1995, **59**, 93-99.

73. Y. Asano and Y. Kato, *FEMS Microbioolgy Letters,* 1994, **118**, 255-258.

74. Y. Kato and Y. Asano, *App. Microbiol. Biotech.,* 1998, **50**, 468-474.

75. M. W. Consevage and A. T. Phillips, *J. Bacteriol.,* 1990, **172**, 2224-2229.

76. T. Furuta, H. Takahashi and Y. Kasuya, *J. Am. Chem. Soc.,* 1990, **112**, 3633-3636.

77. T. Furuta, H. Takahashi, H. Shibasaki and Y. Kasuya, *J. Biol. Chem.*, 1992, **267**, 12600-12605.

78. P. J. White and K. E. Kendrick, *Biochimica and Biophysica Acta*, 1993, **1163**, 273-279.

79. M. Oda, A. Sugishita and K. Furukawa, *J. Bacteriol.*, 1988, **170**, 3199-3205.

80. P. C. Wu, T. A. Kroening, P. J. White and K. E. Kendrick, *J. Bacteriol.*, 1992, **174**, 1647-1655.

81. V. G. Zannoni and B. N. L. Du, *Biochem. J.*, 1963, **88**, 160-163.

82. L. M. Brand and A. E. Harper, *Biochem. Biophys. Acta*, 1976, **444**, 294-306.

83. R. G. Taylor, M. A. Lambert, E. Sexsmith, S. J. Sadler, P. N. Ray, D. J. Mahuran and R. R. McInnes, *J. Biol. Chem.*, 1990, **265**, 18192-18199.

84. K. Weber and J. Retey, *Bioorg. Med. Chem.*, 1996, **4**, 1001-1006.

85. D. Hernandez, J. G. Stroh and A. T. Phillips, *Arch. Biochem. Biophys.*, 1993, **307**, 126-132.

86. M. Consevage and A. T. Phillips, *Biochemistry*, 1985, **24**, 301-308.

87. D. Hernandez and A. T.Phillips, *Biochem. Biophys. Res. Com.*, 1994, **201**, 1433-1438.

88. M. Langer, A. Lieber and J. Retey, *Biochemistry*, 1994, **33**, 14034-14038.

89. M. Langer, A. Pauling and J. Retey, *Angew. Chem.*, 1995, **34**, 1464-1465.

90. B. Schuster and J. Retey, *Proc. Natl. Acad. Sci*, 1995, **92**, 8433-8437.

91. J. Retey, *Natur Wissenschaften Aufsatze*, 1996, **83**, 439-447.

92. T. F. Schwede, J. Retey and G. E. Schulz, *Biochemistry*, 1999, **38**, 5355-5361.

93. J. D. Galpin, B. E. Ellis and M. E. Tanner, *J. Am. Chem. Soc.*, 1999, **121**, 10840-10841.

94. K. R. Hanson and E. A. Havir, *The Biochemistry of Plants*, 1981,

95. H. V. Marsh, E. A. Havir and K. R. Hanson, *Biochemistry*, 1967, 1915-1918.

96. G. B. D'cunha, V. Satyanarayan and P. M. Nair, *Enzymes and Microbiological Technology*, 1994, **16**, 318-322.

97. W. Schulz, H.-G. Eiben and K. Hahlbrock, *FEBS Letters*, 1989, **258**, 335-338.

98. H. J. Gilbert and M. Tully, *J. Bacteriol.*, 1982, 498-505.

99. W. Orczyk, J. Hipskind, E. D. Neergaard, P. Goldsbrough and R. L. Nicholson, *Physiological and Molecular Plant Pathology*, 1996, **48**, 55-64.

100. Y. Tanaka, M. Matuoka, N. Yamanoto, Y. Ohashi, Y. Kano-Murakami and Y. Ozeki, *Plant Physiology*, 1989, **90**, 1403-1407.

101. J. A. Hoskins, *The Lancet*, 1980, 392-394.

102. C. N. Sarkissian, Z. Q. Shao, F. Blain, R. Peevers, H. S. Su and R. Heft, *Proc. Natl. Acad. Sci*, 1999, **96**, 2339-2344.

103. D. Pane, *Nature*, 2000, 515.

104. G. Jack, J. D. Peiris, D. J. T. Starr, H. E. Wade and E. C. Wright, *The Lancet*, 1980, 392-394.

105. J. D. Hermes, P. M. Weiss and W. W. Cleland, *Biochemistry*, 1985, **24**, 2959-2967.

106. K. R. Hanson, E. A. Havir and C. Ressler, *Biochemistry*, 1979, **18**, 1431-1438.

107. E. A. Havir and K. R. Hanson, *Biochemistry*, 1975, **14**, 1620-1626.

108. E. A. Havir and K. R. Hanson, *Biochemistry*, 1973, **12**, 1583-1591.

109. A. Glog, L. Poppe and J. Retey, *Arch. Biochem. Biophys.*, 1998, **359**, 1-7.

110. J. Zon and B. Laber, *Phytochemistry*, 1988, **27**, 711-714.

111. J. Zon and N. Amrhein, *Liebigs. Ann. Chem.*, 1992, 625-628.

112. E. A. Havir and K. R. Hanson, *Methods in Enzymology*, 1970, **17A**, 575-581.

113. E. A. Havir and K. R. Hanson, *Biochemistry*, 1968, **7**, 1904-1914.

114. N. Ida and M. Tokushige, *J. Biochem.*, 1984, **96**, 1315-1321.

115. C. J. Falzone, W. E. Karsten, J. D. Conley and R. E. Viola, *Biochemistry*, 1988, **27**, 9089-9093.

116. I. I. Nuiry, J. D. Hermes, P. M. Weiss, C.-Y. Chen and P. F. Cook, *Biochemistry*, 1984, **23**, 5168-5175.

117. J. S. Takagi, N. Ida, M. Tokushige, H. Sakamoto and Y. Shimura, *Nucleic Acids Res.*, 1985, **13**, 2063-2074.

118. S. A. Woods, J. S. Miles, R. E. Roberts and J. R. Guest, *Biochem. J.*, 1986, **237**, 547-557.

119. J. S. Takagi, R. Fukunaga, M. Tokushige and H. Katsuki, *J. Biochem.*, 1984, **96**, 545-552.

120. A. S. Saribas, J. F. Schindler and R. E. Viola, *J. Biol. Chem.*, 1994, **269**, 6313-6319.

121. S. Suzuki, J. Yamaguchi and M. Tokushige, *Biochem. Biophys. Acta*, 1973, **321**, 369-381.

122. W. E. Karsten and R. E. Viola, *Arch. Biochem. Biophys.*, 1991, **287**, 60-67.

123. Y. Higashi, M. Tokushige and H. Umezawa, *Biochem. Int.*, 1988, **16**, 449-452.

124. N. Ida and M. Tokushige, *J. Biochem.*, 1985, **98**, 793-797.

125. F. Giorgianni, S. Beranova, C. Wesdemiotis and R. E. Viola, *Arch. Biochem. Biophys.*, 1997, **341**, 329-336.

126. S. Murase, J. S. Takagi, Y. Higashi, H. Imaishi, N. Yumoto and M. Tokushige, *Biochem. Biophys. Res. Com.*, 1991, **177**, 414-419.

127. F. Giorgianni, S. Beranova, C. Wesdemiotis and R. E. Viola, *Biochemistry*, 1995, **34**, 3529-3535.

128. M. M. K. Jayasekera, W. Shi, G. K. Farber and R. E. Viola, *Biochemistry*, 1997, **36**, 9145-9150.

129. W. Shi, J. Dunbar, M. M. K. Jayasekera, R. E. Viola and G. K. Farber, *Biochemistry*, 1997, **36**, 9136-9144.

130. D. Ajo, V. Busetti and G. Granozzi, *Tetrahedron*, 1982, **38**, 3329-3334.

131. E. Gross and H. H. Kiltz, *Biochem. Biophys. Res. Com.*, 1973, **50**, 559-565.

132. M. Yamada, T. Miyajima and H. Horikawa, *Tet. Lett.*, 1998, **39**, 289-292.

133. C. J. Pearce and J. Kenneth L. Rinehart, *J. Am. Chem. Soc.*, 1979, **101**, 5069-5070.

134. H. Depaire, J.-P. Thomas and A. Brun, *Tet. Lett.*, 1977, **16**, 1403-1406.

135. D. E. Palmer, C. Pattaroni, K. Nunami, R. K. Chadha, M. Goodman, T. Wakamiya, K. Fukase, S. Horimoto, M. Kitazawa, H. Fujita, A. Kubo and T. Shiba, *J. Am. Chem. Soc.*, 1992, **114**, 5634-5642.

136. A. Gupta and V. S. Chauhan, *Biopolymers*, 1990, **30**, 395-403.

137. R. S. Asquith, K. W. Yeung and M. S. Otterburn, *Tetrahedron*, 1977, **33**, 1633-1635.

138. A. J. Jones, E. Helmerhorst and G. B. Stokes, *Biochem. J.*, 1983, **211**, 499-502.

139. D. Ajo, M. Casarin, R. Bertoncello, V. Busetti, H. C. J. Ottenheijm and R. Plate, *Tetrahedron,* 1985, **41**, 5543-5552.

140. D. Crich and J. W. Davies, *Tetrahedron.,* 1989, **45**, 5641-5654.

141. A. L. J. Beckwith and C. L. L. Chai, *J. Chem. Soc. Chem. Com.,* 1990, 1087-1088.

142. R. G. Gasanov, L. V. Il'inskaya, M. A. Misharin, V. I. Maleev, N. I. Raevski, N. S. Ikonnikov, S. A. Orlova, N. A. Kuzmina and Y. N. Belokon, *J. Chem. Soc., Perkin I,* 1994, 3343-3348.

143. S. A. Burrage, T. Raynham and M. Bradley, *Tet. Lett.,* 1998, **39**, 2831-2834.

144. L. J. Mathias and R. E. Hermes, *Macromolecules,* 1988, **21**, 11-13.

145. D. Ajo, M. Casarin, G. Granozzi and V. Busetti, *Tetrahedron,* 1981, **37**, 3507-3512.

146. T. L. Sommerfeld and D. Seebach, *Helvetica Chimica Acta,* 1993, **76**, 1702-1714.

147. C. Blettner and M. Bradley, *Tet. Lett.,* 1994, **35**, 476-470.

148. T. Neal, Ph.D Thesis, University of St Andrews, 1998.

149. S. McMahon, Personal Communication, 1998.

150. S. H. W. Beiboer, B. vandenberg, N. Dekker, R. C. Coc and H. M. Verheij, *Protein engineering,* 1996, **9**, 345-352.

151. R. Quarrell, T. D. W. Claridge, G. W. Weaver and G. Lowe, *Molecular Diversity,* 1995, **1**, 223-232.

152. E. Bayer, *Angew. Chem.,* 1991, **30**, 113-216.

153. G. C. Cook, C. P. Holmes, J. P. Chinn and M. A. Gallop, *J. Org. Chem.,* 1994, **59**, 7588-7590.

154. B. J. Egner, G. J. Lamgley and M. Bradley, *J. Org. Chem.,* 1995, **60**, 2652-2653.

155. B. J. Egner, M. Cardno and M. Bradley, *J. Chem. Soc. Chem. Com.*, 1995, 2163-2164.

156. M. M. Bradford, *Anal. Biochim.*, 1976, **72**, 248-254.

157. V. L. Davidson and L. H. Jones, *Biochem. Biophys. Acta*, 1995, **1252**, 146-150.

158. A. Mazumdar, S. Adak, R. Chatterjee and R. K. Banerjee, *Biochem. J.*, 1997, **324**, 713-719.

159. J. Y. Han, J. C. Swarts and A. G. Sykes, *Inorganic Chemistry*, 1996, **35**, 4629-4634.

160. K. Mosinska, *Chemia Analityczna*, 1980, **25**, 859-863.

161. E. B. Getz, M. Xiao, T. Chakrabarty, R. Cooke and P. R. Selvin, *Anal. Biochem.*, 1999, **273**, 73-80.

162. U. T. Ruegg and J. Fudinger, *Methods in Enzymology*, 1977, **47**, 111-126.

163. *Organic Syntheses*; J. Wiley and Sons: London, 1932.

164. W. C. Still, M. Kahn and A. Mitra, *J. Org. Chem.*, 1978, **43**, 2923.

165. U. K. Laemmli, *Nature*, 1973, **227**, 680.

166. Kodak, *Chemical Abstracts.*, 1966, **54**, 4220.

167. L. Spialter, D. H. O'Brien, G. L. Untereiner and W. A. Rush, *J. Org. Chem.*, 1965, **30**, 3278-3283.